

INFORMATION TO USERS

This reproduction was made from a copy of a manuscript sent to us for publication and microfilming. While the most advanced technology has been used to photograph and reproduce this manuscript, the quality of the reproduction is heavily dependent upon the quality of the material submitted. Pages in any manuscript may have indistinct print. In all cases the best available copy has been filmed.

The following explanation of techniques is provided to help clarify notations which may appear on this reproduction.

1. Manuscripts may not always be complete. When it is not possible to obtain missing pages, a note appears to indicate this.
2. When copyrighted materials are removed from the manuscript, a note appears to indicate this.
3. Oversize materials (maps, drawings, and charts) are photographed by sectioning the original, beginning at the upper left hand corner and continuing from left to right in equal sections with small overlaps. Each oversize page is also filmed as one exposure and is available, for an additional charge, as a standard 35mm slide or in black and white paper format.*
4. Most photographs reproduce acceptably on positive microfilm or microfiche but lack clarity on xerographic copies made from the microfilm. For an additional charge, all photographs are available in black and white standard 35mm slide format.*

***For more information about black and white slides or enlarged paper reproductions, please contact the Dissertations Customer Services Department.**

U·M·I Dissertation
Information Service

University Microfilms International
A Bell & Howell Information Company
300 N. Zeeb Road, Ann Arbor, Michigan 48106

8618806

Lee, Tak-Yee

PART 1. COMPUTER AIDED DOSAGE FORM DESIGN: THEORY AND APPLICATIONS. PART 2. KINETICS AND MECHANISM OF CAPTOPRIL OXIDATION IN AQUEOUS SOLUTIONS UNDER CONTROLLED OXYGEN PARTIAL PRESSURE

The Ohio State University

PH.D. 1986

University
Microfilms
International

300 N. Zeeb Road, Ann Arbor, MI 48106

PLEASE NOTE:

In all cases this material has been filmed in the best possible way from the available copy. Problems encountered with this document have been identified here with a check mark ✓.

1. Glossy photographs or pages _____
2. Colored illustrations, paper or print _____
3. Photographs with dark background _____
4. Illustrations are poor copy _____
5. Pages with black marks, not original copy _____
6. Print shows through as there is text on both sides of page _____
7. Indistinct, broken or small print on several pages ✓
8. Print exceeds margin requirements _____
9. Tightly bound copy with print lost in spine _____
10. Computer printout pages with indistinct print _____
11. Page(s) _____ lacking when material received, and not available from school or author.
12. Page(s) _____ seem to be missing in numbering only as text follows.
13. Two pages numbered _____. Text follows.
14. Curling and wrinkled pages _____
15. Dissertation contains pages with print at a slant, filmed as received _____
16. Other _____

University
Microfilms
International

Part 1

Computer Aided Dosage Form Design: Theory and Applications

Part 2

**Kinetics and Mechanism of Captopril Oxidation in Aqueous
Solutions under Controlled Oxygen Partial Pressure**

DISSERTATION

Presented in Partial Fulfillment of the Requirements for
the Degree Doctor of Philosophy in the Graduate
School of The Ohio State University

By

Tak-Yee Lee, B.S.

* * * * *

The Ohio State University

1986

Dissertation Committee:

Robert E. Notari, Ph.D.

Louis Malspeis, Ph.D.

Theodore D. Sokoloski, Ph.D.

Approved by



Robert E. Notari, Advisor
College of Pharmacy

To My Parents

ACKNOWLEDGEMENTS

I wish to express my sincerest gratitude to Professor Robert E. Notari, for his guidance, valuable advice, and thoughtful help throughout my entire period of graduate studies. Without his continuous involvement and challenges, this piece of work will not be possible. He is the best teacher and adviser I have ever had.

Thanks also go to the faculty members of the Division of Pharmaceutics and Pharmaceutical Chemistry, Drs. Sylvan G. Frank, Louis Malspeis, Theodore D. Sokoloski, and Alfred E. Staubus, for their contribution to my education. To my fellow graduate students, thanks for their friendship which made past few years most memorable.

I especially like to thank my wife and parents, for their love, support, understanding and encouragement.

The financial support from College of Pharmacy is appreciated.

VITA

June 23, 1955..... Born - Taipei, Taiwan,
Republic of China

1978..... B.S., in Pharmacy
School of Pharmacy
National Taiwan University
Taipei, Taiwan, R.O.C.

1978-1980..... Second Lieutenant, Army

1980-1981..... Research Assistant
National Taiwan University Hospital
Taipei, Taiwan, R.O.C.

1981-1986..... Graduate Teaching Associate
The Division of Pharmaceutics
and Pharmaceutical Chemistry
College of Pharmacy
The Ohio State University
Columbus, Ohio

FIELD of STUDY

Major Field: Pharmaceutics and Pharmaceutical Chemistry

TABLE OF CONTENTS

	Page
ACKNOWLEDGEMENTS	iii
VITA	iv
LIST OF TABLES	vii
LIST OF FIGURES	ix
 CHAPTER	
 I. COMPUTER AIDED DOSAGE FORM DESIGN I: THEORETICAL CONSIDERATIONS FOR CONTROLLED RELEASE DRUG DELIVERY SYSTEMS	 1
Summary	2
Introduction	4
Theoretical Section	7
Experimental	15
Results and Discussion	16
Conclusions	39
Derivations	42
References	48
 II. COMPUTER AIDED DOSAGE FORM DESIGN II: CONTROLLED RELEASE THEOPHYLLINE DELIVERY SYSTEMS	 79
Summary	80
Introduction	81
Theoretical Section	83
Experimental	89

Results and Discussion	91
Conclusions	98
References	100

**III. KINETICS AND MECHANISM OF CAPTOPRIL
OXIDATION IN AQUEOUS SOLUTIONS UNDER
CONTROLLED OXYGEN PARTIAL PRESSURE . . 116**

Summary	117
Introduction	118
Experimental	120
Results	127
Discussion	132
Conclusion	140
References	142

LIST OF TABLES

TABLE	PAGE
1.1	Single Dose Plasma Concentration-Time Equations for Drug Delivery Systems Described by Scheme I and II. 50
1.2	Effect of Therapeutic Window on the Duration-Dose Profile for a Successful Zero-order Release DDS. ^a . . . 52
1.3	Comparison of T_{min} Predicted Using Eq. 1.40 to those Observed for One and Two Compartment Zero-order DDS. 53
1.4	Comparison of Required k_1 for First-order DDS which Release a Defined Percentage of Its Payloads in 10 and 12 Hours 54
2.1	The Minimum Required Duration (T_{min}) of Theophylline Zero-Order Release DDS for Children . . 102
2.2	The Minimum Required Duration (T_{min}) of Theophylline Zero-Order Release DDS for Adults . . . 103
2.3	Individual 12-Hour Maintenance Dose Range for Oral Theophylline Delivery Systems in Children. 104
2.4	Individual 12-Hour Maintenance Dose Range for Oral Theophylline Delivery Systems in Adults. 105
3.1	HPLC analyses and chromatographic characteristics for captopril and captopril disulfide 144
3.2	Mass balance for captopril oxidation at pH 6.62, 0.1M phosphate buffer ($\mu=0.18$), $pO_2=732.9\text{mmHg}$, 32°C in absence of light 145
3.3	Mass balance for captopril oxidation at pH 6.62, $pO_2=729\text{mmHg}$, $\text{Cu}^{++}=1.35\times 10^{-5}\text{M}$, 32°C in absence of light. 146
3.4	Mass balance for captopril oxidation at pH 6.62,

	pO ₂ =322mmHg, Cu ⁺⁺ =1.35x10 ⁻⁵ M, 32°C in absence of light.	147
3.5	Selection of experimental conditions which simulate the continuous flow of oxygen bubbles through the reaction mixture. ^a	148
3.6	Summary of reaction conditions at 32°C	149
3.7	Effect of captopril initial concentration on observed rates. ^a	150
3.8	Effect of added cupric ion on observed rates. ^a	151
3.9	Effect of oxygen partial pressures on observed rates. ^a	152
3.10	Effect of cyclodextrins on observed rates of captopril oxidation. ^a	153

LIST OF FIGURES

FIGURE		PAGE
1.1	Repetitive dose steady state concentration-time profiles for DDS described by Scheme I(A) and II(B)	55
1.2	Typical release rate constant-dose profiles for a zero-order or first-order release DDS described by Scheme I	56
1.3	Release rate constant-dose profile (a) and transformed duration-dose profile (b) for a zero-order DDS described by Scheme I	57
1.4	Steady state plasma concentration-time profiles for the corresponding DDS and doses indicated in Fig. 1.3.	58
1.5	Release rate constant-dose profile for a first-order DDS described by Scheme I	59
1.6	Steady state plasma concentration-time profiles for the corresponding DDS and doses indicated in Fig. 1.5	60
1.7	Release rate constant-dose profile for a zero-order DDS described by Scheme I	61
1.8	Release rate constant-dose profile for a zero-order DDS described by Scheme II	62
1.9	Release rate constant-dose profile for a first-order DDS described by Scheme I	63
1.10	Release rate constant-dose profile for a first-order DDS described by Scheme II	64
1.11	Release rate constant-dose profile for a zero-order DDS described by Scheme I with acceptable duration up to 4	65
1.12	Influence of therapeutic window on the duration-	

	dose profile for zero-order DDS	66
1.13	Influence of absorption on the duration-dose profile for zero-order DDS	67
1.14	Influence of distribution on the duration-dose profile for zero-order DDS	68
1.15	Influence of elimination on the duration-dose profile for zero-order DDS	69
1.16	Influence of elimination on the duration-dose profile for zero-order DDS with constant	70
1.17	Comparison of duration-dose profiles for a one and two compartment zero-order DDS	71
1.18	Comparison of duration-dose profiles for a one and two compartment zero-order DDS	72
1.19	Dosage form index <u>vs</u> duration of DDS for one compartment zero-order DDS containing different half-lives drugs	73
1.20	Influence of therapeutic window on the release rate constant-dose profiles for a first-order DDS described by Scheme II	74
1.21	Influence of absorption on the release rate constant-dose profiles for a first-order DDS described by Scheme II	75
1.22	Influence of elimination on the release rate constant-dose profiles for a first-order DDS described by Scheme II	76
1.23	Possible specified targets for zero-order DDS design	77
1.24	Determination of DDS specifications for a drug candidate with intersubject variation on the duration-dose profiles:	78
2.1	Duration <u>versus</u> dose profiles for zero-order delivery systems orally administered every 12 hours to children	106
2.2	Duration <u>versus</u> dose profiles for zero-order delivery systems orally administered every 12 hours to the ten	107

2.3	Duration <u>versus</u> dose profiles for zero-order delivery systems orally administered every 12 hours to adults(1 and	108
2.4	Zero-order dosage form duration <u>versus</u> dose profiles for the seven adults in Table 2.2 based on a 12-hour dosage	109
2.5	The percentage of patients having steady-state theophylline plasma concentrations between 10 and 20 mg/L as a function of th	110
2.6	The range of the acceptable dose size as a function of the duration of the zero-order delivery system given every 12 hours	111
2.7	Release rate constant <u>versus</u> dose profiles for first-order systems administered orally every 12 hours to	112
2.8	Release rate constant <u>versus</u> dose profiles for first-order systems administered orally every 12 hours to	113
2.9	The percentage of patients having steady-state theophylline plasma concentrations between 10 and 20 mg/L as a function of	114
2.10	Comparison of the calculated release rate profiles for zero-order and first-order theophylline delivery system for children	115
3.1	Schematic representation of the reaction vessel used in the study of captopril oxidation under various oxygen pressures	154
3.2	Standard curves for captopril and captopril disulfide	155
3.3	HPLC Chromatograms of reaction mixture samples taken at different time points during the reaction	156
3.4	UV spectra taken at various points of the peak and that of reference standards for captopril (A) and captopril disulfide (B)	157
3.5	Examples of mass balance for captopril oxidation	158
3.6	Captopril (A) and captopril disulfide (B) concentrations as a function of time under various oxygen partial pressures	159

3.7	Captopril (A) and captopril disulfide (B) concentrations as a function of time under various Cupric ion concentrations	160
3.8	Captopril (A) and captopril disulfide (B) concentrations as a function of time with various initial captopril concentrations	161
3.9	Initial rates as a function of initial captopril concentrations	162
3.10	Semi-logrithmic plots of captopril (A) and captopril disulfide (B) <u>vs</u> time with various initial captopril concentrations	163
3.11	Zero-order(A) and first-order(B) plots of captopril as a function of time under various Cupric ion concentrations	164
3.12	Zero-order(A) and first-order(B) plots of captopril as a function of time under various oxygen partial pressures	165
3.13	Zero-order(A) and first-order(B) plots of captopril as a function of time at various pH	166
3.14	Paired apparent zero-(.	167
3.15	Comparison of captopril concentration as a function of time with the presence of chelating agents	168
3.16	Apparent first-order(A) and zero-order(B) rate constants as a function of cupric ion concentrations	169
3.17	Apparent first-order(A) and zero-order(B) rate constants as a function of oxygen partial pressures	170

CHAPTER I
COMPUTER AIDED DOSAGE FORM DESIGN I:
THEORETICAL CONSIDERATIONS FOR CONTROLLED
RELEASE DRUG DELIVERY SYSTEMS

SUMMARY

Theories employing the clinical pharmacokinetic characteristics of a drug candidate were developed to define the required release rate constants and payloads for controlled zero-order and first-order release delivery systems (DDS). Both one and two compartmental drugs were considered. The goal is to maintain steady state plasma drug concentrations within a selected concentration range when a DDS is administered at a constant dosing interval. Steady state plasma concentration equations were derived. All the acceptable combinations of release rate constants and doses were determined using the steady state equations and computer reiterative simulation method.

Mathematical descriptions for the resultant release rate constant - dose profiles were also developed based on the steady state equations and the selected concentration range (or therapeutic window). The effects of absorption (k_a), distribution (k_{12} and k_{21}), elimination (k for one compartment and k_{10} for two compartment), clearance (CL), and the window on the release rate constant - dose profiles were examined. In the case of zero-order systems, a maximum dosage range was observed. This range appears when the duration of the DDS is an integral multiple of the dosing interval. It is dependent only on the window, clearance, and the dosing interval. A minimum required duration was also observed for zero-order systems. This duration can be estimated from the dosing interval, the therapeutic index, and the apparent half-life of the drug candidate. However, in the case of first-order systems, the dosage range increases as the release rate

constant decreases and no maximum dosage range was observed. The utilization of these theories requires values for the micro rate constants, the volume of distribution, the dosing interval and a selected window. The application of these theories to the description of a specific goal in DDS design was also illustrated.

INTRODUCTION

The purpose of a controlled release drug delivery system (DDS) is to control the rate of drug delivery and thereby control the drug concentration at the target site. A well designed system may fail to achieve its clinical goals if the drug which it delivers represents an irrational choice for the performance characteristics of the system. Therefore, defining the required delivery system specifications for a drug candidate can provide an a priori basis for: (1) deciding whether or not to begin formulation work by comparing the required behavior to that achievable by the available technology; (2) establishing the widest range of acceptable performance criteria; and (3) providing a reference standard to measure the degree of success if formulation is undertaken.

Drug disposition is determined by the pharmacokinetic properties of the drug itself. The associated pharmacokinetic parameters can be used to establish quantitative relationships between the rate of administration and the steady state drug concentrations in the plasma. Since this is the basis for the design of controlled release drug delivery systems, the utilization of clinical pharmacokinetic characteristics to define performance specifications is expeditious.

The goal for a controlled release drug delivery system may be to maintain steady state concentrations within a recognized therapeutic window or to duplicate the range encountered with the usual dosage forms on a normal regimen. Repetitively dosing a zero-order DDS at a

dosage interval of τ equal to the duration of the system (T) will provide constant steady state concentrations similar to those obtained by constant-rate i.v. infusion.¹ This product specification is restrictive since it requires a DDS to behave according to $T = D/k_0 = \tau$.

Several reports discuss controlled release drug delivery system design using pharmacokinetic approaches.¹⁻¹¹ However, most of these studies use a single dose plasma concentration time course to define these parameters.²⁻¹⁰ In addition, previous studies used only a one compartment model drug which is released from the delivery system either by a zero-order¹⁻⁷ or a first-order^{4,8-10} process. Nelson², Rowland and Beckett³, Robinson and Eriksen⁴, Dobrinska and Welling⁵ and Kwan⁶ have proposed methods to calculate the zero-order release rate and dose for the maintenance portion of the delivery system and the required instantaneous dose to provide a rapid and constant drug level. However, a single dose plasma concentration time course equation was used and a single product specification, not a range, was defined in all previous reports.¹⁻¹¹

Consequently, certain limitations have been imposed when controlled release drug delivery systems are designed according to the methods proposed by these authors¹⁻¹⁰:

- (1) The use of a single dose equation for the determination of release rate and dosage size may not be adequate when multiple dosing is required.
- (2) The calculated zero-order release pattern and dosage size are

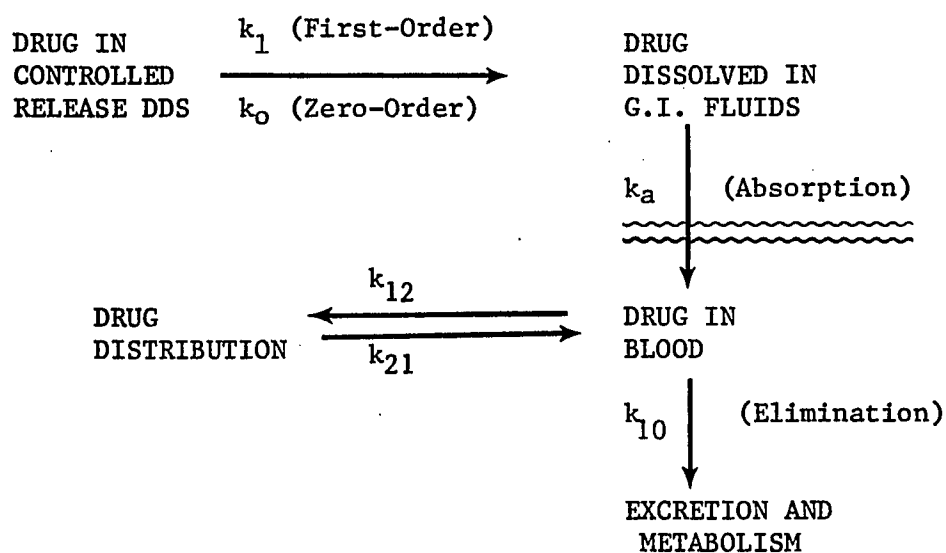
restricted to delivery systems whose functioning duration T is equal to the multiple dosing interval, τ .

The current study avoids these limitations by defining the widest range of product specifications which will satisfy the product goal. The design and evaluation of these delivery systems is based on multiple dosing. The criterion used for an acceptable delivery system is the maintenance of steady state plasma drug concentrations within a desired concentration range, such as the therapeutic window for the drug on a repetitive dosage schedule. Moreover, the functioning duration of the zero-order DDS (T) is not be limited to $T = \tau$. Multiple dose steady-state plasma drug concentration equations have been derived and successfully employed to define the required product specifications by comparing the simulated steady state concentrations to those desired for the drug candidate.

The method involves three steps to define the release rate and dosage size profiles for controlled release drug delivery systems using pharmacokinetic parameters: (1) a mathematical model is established to describe drug release, absorption, distribution, and elimination; (2) the behavior of the drug in each component of the model, and the interdependency of these kinetics, are characterized mathematically; (3) the performance characteristics for the delivery systems are then determined by comparing simulated steady-state plasma concentration-time courses to the desired concentrations and establishing the maximum range of acceptable specifications by reiteration.

THEORETICAL SECTION

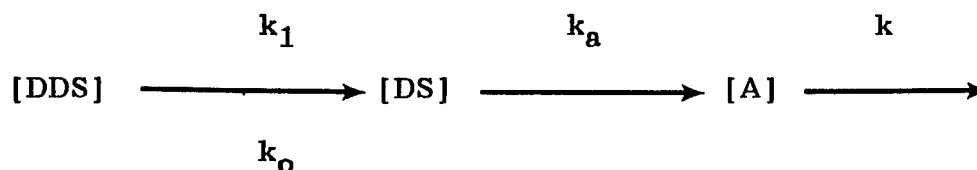
Scheme I represents zero-order (k_0) or first-order (k_1) release from an orally administered drug delivery system, DDS, followed by first-order absorption (k_a) and disposition (k_{12} , k_{21} , and k_{10}).



Scheme I

The amount contained in each phase as a function of time will be designated: $[DDS]$ = drug in the DDS; $[DS]$ = drug in solution in the g.i. tract; $[A1]$ = drug in the central compartment; $[A2]$ = drug in the peripheral compartment.

Scheme II represents the oral administration of a drug described by one compartment model disposition,



Scheme II

where [A] is the amount of drug in the body and k is the elimination rate constant.

In both cases, the bioavailability of dissolved drug [DS] will be assumed to be complete ($F = 1$). This is a reasonable criterion for an oral controlled release drug candidate.¹²

Zero-order Release, General. -- The following assumptions have been invoked to provide all-inclusive solutions. The results are easily translated to more restrictive situations where limiting assumptions apply. Previous investigations have assumed that absorption is much faster than release from the DDS and that T is smaller than the dosage interval, τ . The current treatment places no restrictions on either k_a or T .

In deriving the steady-state equations, it is assumed that all of the drug is eventually released and absorbed. However, when the duration of the device (T) is longer than its gastrointestinal transit time (GIT), part of the dose will be expelled before delivery is complete. This situation is accommodated by presenting results as profiles showing the duration of the drug delivery system versus dose

(T vs D). This allows one to select any GIT value and directly identify from the profiles those products wherein $T \leq GIT$. These profiles also provide a means to define the minimum possible duration which would result in an effective product.

The overall zero-order release rate at any given time, t , depends upon the number of functioning units present. When $t < T$, this number equals the total number of administered doses (n) since none have expired. During each dosing interval, when $t > T$, this number repetitively alternates between the two values $(M + 1)$ and M where

$$T = M(\tau) + \Delta t \quad (1.1)$$

When $T < \tau$, $M = 0$ and $\Delta t = T$. When $T > \tau$, M is a positive integer defined as $M = \text{INT}(T/\tau)$ and the limits for Δt are therefore, $0 \leq \Delta t < \tau$.

Repetitive dosing equations for zero-order systems have therefore been derived under two conditions: $t \leq M(\tau)$ and $t > M(\tau)$. When $t \leq M(\tau)$, each newly administered dose increases the release rate but a single multiple dose equation containing the dose number describes the drug plasma concentration time course. When $t > M(\tau)$, one unit expires at $t' = \Delta t$ during each τ interval where $0 \leq t' \leq \tau$. This requires two separate equations to describe the time course during a dosing interval: one during the period $t' \leq \Delta t$ and another for $t' > \Delta t$.

Two Compartment, Zero-order, n-th Dose, Condition 1: $t < M(\tau)$ --

The total rate of release is nk_0 during the period, $0 < t \leq M(\tau)$, since the number of functioning units equals the total number of administered doses, n . The differential equations for the amount of drug in each site in Scheme I during this period are:

$$-d[DDS]/dt = nk_0 \quad (1.2)$$

$$d[DS]/dt = nk_0 - k_a[DS] \quad (1.3)$$

and those for any time period are

$$d[A1]/dt = k_a[DS] - (k_{12} + k_{10})[A1] + k_{21}[A2] \quad (1.4)$$

$$d[A2]/dt = k_{12}[A1] - k_{21}[A2] \quad (1.5)$$

Equation (1.4) may be solved for the drug concentration in plasma during each dosing interval, $0 \leq t' \leq \tau$:

$$C = \frac{l}{V_1} \left\{ \frac{nk_0 k_{21} k_a}{k_a \alpha \beta} - \frac{k_0 k_a (k_{21} - k_a) (1 - e^{-nk_a \tau})}{k_a (\alpha - k_a) (\beta - k_a) (1 - e^{-k_a \tau})} e^{-k_a t'} - \frac{k_0 k_a (k_{21} - \alpha) (1 - e^{-n\alpha \tau})}{\alpha (k_a - \alpha) (\beta - \alpha) (1 - e^{-\alpha \tau})} e^{-\alpha t'} - \frac{k_0 k_a (k_{21} - \beta) (1 - e^{-n\beta \tau})}{\beta (k_a - \beta) (\alpha - \beta) (1 - e^{-\beta \tau})} e^{-\beta t'} \right\} \quad (1.6)$$

where V_1 is the volume of the central compartment.

Two Compartment, Zero-order, n-th Dose, Condition 2: $t > M(\tau)$ --

When $t > M(\tau)$, one unit expires every time t' reaches Δt . Therefore, $(M + 1)$ units function from $t' = 0$ to Δt and M units function from Δt to τ yielding two release rates: $(M + 1)k_0$ and $(M)k_0$.

Once the condition, $t > M(\tau)$, is satisfied, the same alternating input pattern is repeated during each dosing interval. The dose number corresponding to this constantly repeating input pattern is $j = n - M$ which has an initial value of 1 at $t = M(\tau)$. The initial period during each τ interval, $0 \leq t' \leq \Delta t$, is described by

$$\begin{aligned}
 C = \frac{1}{V_1} & \left\{ \frac{(M+1)k_0k_a k_{21}}{k_a \alpha \beta} - \frac{k_0k_a(k_{21}-k_a)}{k_a(\alpha-k_a)(\beta-k_a)} \left(1 - \frac{e^{-k_a \tau}(e^{k_a(\Delta t)}-1)(1-e^{-(j-2)k_a \tau})}{(1-e^{-k_a \tau})} - e^{-(j-1)k_a \tau}(e^{k_a(\Delta t)}-X_{k_a}) \right) e^{-k_a t'} \right. \\
 & - \frac{k_0k_a(k_{21}-\alpha)}{\alpha(k_a-\alpha)(\beta-\alpha)} \left(1 - \frac{e^{-\alpha \tau}(e^{\alpha(\Delta t)}-1)(1-e^{-(j-2)\alpha \tau})}{(1-e^{-\alpha \tau})} - \frac{e^{-(j-1)\alpha \tau}(e^{\alpha(\Delta t)}-X_{\alpha})}{\beta(k_a-\beta)(\alpha-\beta)} e^{-\alpha t'} - \frac{k_0k_a(k_{21}-\beta)}{\beta(k_a-\beta)(\alpha-\beta)} \left(1 - \frac{e^{-\beta \tau}(e^{\beta(\Delta t)}-1)(1-e^{-(j-2)\beta \tau})}{(1-e^{-\beta \tau})} - e^{-(j-1)\beta \tau}(e^{\beta(\Delta t)}-X_{\beta}) \right) e^{-\beta t'} \right) \left. \right\} \quad (1.7)
 \end{aligned}$$

The terminal period, $\Delta t \leq t' \leq \tau$, is described by

$$\begin{aligned}
 C = \frac{1}{V_1} & \left\{ \frac{Mk_0k_a k_{21}}{k_a \alpha \beta} + \frac{k_0k_a(k_{21}-k_a)}{k_a(\alpha-k_a)(\beta-k_a)} \left(\frac{(e^{k_a(\Delta t)}-1)(1-e^{-(j-1)k_a \tau})}{(1-e^{-k_a \tau})} + \frac{e^{-(j-1)k_a \tau}(e^{k_a(\Delta t)}-X_{k_a})}{\alpha(k_a-\alpha)(\beta-\alpha)} \right) e^{-k_a t'} + \frac{k_0k_a(k_{21}-\alpha)}{\alpha(k_a-\alpha)(\beta-\alpha)} \left(\frac{(e^{\alpha(\Delta t)}-1)(1-e^{-(j-1)\alpha \tau})}{(1-e^{-\alpha \tau})} + e^{-(j-1)\alpha \tau}(e^{\alpha(\Delta t)}-X_{\alpha}) \right) e^{-\alpha t'} + \frac{k_0k_a(k_{21}-\beta)}{\beta(k_a-\beta)(\alpha-\beta)} \left(\frac{(e^{\beta(\Delta t)}-1)(1-e^{-(j-1)\beta \tau})}{(1-e^{-\beta \tau})} + e^{-(j-1)\beta \tau}(e^{\beta(\Delta t)}-X_{\beta}) \right) e^{-\beta t'} \right\} \quad (1.8)
 \end{aligned}$$

where each X factor is $X_i = (1 - e^{-(M+1)i\tau}) / (1 - e^{-i\tau})$ and i represents k_a , α , or β .

Two-Compartment, Zero-order, Steady State. -- These equations will describe steady state drug plasma concentration time courses when $j = \infty$ so that eq. (1.7) becomes

$$C_{SS} = \frac{1}{V_1} \left\{ \frac{(M+1)k_0 k_a k_{21}}{k_a \alpha \beta} - \frac{k_0 k_a (k_{21} - k_a)}{k_a (\alpha - k_a) (\beta - k_a)} \left(1 - \frac{(e^{k_a(\Delta t)} - 1) e^{-k_a \tau}}{(1 - e^{-k_a \tau})} \right) e^{-k_a t'} \right. \\ \left. - \frac{k_0 k_a (k_{21} - \alpha)}{\alpha (k_a - \alpha) (\beta - \alpha)} \left(1 - \frac{(e^{\alpha(\Delta t)} - 1) e^{-\alpha \tau}}{(1 - e^{-\alpha \tau})} \right) e^{-\alpha t'} - \frac{k_0 k_a (k_{21} - \beta)}{\beta (k_a - \beta) (\alpha - \beta)} \left(1 - \frac{(e^{\beta(\Delta t)} - 1) e^{-\beta \tau}}{(1 - e^{-\beta \tau})} \right) e^{-\beta t'} \right\} \quad (1.9)$$

and eq. (1.8) becomes

$$C_{SS} = \frac{1}{V_1} \left\{ \frac{M k_0 k_a k_{21}}{k_a \alpha \beta} + \frac{k_0 k_a (k_{21} - k_a) (e^{k_a(\Delta t)} - 1)}{k_a (\alpha - k_a) (\beta - k_a) (1 - e^{-k_a \tau})} e^{-k_a t'} + \right. \\ \left. \frac{k_0 k_a (k_{21} - \alpha) (e^{\alpha(\Delta t)} - 1)}{\alpha (k_a - \alpha) (\beta - \alpha) (1 - e^{-\alpha \tau})} e^{-\alpha t'} + \frac{k_0 k_a (k_{21} - \beta) (e^{\beta(\Delta t)} - 1)}{\beta (k_a - \beta) (\alpha - \beta) (1 - e^{-\beta \tau})} e^{-\beta t'} \right\} \quad (1.10)$$

One Compartment, Zero-order, Steady State. -- Using the same approach for Scheme II, where commonly employed literature restrictions on T and k_a are again omitted, leads to

$$C^{SS} = \frac{1}{V} \left\{ \frac{(M+1)k_0}{k} - \frac{k_0 k_a}{k_a(k-k_a)} \left(1 - \frac{(e^{k_a(\Delta t)} - 1)e^{-k_a \tau}}{(1-e^{-k_a \tau})} \right) e^{-k_a t'} \right. \\ \left. - \frac{k_0 k_a}{k(k_a-k)} \left(1 - \frac{(e^{k(\Delta t)} - 1)e^{-k \tau}}{(1-e^{-k \tau})} \right) e^{-k t'} \right\} \quad (1.11)$$

when $0 \leq t' \leq \Delta t$ and

$$C^{SS} = \frac{1}{V} \left\{ \frac{Mk_0}{k} + \frac{k_0 k_a e^{k_a(\Delta t)} - 1}{k_a(k-k_a)(1-e^{-k_a \tau})} e^{-k_a t'} + \frac{k_0 k_a (e^{k(\Delta t)} - 1)}{k(k_a-k)(1-e^{-k \tau})} e^{-k t'} \right\} \quad (1.12)$$

when $\Delta t \leq t' \leq \tau$.

First-order Release, General. -- Contrary to zero-order release, a first-order process approaches completion asymptotically making the mathematical solution for the time required to release the full dose approaches ∞ . A practical approach is to consider the effective duration of the DDS as the time required to release some acceptable percentage of the total dose. The influence of the time to deliver a selected fraction of the dose upon the product specifications will be presented later in the discussion.

Two Compartment, First order, Steady State. -- Solving the differential equations for Scheme I, where release is first order, applying the multiple dosing factor¹² and setting $n = \infty$ provides

$$\begin{aligned}
C^{SS} = \frac{k_1 k_a D_0}{V_1} \left\{ \frac{(k_{21} - k_1)}{(k_a - k_1)(\alpha - k_1)(\beta - k_1)(1 - e^{-k_1 \tau})} e^{-k_1 t'} + \right. \\
\frac{(k_{21} - k_a)}{(k_1 - k_a)(\alpha - k_a)(\beta - k_a)(1 - e^{-k_a \tau})} e^{-k_a t'} + \\
\frac{(k_{21} - \alpha)}{(k_1 - \alpha)(k_a - \alpha)(\beta - \alpha)(1 - e^{-\alpha \tau})} e^{-\alpha t'} + \\
\left. \frac{(k_{21} - \beta)}{(k_1 - \beta)(k_a - \beta)(\alpha - \beta)(1 - e^{-\beta \tau})} e^{-\beta t'} \right\} \quad (1.13)
\end{aligned}$$

One Compartment, First order, Steady State. -- Applying the same treatment to Scheme II yields

$$\begin{aligned}
C^{SS} = \frac{k_1 k_a D_0}{V} \left\{ \frac{1}{(k_a - k_1)(k - k_1)(1 - e^{-k_1 \tau})} e^{-k_1 t'} + \right. \\
\frac{1}{(k_1 - k_a)(k - k_a)(1 - e^{-k_a \tau})} e^{-k_a t'} + \left. \frac{1}{(k_1 - k)(k_a - k)(1 - e^{-k \tau})} e^{-k t'} \right\} \quad (1.14)
\end{aligned}$$

EXPERIMENTAL

Reiterative Simulations of Steady State Concentration-Time Courses To Describe DDS Specifications. -- Since eqs. 1.9-1.14 contain both dose size and release rate constants, there exists the possibility for an infinite number of combinations capable of maintaining steady-state concentrations within a selected therapeutic window. These successful combinations can be found using computer simulations by the following procedure.

For a given set of values for τ and the pharmacokinetic parameters in Schemes I or II, eqs. 1.9 - 1.14 are initialized with small values for dose and release rate constants. Resultant steady state levels are then compared to the desired limits (Fig. 1.1). For each release rate constant, the dose size is reiteratively increased and the levels are tested until all successful dose sizes are found. Then the release rate constant value is increased and the process repeated. The resultant release rate-dose profiles (illustrated in Fig. 1.2) can then be employed to choose final product specifications.

RESULTS AND DISCUSSION

Onset of Steady State -- Onset time may be defined as the time required to reach 94% of the steady state concentration which normally requires four times the terminal half-life ($t_{1/2}^*$).¹² The onset for first-order systems was observed to occur at four half lives after initiating the regimen. However, the onset for zero-order systems was found to be four times the biological half-life plus $M(\tau)$ since the release pattern becomes repetitive only after $t = M(\tau)$. Then $(M + 1)k_0$ is operating during $0 \leq t' \leq \Delta t$ and Mk_0 is in effect during $\Delta t \leq t' \leq \tau$.

Verification of Steady State Equations by Comparison to Superposition

Method -- Single dose equations for the four cases represented in Schemes I and II for k_0 and k_1 were derived in the usual manner (Table 1.1) and the method of superposition was used to generate steady state time courses using the computer.¹³ The data points in Fig. 1.1 are steady state concentrations using superposition while the curves are calculated using eqs. 1.9 to 1.14. All tests showed agreement between the two methods thus verifying the validity of eqs. 1.9 to 1.14.

Reiterative Simulations of Steady State Concentrations to Define

Release Rate-Dose Profiles -- Figure 1.2 shows typical release rate constant - dose profiles (delivery profiles) for zero-order and first-order systems as obtained by reiteration of release rate constants and dose sizes in eqs. 1.9 to 1.14 using the therapeutic window and

rate constant values indicated in the figure. The enclosed area represents the release rate constant and dose combinations that can provide steady state concentrations within the therapeutic window. The shapes of these profiles are similar for both Schemes I and II.

Relationship of the Delivery Profiles to the Steady State Plasma

Concentration - Time Courses, Zero-order DDS -- Figure 1.3 shows a zero-order release rate profile and its transformed duration-dose profile (duration profile) for a DDS given every 12 hours with a therapeutic window of 10 to 20 mg/L. Any DDS on curve A-E will provide a steady state minimum concentration equal to the lower limit of the window, $C_{\min}^{SS} = C_{\min} = 10$ mg/L. Any DDS located on curve A-F will provide a steady state maximum concentration equal to the upper limit of the window, $C_{\max}^{SS} = C_{\max} = 20$ mg/L. The Systems described within these boundaries have steady state concentrations which lie within the window without reaching the upper or lower limits. Furthermore, the DDS at position A will produce a steady state concentration profile which traverses the entire window, $C_{\min}^{SS} = C_{\min}$ and $C_{\max}^{SS} = C_{\max}$, since it lies on the intersection of curves A-E and A-F. Those systems located on dotted line E-F all have a duration equal to the dosage interval: $T = \tau = 12$ hours. These will maintain constant steady state concentrations similar to a continuous constant rate i.v. infusion. Each of these examples (A through F) are illustrated in Fig. 1.4.

Relationship of the Delivery Profile to the Steady State Plasma

Concentration - Time Courses; First-order DDS -- Figure 1.5 shows the delivery profile for a first-order release DDS when it is given every 12 hours. Under the conditions given in the figure the resultant correlations with steady state plasma concentration profiles are similar to those produced by zero-order release DDS. Any DDS located on curve A-E will provide $C_{\min}^{SS} = C_{\min}$ while any DDS on curve A-F will result in $C_{\max}^{SS} = C_{\max}$. Furthermore, a system at point A will produce a steady state plasma concentration-time course which traverses the entire window since it is located on the intersection of these two curves (Fig. 1.6). However, unlike the zero-order DDS, there are no first-order systems which can provide constant steady state plasma concentrations.

Basis for Direct Calculation of Release Rate - Dose Profiles -- Assume that a successful DDS must provide steady state concentrations which fall within a desired range; $C_{\min} \leq C^{SS} \leq C_{\max}$. Since curve A-F is associated with C_{\max} (Figs. 1.3 and 1.5) and A-E is associated with C_{\min} , setting $C_{\max}^{SS} = C_{\max}$ and $C_{\min}^{SS} = C_{\min}$ allows direct calculation of the upper and lower dosage boundaries of these rate constant-dose profiles. This calculation requires values for the time of maximum (t_{\max}) and minimum (t_{\min}) concentration during each τ interval. These values can be calculated for the zero-order case in Scheme II and approximated by computer reiterative techniques which solve the equations for $dC^{SS}/dt' = 0$ in the three remaining cases (see section on Derivations). The bisectional method used to solve for t_{\max} and t_{\min}

is a successive approximation similar to that known as Regula Falsi.¹⁴ It locates a root of a function by determining a small interval during which the function changes sign. This direct calculation method of boundaries is demonstrated in the following treatment.

Direct Calculations for Delivery Profiles for Zero-order, Two

Compartment -- For a zero-order DDS described by Scheme I, t_{\min} , the time at which C_{\min}^{SS} occurs, is always during the period 0 to Δt (confirmed in Derivations). Therefore eq. 1.9 can be used to define C^{SS} as follows:

$$C_{\min}^{SS} = \frac{k_0}{V_1} \left\{ \frac{(M+1)}{k_{10}} - \frac{(k_{21}-\alpha)}{\alpha(\beta-\alpha)} \left[1 - \frac{(e^{\alpha(\Delta t)}-1)e^{-\alpha\tau}}{(1-e^{-\alpha\tau})} \right] e^{-\alpha t_{\min}} - \frac{(k_{21}-\beta)}{\beta(\alpha-\beta)} \left[1 - \frac{(e^{\beta(\Delta t)}-1)e^{-\beta\tau}}{(1-e^{-\beta\tau})} \right] e^{-\beta t_{\min}} \right\} \quad (1.15)$$

where t_{\min} is expressed in terms of t' . Substituting C_{\min} for C_{\min}^{SS} in eq. 1.15 provides $k_0(\min)$, the minimum zero-order release rate, for a DDS of specified duration is defined by eq. 1.16.

$$k_0(\min) = \{C_{\min}V_1\} \div \left\{ \frac{(M+1)}{k_{10}} - \frac{(k_{21}-\alpha)}{\alpha(\beta-\alpha)} \left[1 - \frac{(e^{\alpha(\Delta t)}-1)e^{-\alpha\tau}}{(1-e^{-\alpha\tau})} \right] e^{-\alpha t_{\min}} - \frac{(k_{21}-\beta)}{\beta(\alpha-\beta)} \left[1 - \frac{(e^{\beta(\Delta t)}-1)e^{-\beta\tau}}{(1-e^{-\beta\tau})} \right] e^{-\beta t_{\min}} \right\} \quad (1.16)$$

Since $D = k_0T = k_0[M(\tau) + \Delta t]$, the minimum required dose, D_{\min} may be calculated from $k_0(\min)[M(\tau) + \Delta t]$, which follow from eq. 1.16:

$$D_{\min} = \{C_{\min}V_1(M\tau + \Delta t)\} \div \left\{ \frac{(M+1)}{k_{10}} - \frac{(k_{21}-\alpha)}{\alpha(\beta-\alpha)} \left[1 - \frac{(e^{\alpha(\Delta t)}-1)e^{-\alpha\tau}}{(1-e^{-\alpha\tau})} \right] e^{-\alpha t_{\min}} \right. \\ \left. - \frac{(k_{21}-\beta)}{\beta(\alpha-\beta)} \left[1 - \frac{(e^{\beta(\Delta t)}-1)e^{-\beta\tau}}{(1-e^{-\beta\tau})} \right] e^{-\beta t_{\min}} \right\} \quad (1.17)$$

These equations require reiterative computer techniques to establish the true value for t_{\min} . Simplified equations were also developed using the approximation, $t_{\min} = 0$, based on the observation that t_{\min} is close to 0 because: (1) the release rate increases when a new dose is introduced at $t' = 0$ and (2) the C_{\min}^{SS} value calculated from eq. 1.15 using the true t_{\min} value is greater than or equal to that approximated by setting $t_{\min} = 0$. Consequently, eqs. 1.16 and 1.17 can be simplified to:

$$k_o(\min) = \{C_{\min}V_1\} \div \left\{ \frac{(M+1)}{k_{10}} - \frac{(k_{21}-\alpha)}{\alpha(\beta-\alpha)} \left[1 - \frac{(e^{\alpha(\Delta t)}-1)e^{-\alpha\tau}}{(1-e^{-\alpha\tau})} \right] \right. \\ \left. - \frac{(k_{21}-\beta)}{\beta(\alpha-\beta)} \left[1 - \frac{(e^{\beta(\Delta t)}-1)e^{-\beta\tau}}{(1-e^{-\beta\tau})} \right] \right\} \quad (1.18)$$

$$D_{\min} = \{C_{\min}V_1(M\tau + \Delta t)\} \div \left\{ \frac{(M+1)}{k_{10}} - \frac{(k_{21}-\alpha)}{\alpha(\beta-\alpha)} \left[1 - \frac{(e^{\alpha(\Delta t)}-1)e^{-\alpha\tau}}{(1-e^{-\alpha\tau})} \right] \right. \\ \left. - \frac{(k_{21}-\beta)}{\beta(\alpha-\beta)} \left[1 - \frac{(e^{\beta(\Delta t)}-1)e^{-\beta\tau}}{(1-e^{-\beta\tau})} \right] \right\} \quad (1.19)$$

Therefore the $k_o(\min)$ and D_{\min} values can be estimated for any chosen duration, $T = [M(\tau) + \Delta t]$, since the remaining variables in

eqs. 1.18 and 1.19 are pharmacokinetic parameters of the drug itself. The error is small and always errors on the safe side as shown later.

Applying reiterative computer techniques to establish the t_{\max} values, substituting in eq. 1.10 and applying the condition, $C_{\max}^{SS} = C_{\max}$, leads to

$$k_o(\max) = \{C_{\max}V_1\} \div \left\{ \frac{M}{k_{10}} + \frac{(k_{21}-\alpha)(e^{\alpha(\Delta t)}-1)}{\alpha(\beta-\alpha)(1-e^{-\alpha\tau})} e^{-\alpha t_{\max}} + \frac{(k_{21}-\beta)(e^{\beta(\Delta t)}-1)}{\beta(\alpha-\beta)(1-e^{-\beta\tau})} e^{-\beta t_{\max}} \right\} \quad (1.20)$$

$$D_{\max} = \{C_{\max}V_1(M\tau+\Delta t)\} \div \left\{ \frac{M}{k_{10}} + \frac{(k_{21}-\alpha)(e^{\alpha(\Delta t)}-1)}{\alpha(\beta-\alpha)(1-e^{-\alpha\tau})} e^{-\alpha t_{\max}} + \frac{(k_{21}-\beta)(e^{\beta(\Delta t)}-1)}{\beta(\alpha-\beta)(1-e^{-\beta\tau})} e^{-\beta t_{\max}} \right\} \quad (1.21)$$

Simplified equations were developed using the approximation, $t_{\max} = \Delta t$, based on the observations that t_{\max} is close to Δt since: (1) the number of functioning units decreases from $(M + 1)$ to M at Δt and (2) the true C_{\max}^{SS} is less than or equal to that approximated using $t_{\max} = \Delta t$. Equations 1.20 and 1.21 were thus simplified to

$$k_o(\max) = \{C_{\max}V_1\} \div \left\{ \frac{M}{k_{10}} + \frac{(k_{21}-\alpha)(1-e^{-\alpha(\Delta t)})}{\alpha(\beta-\alpha)(1-e^{-\alpha\tau})} + \frac{(k_{21}-\beta)(1-e^{-\beta(\Delta t)})}{\beta(\alpha-\beta)(1-e^{-\beta\tau})} \right\} \quad (1.22)$$

$$D_{\max} = \{C_{\max}V_1(M\tau+\Delta t)\} \div \left\{ \frac{M}{k_{10}} + \frac{(k_{21}-\alpha)(1-e^{-\alpha(\Delta t)})}{\alpha(\beta-\alpha)(1-e^{-\alpha\tau})} + \frac{(k_{21}-\beta)(1-e^{-\beta(\Delta t)})}{\beta(\alpha-\beta)(1-e^{-\beta\tau})} \right\} \quad (1.23)$$

Direct Calculations of Delivery Profiles for Zero-order, One

Compartment -- Applying the same approach used for the two compartment zero-order DDS, the minimum and maximum required release rates and doses for each specific duration for a DDS which behaves according to Scheme II can be described by eqs. 1.24 to 1.29 based on the computer-calculated values for t_{\min} and t_{\max} :

$$t_{\min} = \ln\left(\frac{1 - (e^{k_a(\Delta t)} - 1)e^{-k_a\tau}/(1 - e^{-k_a\tau})}{1 - (e^{k(\Delta t)} - 1)e^{-k\tau}/(1 - e^{-k\tau})}\right) \div (k_a - k) \quad (1.24)$$

$$t_{\max} = \ln\left(\frac{(e^{k_a(\Delta t)} - 1)/(1 - e^{-k_a\tau})}{(e^{k(\Delta t)} - 1)/(1 - e^{-k\tau})}\right) \div (k_a - k) \quad (1.25)$$

$$k_o(\min) = \{C_{\min}CL\} \div \left\{ (M+1) - \left[1 - \frac{(e^{k(\Delta t)} - 1)e^{-k\tau}}{(1 - e^{-k\tau})} \right] e^{-kt_{\min}} \right\} \quad (1.26)$$

$$D_{\min} = \{C_{\min}CL(M\tau + \Delta t)\} \div \left\{ (M+1) - \left[1 - \frac{(e^{k(\Delta t)} - 1)e^{-k\tau}}{(1 - e^{-k\tau})} \right] e^{-kt_{\min}} \right\} \quad (1.27)$$

$$k_o(\max) = \{C_{\max}CL\} \div \left\{ M + \frac{(e^{k(\Delta t)} - 1)}{(1 - e^{-k\tau})} e^{-kt_{\max}} \right\} \quad (1.28)$$

$$D_{\max} = \{C_{\max}CL(M\tau + \Delta t)\} \div \left\{ M + \frac{(e^{k(\Delta t)} - 1)}{(1 - e^{-k\tau})} e^{-kt_{\max}} \right\} \quad (1.29)$$

Simplified equations were also developed using the approximations $t_{\min} = 0$ and $t_{\max} = \Delta t$ based on observations similar to those described for the two compartment zero-order DDS. In this way, eqs. 1.26 to 1.29 were simplified to eqs. 1.30 to 1.33.

$$k_o(\min) = \{C_{\min}CL\} \div \left\{ (M+1) - \left[1 - \frac{(e^{k(\Delta t)} - 1)e^{-k\tau}}{(1 - e^{-k\tau})} \right] \right\} \quad (1.30)$$

$$D_{\min} = \{C_{\min}CL(M\tau + \Delta t)\} \div \left\{ (M+1) - \left[1 - \frac{(e^{k(\Delta t)} - 1)e^{-k\tau}}{(1 - e^{-k\tau})} \right] \right\} \quad (1.31)$$

$$k_o(\max) = \{C_{\max}CL\} \div \left\{ M + \frac{(1 - e^{-k(\Delta t)})}{(1 - e^{-k\tau})} \right\} \quad (1.32)$$

$$D_{\max} = \{C_{\max}CL(M\tau + \Delta t)\} \div \left\{ M + \frac{(1 - e^{-k(\Delta t)})}{(1 - e^{-k\tau})} \right\} \quad (1.33)$$

Direct Calculations of Delivery Profiles for First-order, Two

Compartment -- Using the eq. 1.13, after substituting C_{\min} and C_{\max} for C_{\min}^{ss} and C_{\max}^{ss} , the minimum and maximum dose size for a given k , can be defined by eqs. 1.34 and 1.35 using the t_{\min} and t_{\max} values obtained by computer reiterations.

$$\begin{aligned}
D_{\min} = \left\{ \frac{C_{\min} V_1}{k_1 k_a} \right\} \div \left\{ \frac{(k_{21} - k_1)}{(k_a - k_1)(\alpha - k_1)(\beta - k_1)(1 - e^{-k_1 \tau})} e^{-k_1 t_{\min}} + \right. \\
\frac{(k_{21} - k_a)}{(k_1 - k_a)(\alpha - k_a)(\beta - k_a)(1 - e^{-k_a \tau})} e^{-k_a t_{\min}} + \\
\frac{(k_{21} - \alpha)}{(k_1 - \alpha)(k_a - \alpha)(\beta - \alpha)(1 - e^{-\alpha \tau})} e^{-\alpha t_{\min}} + \\
\left. \frac{(k_{21} - \beta)}{(k_1 - \beta)(k_a - \beta)(\alpha - \beta)(1 - e^{-\beta \tau})} e^{-\beta t_{\min}} \right\} \quad (1.34)
\end{aligned}$$

$$\begin{aligned}
D_{\max} = \left\{ \frac{C_{\max} V_1}{k_1 k_a} \right\} \div \left\{ \frac{(k_{21} - k_1)}{(k_a - k_1)(\alpha - k_1)(\beta - k_1)(1 - e^{-k_1 \tau})} e^{-k_1 t_{\max}} + \right. \\
\frac{(k_{21} - k_a)}{(k_1 - k_a)(\alpha - k_a)(\beta - k_a)(1 - e^{-k_a \tau})} e^{-k_a t_{\max}} + \\
\frac{(k_{21} - \alpha)}{(k_1 - \alpha)(k_a - \alpha)(\beta - \alpha)(1 - e^{-\alpha \tau})} e^{-\alpha t_{\max}} + \\
\left. \frac{(k_{21} - \beta)}{(k_1 - \beta)(k_a - \beta)(\alpha - \beta)(1 - e^{-\beta \tau})} e^{-\beta t_{\max}} \right\} \quad (1.35)
\end{aligned}$$

Since the controlled release of drug should be the rate-limiting step relative to absorption ($k_1 \ll k_a$), t_{\min} can be approximated as zero. However, t_{\max} must be reiteratively determined by computer methods. Therefore, approximate equations were not examined as substitutes for eqs. 1.34 and 1.35.

Direct Calculation of Delivery Profiles for First-order, One

Compartment -- The minimum and maximum required doses for each first-order release rate constant can be calculated from eq. 1.14 by substituting the t_{\min} and t_{\max} values to give:

$$D_{\min} = \frac{C_{\min}V}{k_1 k_a} \left\{ \frac{1}{(k_a - k_1)(k - k_1)(1 - e^{-k_1 \tau})} e^{-k_1 t_{\min}} + \frac{1}{(k_1 - k_a)(k - k_a)(1 - e^{-k_a \tau})} e^{-k_a t_{\min}} + \frac{1}{(k_1 - k)(k_a - k)(1 - e^{-k \tau})} e^{-k t_{\min}} \right\} \quad (1.36)$$

$$D_{\max} = \frac{C_{\max}V}{k_1 k_a} \left\{ \frac{1}{(k_a - k_1)(k - k_1)(1 - e^{-k_1 \tau})} e^{-k_1 t_{\max}} + \right. \\ \left. \frac{1}{(k_1 - k_a)(k - k_a)(1 - e^{-k_a \tau})} e^{-k_a t_{\max}} + \right. \\ \left. \frac{1}{(k_1 - k)(k_a - k)(1 - e^{-k \tau})} e^{-k t_{\max}} \right\} \quad (1.37)$$

Verification of Boundary Equations for Delivery Profiles by Comparison to Simulation Method -- Typical boundaries for delivery profiles

calculated by eqs. 1.16 to 1.37 are shown in Figs. 1.7-1.10. Solid curves represent the boundaries determined using the t_{\min} and t_{\max} values. The dashed curves represent boundaries calculated using the approximate t_{\min} and t_{\max} values. The data points were determined by the simulation method. In all cases, good agreement between these three methods verified the validity of eqs. 1.16 to 1.37. The profiles determined with approximate t_{\min} and t_{\max} values showed minor differences compared to those determined by the other two methods. However, the differences are small and the estimates describe a slightly reduced profile which is contained within the profile described by simulations for successful systems.

Since the equations for zero-order systems do not restrict duration (T) relative to τ , this unique approach can define performance specifications for systems of any T. Figure 1.11 shows a typical duration profile for durations up to 4τ . However, for an orally administered DDS, a practical limit is imposed on the duration by the gastrointestinal transit time. The following discussions for oral zero-order DDS will be limited to those systems where $\tau = 12$ hours and the duration is less than or equal to 2τ . Any estimated G.I. transit time less than 24 hours can be accommodated using the resultant profiles.

In order to better understand the delivery profiles and the duration profiles, those factors which influence their boundaries were investigated.

Influence of Therapeutic Window on the Zero-order Duration Profiles --

As shown in Fig. 1.12, the duration profile is reduced when the therapeutic window is reduced. The D_{\max} and D_{\min} for a DDS of specified duration is proportional to the C_{\max} and C_{\min} as shown by eqs. 1.21 and 1.17. It was found that the minimum required duration (T_{\min}) observed on any duration profile was dependent upon the therapeutic index (T.I.), or C_{\max}/C_{\min} . The T_{\min} for a successful DDS increased when the T.I. was reduced (Table 1.2). In addition, the observed T_{\min} values are in agreement with those predicted by $T_{\min} = \tau - \ln(C_{\max}/C_{\min})/k$ or $T_{\min} = \tau - \ln(C_{\max}/C_{\min})/\beta$ provided that the β -phase is predominant during $t' > t_{\max}$.

Influence of Absorption on the Zero-Order Duration Profiles -- For a long-acting orally administered DDS, release should be the rate-limiting step. If absorption is rate-determining, the delivery of drug to the blood will not be controlled by the DDS. As indicated in Fig. 1.13, the duration profile for a successful delivery system is reduced as the absorption rate constant, k_a , is increased if k_a is involved in the plasma time course. When k_a is increased, the T_{\min} values increase and the dose range decreases except for the unique case where T , the duration, is equal to τ (or its integer multiples). When $T=n\tau$, the maximum dose range is independent of k_a . Once k_a increases beyond a certain value, further increase will not change the profile. Then the profiles are identical to those described by eqs. 1.18, 1.19, 1.22, and 1.23 wherein release is rate limiting. Such a profile represents the best goal for zero-order DDS design since this profile is governed by the behavior of the DDS.

Influence of Distribution on the Zero-Order Duration Profiles -- The influence of apparent volume of distribution was simulated by examining the effect of changing the k_{21}/k_{12} values. As shown in Fig. 1.14, T_{\min} is increased when the k_{21}/k_{12} ratio is increased. The dose range for a DDS with a specified T is decreased when k_{21}/k_{12} is increased except for the special case, $T = n\tau$, where the dose range remains constant and independent of k_{21}/k_{12} .

Influence of Elimination on the Zero-Order Duration Profiles -- The influence of elimination on the product specifications for successful

delivery systems was investigated by changing the values for total body clearance (CL) and biological half-life ($t_{1/2}$).

In the case of Scheme I, this was implemented by changing the k_{10} values. As the clearance value increases (with concomitant decrease in half-life), the dose and minimum required duration also increase (Fig. 1.15). However, the observed required dose is not directly proportional to the clearance value except when the duration is an integral multiple of τ . This special case ($T=n\tau$) can be verified by setting $\Delta t = 0$ in eqs. 1.17 and 1.21 to give the following equations.

$$D_{\min}^{T=n\tau} = (C_{\min})(CL)(\tau) \quad (1.38)$$

$$D_{\max}^{T=n\tau} = (C_{\max})(CL)(\tau) \quad (1.39)$$

For the other conditions ($T \neq n\tau$), both the dosage sizes and ranges are complicated functions of CL and Δt .

The observed increase in required dose can be explained by the fact that the body eliminates the drug more rapidly when the clearance is increased. As a result, delivery systems designed for drugs with large clearance values may require payloads which are too large to be incorporated into the device.

In contrast, the minimum required duration increases as the biological half-life decreases and clearance increases (Fig. 1.15). However, when the half-life is kept constant while increasing CL (by changing k_{10} , k_{21} , and k_{12}), T_{\min} is maintained nearly constant (Fig. 1.16). Thus the T_{\min} is apparently related to the half-life value rather than to clearance.

The steady state time course for a successful DDS with $T = T_{\min}$ will transverse the entire therapeutic window resulting in $C_{\min}^{SS} = C_{\min}$ and $C_{\max}^{SS} = C_{\max}$. In addition, since t_{\min} may be approximated by $t' = 0$ (or τ) and t_{\max} is approximately $t' = \Delta t$, the time period following C_{\max}^{SS} can be approximated by $\tau - \Delta t$. If the concentration time course during $t' > \Delta t$ is approximated by monoexponential loss, the maximum time for this phase can be approximated by $t_f = -\ln(C_{\min}/C_{\max})/\beta$. Consequently, the minimum required duration for a successful zero-order DDS can be approximated by:

$$T_{\min} = \tau - t_f \quad (1.40)$$

This approximation provides a good estimate for a one compartment zero-order DDS when k_a is not rate limiting. A reasonable estimate is obtained for a two compartment zero-order DDS, when the model collapses to approach that of a one compartment model¹³ (Table 1.3).

Comparison of Zero-order Duration Profiles Between One and Two

Compartment Models -- The duration profiles for one and two compartment models are similar in shape provided that the therapeutic window, clearance and dosage intervals are kept constant. The observed maximum dosage size ranges are then identical and the values can be calculated using eqs. 1.38 and 1.39. The minimum required durations are also similar but not always equal. However, values used for k_{12} and k_{21} in the two compartment model can produce a slightly different duration profile compared to the one compartment model.

As observed in Fig. 1.17, the difference between a one compartment model and its corresponding two compartment model (same CL and $t_{1/2}$) becomes insignificant when k_{21} becomes sufficiently larger than k_{10} . As $k_{21} \gg k_{10}$, the equilibration between central and peripheral compartments becomes sufficiently fast to produce a collapse of the two compartment behavior to that of one compartment.¹³ However, k_{12} does not have a similar effect (Fig. 1.18). As k_{12} becomes larger, the peripheral compartment begins to behave as a second reservoir for the drug.

Determination of Drug Candidacy for Zero-order DDS -- It is both prudent and expedient to establish a priori information regarding the suitability of a particular drug for a DDS. Without the benefit of the current theory, Notari¹² has suggested that half-life is one primary concern for a priori evaluation of drug candidacy. A drug with a long half-life will not require a long acting DDS. On the other hand, a short half-life drug may impose technical difficulties due to the large amount of drug needed to be incorporated in the device. In addition, as shown in Fig. 1.15, a short half-life drug will require a larger T_{\min} thus reducing the tolerance in range of acceptable values for duration.

In the previous discussions, eq. 1.40 was used to estimate T_{\min} for zero-order DDS. Rewriting this equation in terms of the half-life provides:

$$T_{\min} = \tau - [t_{1/2} \ln(C_{\max}/C_{\min})/0.693] \quad (1.41)$$

In addition to either determining T_{\min} from the duration profiles or estimating it from eqs. 1.40 and 1.41, T_{\min} values can also be estimated from plots of the dosage form index (D.I.) versus the DDS duration (Fig. 1.19). The D.I. (as defined by Theeuwes and Bayne¹⁵) is the ratio of the maximum to minimum steady state plasma concentration. This index represents the fluctuation in the steady state time course.

Curves representing D.I. vs. duration can be used to estimate T_{\min} values for a zero-order DDS which would maintain steady state levels within the required window for various biological half-life values. The utilization of these curves can be achieved by first choosing the desired therapeutic index. Since T.I., the chosen therapeutic index, represents the maximum D.I. value for the DDS, a line where D.I. = T.I. (parallel to the x axis) will intersect the curves at the minimum required duration (T_{\min}) for a DDS containing a drug of that $t_{1/2}$. All of those systems having D.I. values less than or equal to this T.I. value will be acceptable. Therefore, the greater the portion of the curve below the D.I. = T.I. line, the wider the range of choices and the better the drug candidate.

For example, assuming that the therapeutic window is 10 to 20 mg/L yields a T.I. value of 2. Assuming that $\tau = 12$ hours, the intersection of curve A for $t_{1/2} = (\tau/12) = 1$ hour and the D.I. = 2 line occurs at $T = 11$ hours. Thus a drug with a one hour half-life will have a T_{\min} value of 11 hours. For the other half-lives

illustrated, the T_{\min} values are 10, 9, 8, and 6 hours when $t_{1/2} = 2, 3, 4,$ and 6 hours respectively. All of the curves converge at the value $D.I. = 1$ which is the resulting ratio during the constant steady state concentrations observed when $T = \tau$

Influence of Therapeutic Window on the First-Order Delivery Profile --

Figure 1.20 shows the delivery profiles for first-order release systems using five different therapeutic windows. As previously observed for zero-order release, increasing the therapeutic window increases both the dosage size and range for a DDS with a specified release rate constant. This increase in the required dose is proportional to the increase in the size of the window. However, the maximum release rate constant is dependent only upon the therapeutic index and independent of the absolute values for C_{\min} and C_{\max} .

Influence of Absorption on the First-Order Delivery Profile --

Figure 1.21 shows delivery profiles for a first-order DDS combined with various absorption rate constants. When k_a increases, the maximum release rate and the dose range both decrease. However, the profiles approach a constant boundary when k_a becomes sufficiently large to ensure that release is rate limiting.

Influence of Elimination on the First-Order Delivery Profiles --

Figure 1.22 shows the effect of k , the elimination rate constant, on the profiles for first-order drug delivery. As k increases, the required dose increases while the maximum release rate constant decreases. This can affect the feasibility for designing a first-order

release DDS in two ways. First, the dose size may become too large to be incorporated into a single unit when the candidate is rapidly eliminated (large k). On the other hand, the combination of a slow release rate constant and a large dose may result in reduced bioavailability owing to expulsion from the G.I. tract. As illustrated, the maximum release rate constant for a candidate with $k = 0.51 \text{ h}^{-1}$ is 0.1 h^{-1} . Assuming the GIT is 12 hours, only 70% of the drug is released from the DDS during this time.

Defining Specifications for Zero-order DDS Design -- The broader the product specification goals, the greater is the likelihood for success in developing a controlled release device. There are two considerations defined by the duration profiles: (1) duration, which is a function of release rate; (2) dosage range, which governs the final product sizes and therefore clinical flexibility. If the widest dosage range is considered, maximum dose range, then the maximum flexibility in product size is obtained. However, in that case the DDS must release its payload uniformly over the exact dosage interval ($T=\tau$). Conversely, if the widest range for the duration is employed, then the acceptable payload range is minimized. The duration profiles can be used to reach a compromise between these two conflicting limitations as illustrated below.

The selection of a dosage size and duration for a twice a day DDS is illustrated in Fig. 1.23. If the maximum dose range is selected as the primary consideration (Fig. 1.23A), the DDS will be required to

uniformly deliver its contents over a period of 12 hours with a release pattern such as that shown in Fig. 1.23B. Although maximum product size flexibility is obtained, this restriction on the release pattern will make formulation difficult and also predispose to clinical failure when products do not perform within this narrow range. On the other hand, the widest range of duration, as shown in Fig. 1.23D, allows specifications for uniform release of the entire contents within the range of 6 to 12 hours. But then only a narrow dosage range would be considered as adequate (Fig. 1.23C). Some compromise must be made to minimize these limitations on the duration and dose range. Figures 1.23E and F represent one such set of choices. Here, a DDS which can uniformly release its contents within 8 to 11 hours shows reasonable flexibility in both the release pattern and also the dosage range.

Thus, in order to provide a broader target for DDS design, the duration and dosage range must be optimized. Neither of the extreme cases, i.e. the widest dosage range or duration range, represent the most feasible specifications since maximizing one range will restrict the other. The goal should provide reasonable flexibility in both the duration and dosage range.

Since intersubject variability in clearance is generally expected, different dosage sizes, ranges, and T_{\min} values are required in clinical practice. An ideal DDS should provide the necessary flexibility to accommodate all the patients. The minimum duration

therefore has to be greater than or equal to the longest required T_{\min} value in a patient population. As illustrated in Fig. 1.24, patients A, B and C have different clearance values thus producing three different duration profiles. Based on these three profiles, a duration of 10 to 12 hours would satisfy the T_{\min} for all three patients. For this release pattern, patient A requires a dose size range of 69-102 mg, B 150-196 mg and C 245-286 mg. The ideal payload for a DDS should accommodate these required dose ranges by changing the number of units administered. As a result, a 90 mg product of 10-12 hour duration is one choice which provides successful therapy for all three patients by administering 1, 2 or 3 doses every 12 hours.

Defining Specifications for First-order DDS Design - In contrast to a zero-order system, 100% delivery from a first-order system occurs as time approaches infinity. Since $t_f = -\ln(1-f)/k_1$, the selected fraction to be released during a given time interval will determine the minimum allowable k_1 value as shown in Table 1.4. The minimum practical release rate constant will depend upon the fraction (f) selected to be released during a specified time (t_f) and the release rate constant vs. dose profile. The selected values can be used to evaluate the number of subjects in a group which may be treated with a given DDS. For example, the 80% and 95% delivery values associated with $t_f = 12$ hours have been entered as dashed lines in Fig. 1.22. At 95% release in 12 hours, only patient A may be treated with the product while at 80%, A, B and C but not D may be treated. In order to treat all four patients, a k_1 value of 0.1 h^{-1} is required which corresponds to only

70% delivery in 12 hours. This would predispose to bioavailability problems. The determination of payloads and dosage ranges is similar to that discussed under the zero order systems.

CONCLUSIONS

A traditional solution for the design of a zero-order controlled release drug delivery system has been to make T , the duration, equal to τ , the dosing interval. This restrictive product specification requires a DDS to behave according to $T = D/k_0 = \tau$. This report employs clinical pharmacokinetics to define a wide range of product specifications for a DDS (zero-order and first-order) which can provide steady state concentrations within a desired range during repetitively dosing schedules. In addition, this study did not apply any restrictions on the duration of the delivery system. Therefore, it provides specifications for a zero-order DDS not only when $T = \tau$, but also when $T < \tau$ and $T > \tau$.

The delivery profiles and duration profiles thus defined provide the widest acceptable range of product specifications. The utilization of these theories requires the pharmacokinetic micro rate constants for the drug candidate and the selection of a desired steady state plasma concentration. In addition, the theories allow a priori feasibility assessment for designing a DDS by comparison of the calculated performance specifications to the available technology.

For a zero-order DDS, the method provides a means to calculate T_{\min} , the minimum required duration, for a DDS to be successful. Furthermore, the method can also provide information on the maximum potential dosage range. These two sets of information can then be used to determine the suitability of the drug candidate for the DDS.

For example, a short half-life drug will require a large dose size which may be impossible to incorporate into the device. Also, it will require a high T_{\min} value close to or equal to τ which limits the flexibility of the duration selection. Consequently, it may be a poor candidate. However, for a first-order DDS, the candidacy of the drug can be determined by examining either the required dose size or by comparing the acceptable release rate constant, k_1 , to the minimum required release rate constant. This is defined as the rate constant which will release a certain fraction of the dose during a selected time period.

Since various subjects may represent different pharmacokinetic behavior for a single drug, the individual pharmacokinetic constants used in the design calculations for a DDS should be representative of all the individual patient requirements. This will restrict the range of the design of an adequate DDS. For example, different T_{\min} values exist for different individuals when a zero-order DDS is examined. The ideal DDS would require a duration that is longer than the largest T_{\min} value among a group of subjects. Therefore, individual pharmacokinetic data for a number of subjects which represent the population are required for the design. In addition, the selection of the product specifications will also depend on the percentage of patients to be satisfied. Since the current theories provide information on the individual requirements based on the delivery profiles and duration profiles, the influence of patient variability, (such as the intersubject variability in the clearance) can be

considered a priori. The ideal DDS which would accommodate this variability could then be defined.

DERIVATIONS

Mathematical Derivation of Boundaries for Delivery Profiles Using Two Compartment Zero-order Release DDS as Example

The steady state plasma concentration - time course during the $(M+1)k_0$ phase ($0 \leq t < \Delta t$) can be described by eq. 1.42.

$$\begin{aligned}
 C^{SS} = \frac{1}{V_1} \left\{ \frac{(M+1)k_0 k_a k_{21}}{k_a \alpha \beta} - \frac{k_0 k_a (k_{21} - k_a)}{k_a (\alpha - k_a) (\beta - k_a)} \left(1 - \frac{(e^{k_a (\Delta t)} - 1) e^{-k_a \tau}}{(1 - e^{-k_a \tau})} \right) e^{-k_a t'} \right. \\
 - \frac{k_0 k_a (k_{21} - \alpha)}{\alpha (k_a - \alpha) (\beta - \alpha)} \left(1 - \frac{(e^{\alpha (\Delta t)} - 1) e^{-\alpha \tau}}{(1 - e^{-\alpha \tau})} \right) e^{-\alpha t'} \\
 \left. - \frac{k_0 k_a (k_{21} - \beta)}{\beta (k_a - \beta) (\beta - \alpha)} \left(1 - \frac{(e^{\beta (\Delta t)} - 1) e^{-\beta \tau}}{(1 - e^{-\beta \tau})} \right) e^{-\beta t'} \right\} \quad (1.42)
 \end{aligned}$$

Since the C_{min}^{SS} appears during this phase, the first derivative of eq. 1.42 at $t' = t_{min}$ will equal to 0, i.e.,

$$\begin{aligned}
 \frac{k_0 k_a (k_{21} - k_a)}{(\alpha - k_a) (\beta - k_a)} \left[1 - \frac{(e^{k_a (\Delta t)} - 1) e^{-k_a \tau}}{(1 - e^{-k_a \tau})} \right] e^{-k_a t_{min}} + \frac{k_0 k_a (k_{21} - \alpha)}{(k_a - \alpha) (\beta - \alpha)} \left[1 - \frac{(e^{\alpha (\Delta t)} - 1) e^{-\alpha \tau}}{(1 - e^{-\alpha \tau})} \right] e^{-\alpha t_{min}} \\
 + \frac{k_0 k_a (k_{21} - \beta)}{(k_a - \beta) (\alpha - \beta)} \left[1 - \frac{(e^{\beta (\Delta t)} - 1) e^{-\beta \tau}}{(1 - e^{-\beta \tau})} \right] e^{-\beta t_{min}} = 0 \quad (1.43)
 \end{aligned}$$

Therefore, C_{min}^{SS} can be expressed as eq. 1.44 when t' in eq. 1.42 is replaced by t_{min} and then being simplified further by using the relationship shown in eq. 1.43 and $\alpha \beta = (k_{10})(k_{21})$.

$$C_{\min}^{SS} = \frac{1}{V_1} \left\{ \frac{(M+1)k_0}{k_{10}} - \frac{k_0(k_{21}-\alpha)}{\alpha(\beta-\alpha)} \left(1 - \frac{(e^{\alpha(\Delta t)}-1)e^{-\alpha\tau}}{(1-e^{-\alpha\tau})} \right) e^{-\alpha t_{\min}} \right. \\ \left. - \frac{k_0(k_{21}-\beta)}{\beta(\beta-\alpha)} \left(1 - \frac{(e^{\beta(\Delta t)}-1)e^{-\beta\tau}}{(1-e^{-\beta\tau})} \right) e^{-\beta t_{\min}} \right\} \quad (1.44)$$

For a successful zero-order released drug delivery system, the C_{\min}^{SS} has to be greater than or equal to the lower limit of the therapeutic window, C_{\min} . Therefore,

$$C_{\min}^{SS} = \frac{1}{V_1} \left\{ \frac{(M+1)k_0}{k_{10}} - \frac{k_0(k_{21}-\alpha)}{\alpha(\beta-\alpha)} \left(1 - \frac{(e^{\alpha(\Delta t)}-1)e^{-\alpha\tau}}{(1-e^{-\alpha\tau})} \right) e^{-\alpha t_{\min}} \right. \\ \left. - \frac{k_0(k_{21}-\beta)}{\beta(\beta-\alpha)} \left(1 - \frac{(e^{\beta(\Delta t)}-1)e^{-\beta\tau}}{(1-e^{-\beta\tau})} \right) e^{-\beta t_{\min}} \right\} \geq C_{\min} \quad (1.45)$$

Consequently,

$$k_0 \geq \{C_{\min}V_1\} \div \left\{ \frac{(M+1)k_0}{k_{10}} - \frac{k_0(k_{21}-\alpha)}{\alpha(\beta-\alpha)} \left(1 - \frac{(e^{\alpha(\Delta t)}-1)e^{-\alpha\tau}}{(1-e^{-\alpha\tau})} \right) e^{-\alpha t_{\min}} \right. \\ \left. - \frac{k_0(k_{21}-\beta)}{\beta(\beta-\alpha)} \left(1 - \frac{(e^{\beta(\Delta t)}-1)e^{-\beta\tau}}{(1-e^{-\beta\tau})} \right) e^{-\beta t_{\min}} \right\} \quad (1.46)$$

As a result, the minimum release rate ($k_0(\min)$) for the successful delivery system with a specific duration $M\tau + \Delta t$ can be expressed by eq. 1.47. Furthermore, since the dose is equal to $(M\tau + \Delta t)(k_0)$, the minimum required dose for these delivery systems can be expressed by eq. 1.48.

$$k_o(\min) = \{C_{\min}V_1\} \div \left\{ \frac{(M+1)k_o}{k_{10}} - \frac{k_o(k_{21}-\alpha)}{\alpha(\beta-\alpha)} \left[1 - \frac{(e^{\alpha(\Delta t)}-1)e^{-\alpha\tau}}{(1-e^{-\alpha\tau})} \right] e^{-\alpha t_{\min}} \right. \\ \left. - \frac{k_o(k_{21}-\beta)}{\beta(\beta-\alpha)} \left[1 - \frac{(e^{\beta(\Delta t)}-1)e^{-\beta\tau}}{(1-e^{-\beta\tau})} \right] e^{-\beta t_{\min}} \right\} \quad (1.47)$$

$$D_{\min} = \{C_{\min}V_1(M\tau+\Delta t)\} \div \left\{ \frac{(M+1)}{k_{10}} - \frac{(k_{21}-\alpha)}{\alpha(\beta-\alpha)} \left[1 - \frac{(e^{\alpha(\Delta t)}-1)e^{-\alpha\tau}}{(1-e^{-\alpha\tau})} \right] e^{-\alpha t_{\min}} \right. \\ \left. - \frac{(k_{21}-\beta)}{\beta(\alpha-\beta)} \left[1 - \frac{(e^{\beta(\Delta t)}-1)e^{-\beta\tau}}{(1-e^{-\beta\tau})} \right] e^{-\beta t_{\min}} \right\} \quad (1.48)$$

To simplified these two eqs, the assumption of $t_{\min}=0$ was made and the results were shown by eqs. 1.49 and 1.50.

$$k_o(\min) = \{C_{\min}V_1\} \div \left\{ \frac{(M+1)}{k_{10}} - \frac{(k_{21}-\alpha)}{\alpha(\beta-\alpha)} \left[1 - \frac{(e^{\alpha(\Delta t)}-1)e^{-\alpha\tau}}{(1-e^{-\alpha\tau})} \right] \right. \\ \left. - \frac{(k_{21}-\beta)}{\beta(\alpha-\beta)} \left[1 - \frac{(e^{\beta(\Delta t)}-1)e^{-\beta\tau}}{(1-e^{-\beta\tau})} \right] \right\} \quad (1.49)$$

$$D_{\min} = \{C_{\min}V_1(M\tau+\Delta t)\} \div \left\{ \frac{(M+1)}{k_{10}} - \frac{(k_{21}-\alpha)}{\alpha(\beta-\alpha)} \left[1 - \frac{(e^{\alpha(\Delta t)}-1)e^{-\alpha\tau}}{(1-e^{-\alpha\tau})} \right] \right. \\ \left. - \frac{(k_{21}-\beta)}{\beta(\alpha-\beta)} \left[1 - \frac{(e^{\beta(\Delta t)}-1)e^{-\beta\tau}}{(1-e^{-\beta\tau})} \right] \right\} \quad (1.50)$$

These simplified eqs. were absorption independent since there is no k_a present in these expressions.

On the other hand, the C_{\max}^{SS} appears during the Mk_0 phase of the steady state plasma concentration - time profile ($\Delta t \leq t' \leq \tau$). The equation describes this phase is shown by eq. 1.51.

$$C^{SS} = \frac{1}{V_1} \left\{ \frac{Mk_0 k_a k_{21}}{k_a \alpha \beta} + \frac{k_0 k_a (k_{21} - k_a) (e^{k_a (\Delta t)} - 1)}{k_a (\alpha - k_a) (\beta - k_a) (1 - e^{-k_a \tau})} e^{-k_a t'} + \frac{k_0 k_a (k_{21} - \alpha) (e^{\alpha (\Delta t)} - 1)}{\alpha (k_a - \alpha) (\beta - \alpha) (1 - e^{-\alpha \tau})} e^{-\alpha t'} + \frac{k_0 k_a (k_{21} - \beta) (e^{\beta (\Delta t)} - 1)}{\beta (k_a - \beta) (\alpha - \beta) (1 - e^{-\beta \tau})} e^{-\beta t'} \right\} \quad (1.51)$$

The first derivative of concentration will equal to 0 when $t' = t_{\max}$ since it is the maximum concentration. Therefore,

$$\frac{k_0 k_a (k_{21} - k_a) (e^{k_a (\Delta t)} - 1)}{(\alpha - k_a) (\beta - k_a) (1 - e^{-k_a \tau})} e^{-k_a t_{\max}} + \frac{k_0 k_a (k_{21} - \alpha) (e^{\alpha (\Delta t)} - 1)}{(k_a - \alpha) (\beta - \alpha) (1 - e^{-\alpha \tau})} e^{-\alpha t_{\max}} + \frac{k_0 k_a (k_{21} - \beta) (e^{\beta (\Delta t)} - 1)}{(k_a - \beta) (\alpha - \beta) (1 - e^{-\beta \tau})} e^{-\beta t_{\max}} = 0 \quad (1.52)$$

As a result of mathematical manipulation, the C_{\max}^{SS} can be expressed as eq. 1.53.

$$C_{\max}^{SS} = \frac{1}{V_1} \left\{ \frac{Mk_0}{k_{l0}} + \frac{k_0 (k_{21} - \alpha) (e^{\alpha (\Delta t)} - 1)}{\alpha (\beta - \alpha) (1 - e^{-\alpha \tau})} e^{-\alpha t_{\max}} + \frac{k_0 (k_{21} - \beta) (e^{\beta (\Delta t)} - 1)}{\beta (\beta - \alpha) (1 - e^{-\beta \tau})} e^{-\beta t_{\max}} \right\} \quad (1.53)$$

For a successful delivery system, the C_{\max}^{SS} can not exceed the upper limit of the therapeutic window, C_{\max} . Therefore, the relationship of $C_{\max}^{SS} \leq C_{\max}$ has to be satisfied. In other words,

$$\begin{aligned}
C_{\max}^{SS} = \frac{k_0}{V_1} \left\{ \frac{M}{k_{10}} + \frac{(k_{21}-\alpha)(e^{\alpha(\Delta t)}-1)}{\alpha(\beta-\alpha)(1-e^{-\alpha\tau})} e^{-\alpha t_{\max}} \right. \\
\left. + \frac{(k_{21}-\beta)(e^{\beta(\Delta t)}-1)}{\beta(\beta-\alpha)(1-e^{-\beta\tau})} e^{-\beta t_{\max}} \right\} \leq C_{\max}
\end{aligned} \tag{1.54}$$

Thus,

$$\begin{aligned}
k_0 \leq \{C_{\max}V_1\} \div \left\{ \frac{M}{k_{10}} + \frac{(k_{21}-\alpha)(e^{\alpha(\Delta t)}-1)}{\alpha(\beta-\alpha)(1-e^{-\alpha\tau})} e^{-\alpha t_{\max}} \right. \\
\left. + \frac{(k_{21}-\beta)(e^{\beta(\Delta t)}-1)}{\beta(\beta-\alpha)(1-e^{-\beta\tau})} e^{-\beta t_{\max}} \right\}
\end{aligned} \tag{1.55}$$

As a result, the maximum release rate ($k_0(\max)$) and the maximum dose (D_{\max}) for the successful DDS with a specific duration $M\tau + \Delta t$ can be determined by using eqs. 1.56 and 1.57.

$$\begin{aligned}
k_0(\max) = \{C_{\max}V_1\} \div \left\{ \frac{M}{k_{10}} + \frac{(k_{21}-\alpha)(e^{\alpha(\Delta t)}-1)}{\alpha(\beta-\alpha)(1-e^{-\alpha\tau})} e^{-\alpha t_{\max}} \right. \\
\left. + \frac{(k_{21}-\beta)(e^{\beta(\Delta t)}-1)}{\beta(\beta-\alpha)(1-e^{-\beta\tau})} e^{-\beta t_{\max}} \right\}
\end{aligned} \tag{1.56}$$

$$\begin{aligned}
D_{\max} = \{C_{\max}V_1(M\tau + \Delta t)\} \div \left\{ \frac{M}{k_{10}} + \frac{(k_{21}-\alpha)(e^{\alpha(\Delta t)}-1)}{\alpha(\beta-\alpha)(1-e^{-\alpha\tau})} e^{-\alpha t_{\max}} \right. \\
\left. + \frac{(k_{21}-\beta)(e^{\beta(\Delta t)}-1)}{\beta(\beta-\alpha)(1-e^{-\beta\tau})} e^{-\beta t_{\max}} \right\}
\end{aligned} \tag{1.57}$$

Further simplification of these two equations were made based on the assumption of $t_{\max} = \Delta t$, and the simplified equations for $k_0(\max)$ and D_{\max} were shown as eqs. 1.58 and 1.59.

$$k_0(\max) = \{C_{\max}V_1\} \div \left\{ \frac{M}{k_{10}} + \frac{(k_{21}-\alpha)(1-e^{-\alpha(\Delta t)})}{\alpha(\beta-\alpha)(1-e^{-\alpha\tau})} + \frac{(k_{21}-\beta)(1-e^{-\beta(\Delta t)})}{\beta(\beta-\alpha)(1-e^{-\beta\tau})} \right\} \quad (1.58)$$

$$D_{\max} = \{C_{\max}V_1(M\tau+\Delta t)\} \div \left\{ \frac{M}{k_{10}} + \frac{(k_{21}-\alpha)(1-e^{-\alpha(\Delta t)})}{\alpha(\beta-\alpha)(1-e^{-\alpha\tau})} + \frac{(k_{21}-\beta)(1-e^{-\beta(\Delta t)})}{\beta(\beta-\alpha)(1-e^{-\beta\tau})} \right\} \quad (1.59)$$

REFERENCES

1. P. G. Welling and M. R. Dobrinska, Multiple Dosing of Sustained Release Systems, in "Sustained and Controlled Release Drug Delivery Systems", J. R. Robinson (Ed.), 631, Marcel Dekker, Inc., New York, N.Y., 1978.
2. E. Nelson, A Note on Mathematics of Oral Sustained Release Products, J. Amer. Pharm. Ass. Sci. Ed., 46, 572 (1957).
3. M. Rowland and A. H. Beckett, Mathematical Treatment of Oral Sustained Release Drug Formulation, J. Pharm. Pharmacol., 16, Suppl., 156T (1964).
4. J. R. Robinson and S. P. Eriksen, Theoretical Formulation of Sustained-Release Dosage Form, J. Pharm. Sci., 55, 1254 (1966).
5. M. G. Dobrinska and P. G. Welling, Blood Level from a Sustained-Release Dosage Form, J. Pharm. Sci., 64, 1728 (1975).
6. K. C. Kwan, Pharmacokinetic Considerations in the Design of Controlled and Sustained Release Drug Delivery Systems, in "Sustained and Controlled Release Drug Delivery Systems", J. R. Robinson (Ed.), 595, Marcel-Dekker, Inc., New York, N.Y., 1978.
7. J. D. Rogers and K. C. Kwan, Pharmacokinetic Requirements for Controlled-Release Dosage Form, in "Controlled-Release Pharmaceuticals", J. Urquhart (Ed.), 95, American Pharmaceutical Associations, Washington D.C., 1981.
8. R. G. Weigand and J. D. Taylor, Kinetics of Plasma Drug Levels after Sustained Release Dosage, Biochem. Pharmacol., 3, 256 (1960).
9. E. Kruger-Thiemer and S. P. Eriksen, Mathematical Model of Sustained-Release Preparations and Its Analysis, J. Pharm. Sci., 55, 1249 (1966).
10. J. R. Robinson and S. P. Eriksen, Theoretical Approach to Sustained-Release Multiple-Dose Therapy: Noncumulative Attainment of Desired Blood Level, J. Pharm. Sci., 59, 1796 (1970).
11. H. Boxenbaum, Pharmacokinetic Determinants in the Design and Evaluation of Sustained-Release Dosage Forms, Pharm. Res., 82 (1984).

12. R. E. Notari, "Biopharmaceutics and Clinical Pharmacokinetics, an Introduction", 3rd. ed., Merce! Dekker, Inc., New York, N.Y., 1980.
13. J. G. Wagner, "Fundamentals of Clinical Pharmacokinetics", Drug Intellegence Publications, Inc., Hamilton, Illinois, 1975, p. 154.
14. M. Abramowitz and I.A. Stegun, Eds., Handbook of Mathematical Functions with Formulas, Graphs, and Mathematical Tables, National Bureau of Standards Applied Mathematics Series 55, U.S. Department of Commerce, U.S. Government Printing Office, Washington, D.C., 1972, p.18.
15. F. Theeuwes and W. Bayne, Controlled-Release Dosage Form Design, in "Controlled-Release Pharmaceuticals", J. Urquhart (Ed.), 61, American Pharmaceutical Associations, Washington, D.C., 1981.

Table 1.1

Single Dose Plasma Concentration-Time Equations for Drug
Delivery Systems Described by Scheme I and II.

Two Compartment, First-Order DDS, Single Dose Equation

$$C = \frac{k_1 k_a D_0}{V_1} \left\{ \frac{(k_{21}-k_1)}{(k_a-k_1)(\alpha-k_1)(\beta-k_1)} e^{-k_1 t} + \frac{(k_{21}-k_a)}{(k_1-k_a)(\alpha-k_a)(\beta-k_a)} e^{-k_a t} \right. \\ \left. + \frac{(k_{21}-\alpha)}{(k_1-\alpha)(k_a-\alpha)(\beta-\alpha)} e^{-\alpha t} + \frac{(k_{21}-\beta)}{(k_1-\beta)(k_a-\beta)(\alpha-\beta)} e^{-\beta t} \right\}$$

One Compartment, First-Order DDS, Single Dose Equation

$$C = \frac{k_1 k_a D_0}{V} \left\{ \frac{1}{(k_a-k_1)(k-k_1)} e^{-k_1 t} + \frac{1}{(k_1-k_a)(k-k_a)} e^{-k_a t} + \frac{1}{(k_1-k)(k_a-k)} e^{-k t} \right\}$$

Two Compartment, Zero-Order DDS, Single Dose Equation
(1) $t \leq T$

$$C = \frac{1}{V_1} \left\{ \frac{k_0}{k_{10}} - \frac{k_0 k_a (k_{21}-k_a)}{k_a (\alpha-k_a) (\beta-k_a)} e^{-k_a t} - \frac{k_0 k_a (k_{21}-\alpha)}{\alpha (k_a-\alpha) (\beta-\alpha)} e^{-\alpha t} \right. \\ \left. - \frac{k_0 k_a (k_{21}-\beta)}{\beta (k_a-\beta) (\alpha-\beta)} e^{-\beta t} \right\}$$

Table 1.1 (Continue)

(2) $t \geq T$

$$C = \frac{1}{V_1} \left\{ \frac{k_0 k_a (k_{21} - k_a) (e^{k_a T} - 1)}{k_a (\alpha - k_a) (\beta - k_a)} e^{-k_a t} + \frac{k_0 k_a (k_{21} - \alpha) (e^{\alpha T} - 1)}{\alpha (k_a - \alpha) (\beta - \alpha)} e^{-\alpha t} \right. \\ \left. + \frac{k_0 k_a (k_{21} - \beta) (e^{\beta T} - 1)}{\beta (k_a - \beta) (\alpha - \beta)} e^{-\beta t} \right\}$$

One Compartment, Zero-Order DDS, Single Dose Equation:

(1) $t \leq T$

$$C = \frac{1}{V} \left\{ \frac{k_0}{k} - \frac{k_0 k_a}{k_a (k - k_a)} e^{-k_a t} - \frac{k_0 k_a}{k (k_a - k)} e^{-kt} \right\}$$

(2) $t \geq T$

$$C = \frac{1}{V} \left\{ \frac{k_0 k_a (e^{k_a T} - 1)}{k_a (k - k_a)} e^{-k_a t} + \frac{k_0 k_a (e^{k T} - 1)}{k (k_a - k)} e^{-kt} \right\}$$

Table 1.2

**Effect of Therapeutic Window on the Duration-Dose Profile
for a Successful Zero-order Release DDS.^a**

Therapeutic Window (mg/L)	Maximum Dose Range ^b (mg)	T.I.	T _{min} (hours)	
			Predicted ^c	Observed ^d
10-15	108-162	1.5	8.7	8.7
20-30	216-324	1.5	8.7	8.7
5-10	54-108	2	6.4	6.3
10-20	108-216	2	6.4	6.3
5-15	54-162	3	3.1	2.9
10-30	108-324	3	3.1	2.9

^a $k_{12}=3.0 \text{ h}^{-1}$, $k_{21}=5.0 \text{ h}^{-1}$, $k_{10}=0.2 \text{ h}^{-1}$, $k_a=5.0 \text{ h}^{-1}$,
 $\alpha=8.076 \text{ h}^{-1}$, $\beta=0.124 \text{ h}^{-1}$, $V_1=4.5 \text{ L}$, $\tau=12 \text{ hours}$.

^bRequired dose size range for DDS with duration $T=n\tau$.

^c $T_{\min} = \tau - \ln(\text{T.I.})/\beta$.

^d T_{\min} determined from the duration-dose profiles.

Table 1.3

Comparison of T_{\min} Predicted Using Eq. 1.40 to those Observed for One and Two Compartment Zero-order DDS.

$A^a(h^{-1})$		$B^b(h^{-1})$			$T_{\min}(\text{Hours})$		
k	k_{12}	k_{21}	k_{10}	β	$A^{a,c}$	$B^{b,c}$	Predicted ^d
0.382	1.0	1.0	1.0	0.382	10.2	10.9	10.2
0.191	0.5	0.5	0.5	0.191	8.3	9.1	8.4
0.293	0.5	1.0	0.5	0.293	9.6	10.1	9.6
0.134	1.0	0.5	0.5	0.134	6.8	8.8	6.8
0.363	1.0	3.0	0.5	0.363	10.1	10.2	10.1
0.114	3.0	1.0	0.5	0.114	5.8	7.0	5.9
0.410	1.0	5.0	0.5	0.410	10.3	10.3	10.3
0.078	5.0	1.0	0.5	0.078	2.9	4.7	3.1

^aOne compartment: $k_a=10.0 h^{-1}$, $V=4.5 L$, and $\tau=12$ hours.

^bTwo compartment: $k_a=10.0 h^{-1}$, $V_1=4.5 L$, and $\tau=12$ hours.

^c T_{\min} observed from duration-dose profiles.

^d T_{\min} calculated using eq. 1.40.

Table 1.4

Comparison of Required k_1 for First-order DDS which
Release a Defined Percentage of Its Payloads in 10 and 12
Hours

% Released	Minimum Required k_1 (h^{-1})	
	$T_f=10$ hours	$T_f=12$ hours
80	0.161	0.134
85	0.190	0.158
90	0.230	0.192
95	0.300	0.250

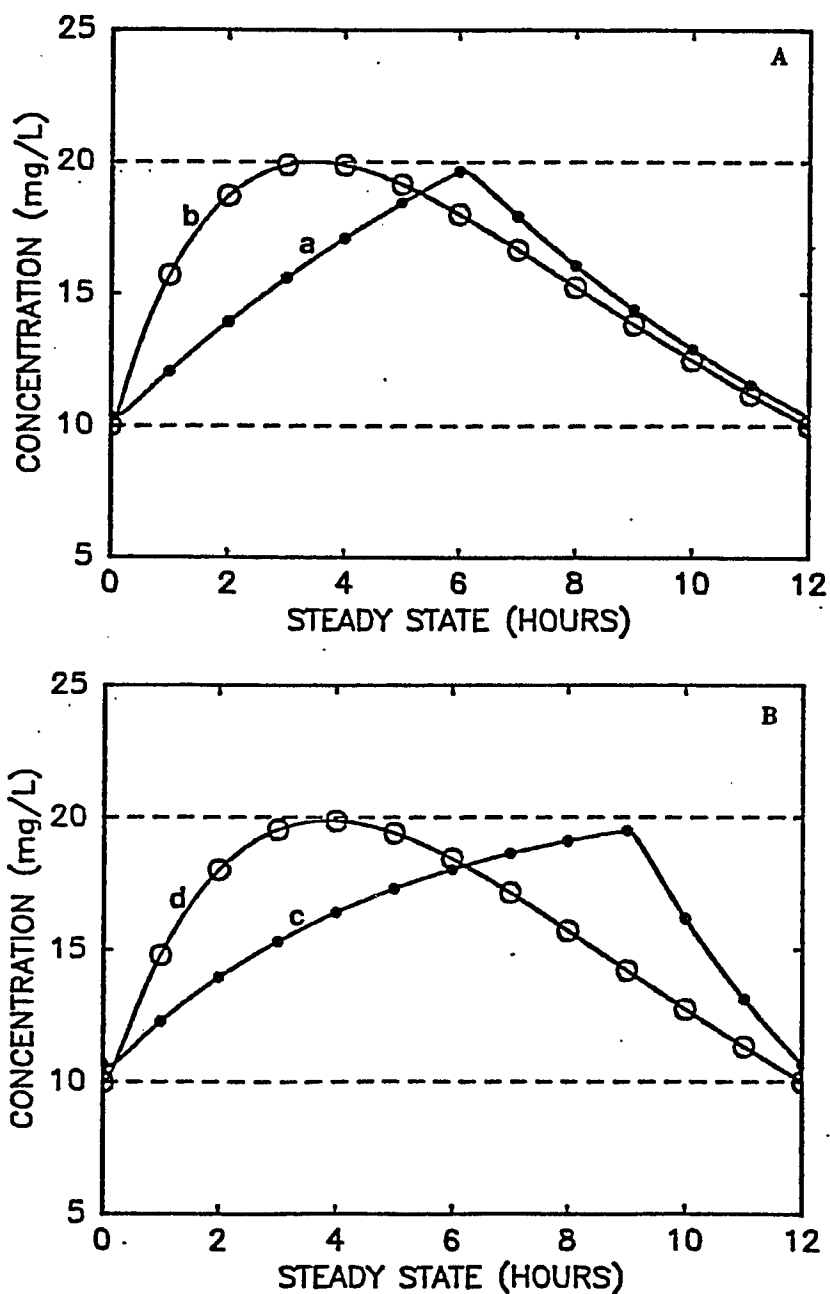


Figure 1.1:

Repetitive dose steady state concentration-time profiles for DDS described by Scheme I(A) and II(B). Solid curves are predicted profiles using eqs. 1.9 - 1.14. (o) and (•) are predicted values using superposition and single dose equations (Table 1.1). • represents zero-order DDS (a and c) and o represents first-order DDS (b and d). Pharmacokinetic parameters used : (A) $k_{12}=3.0 \text{ h}^{-1}$, $k_{21}=5.0 \text{ h}^{-1}$, $k_{10}=0.2 \text{ h}^{-1}$, $k_a=5.0 \text{ h}^{-1}$, $V_1=4.5 \text{ L}$, and $\tau=12 \text{ hours}$ (B) $k=0.21 \text{ h}^{-1}$, $V=4.5 \text{ L}$, and $\tau=12 \text{ hours}$. Dashed lines (-----) represent therapeutic window which is selected as 10 to 20 mg/L.

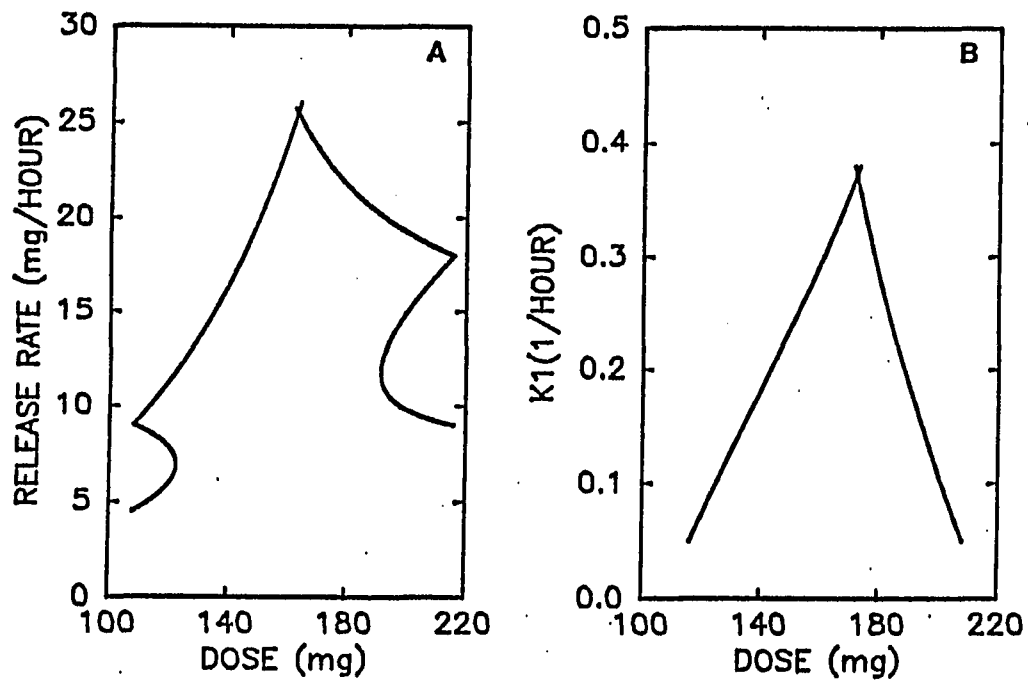


Figure 1.2: Typical release rate constant-dose profiles for a zero-order or first-order release DDS described by Scheme I. Pharmacokinetic values used: $k_{12}=3.0 \text{ h}^{-1}$, $k_{21}=5.0 \text{ h}^{-1}$, $k_{10}=0.2 \text{ h}^{-1}$, $k_a=10 \text{ h}^{-1}$, $V_1=4.5 \text{ L}$, and $\tau=12$ hours. Any combination of dose and release rate constant within the limit will maintain the therapeutic window in Fig. 1.1.

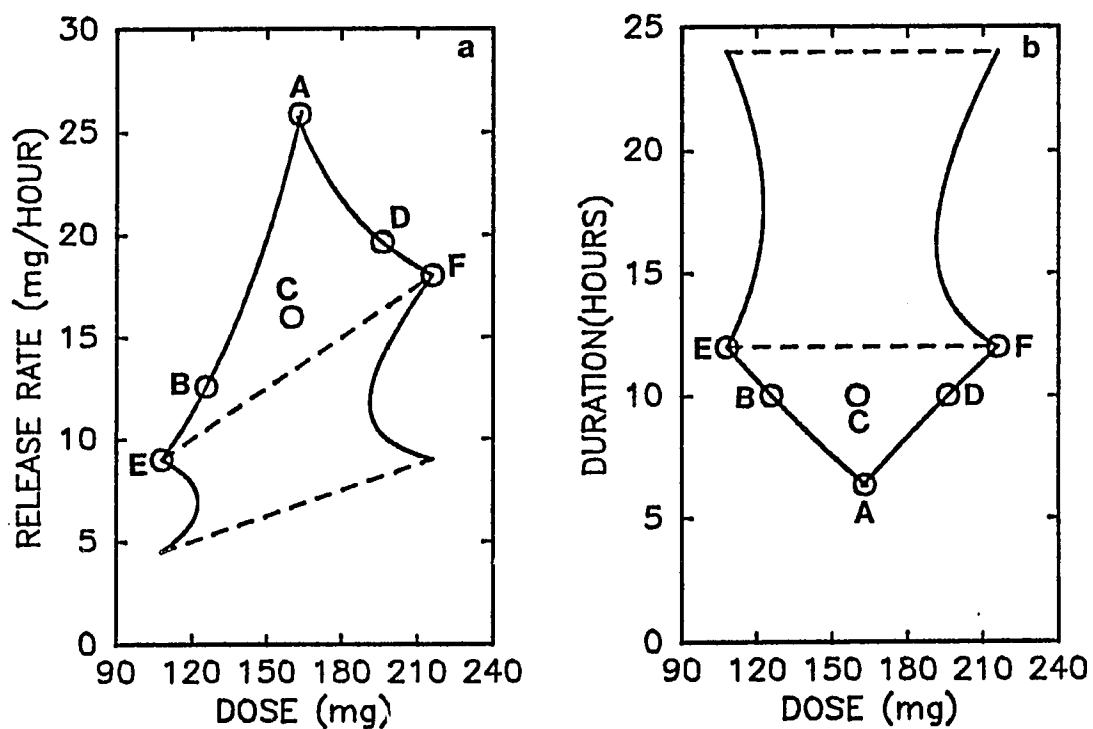


Figure 1.3: Release rate constant-dose profile (a) and transformed duration-dose profile (b) for a zero-order DDS described by Scheme I, with values: $k_{12}=3.0 \text{ h}^{-1}$, $k_{21}=5.0 \text{ h}^{-1}$, $k_{10}=0.2 \text{ h}^{-1}$, $k_a=10 \text{ h}^{-1}$, $V_1=4.5 \text{ L}$, and $\tau=12 \text{ hours}$.

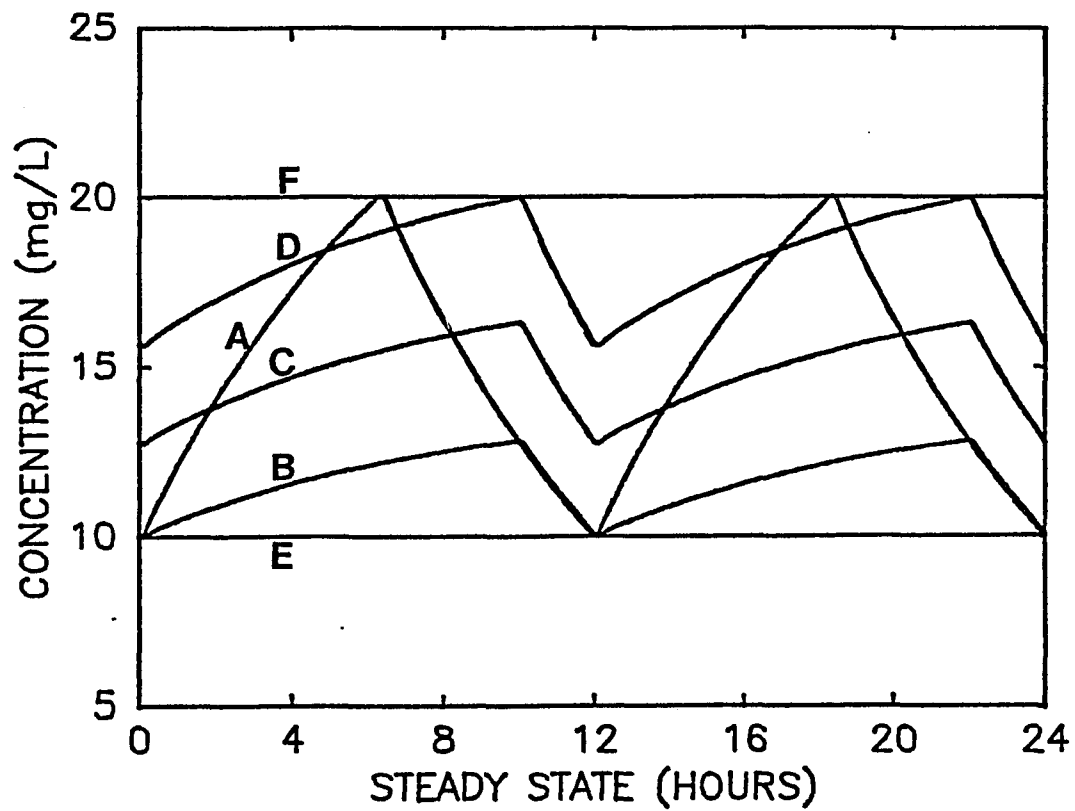


Figure 1.4: Steady state plasma concentration-time profiles for the corresponding DDS and doses indicated in Fig. 1.3.

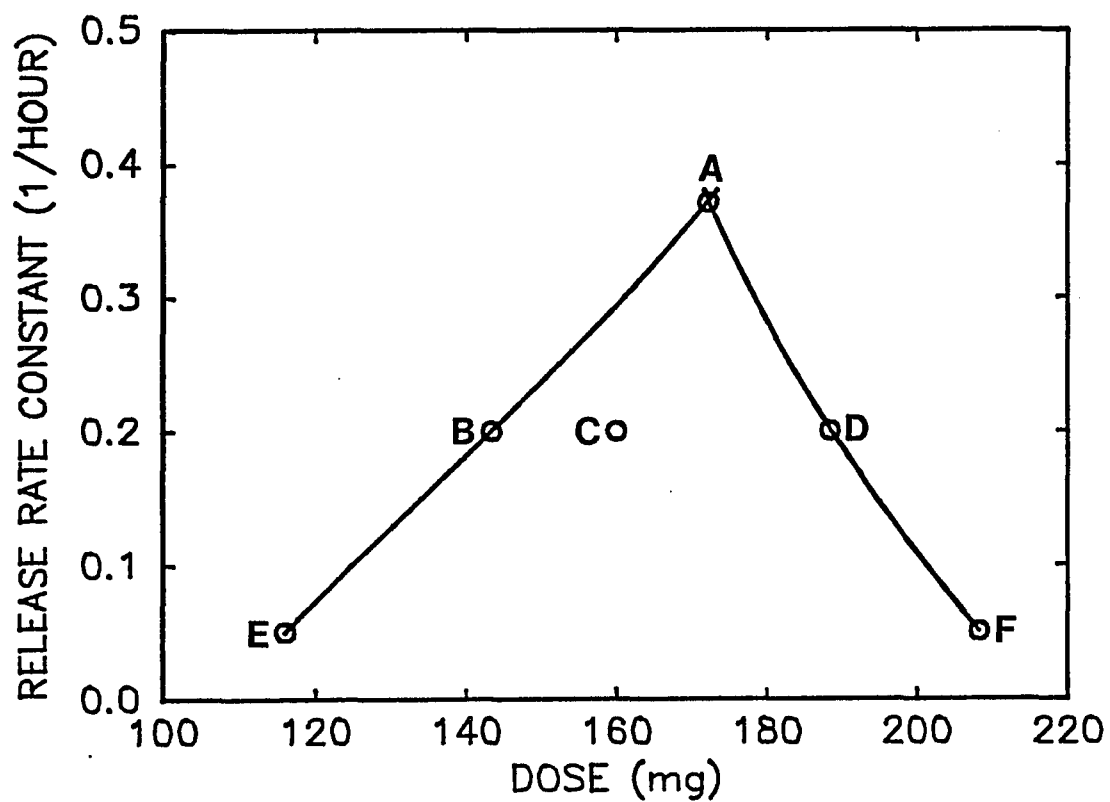


Figure 1.5: Release rate constant-dose profile for a first-order DDS described by Scheme I. with values: $k_{12}=3.0 \text{ h}^{-1}$, $k_{21}=5.0 \text{ h}^{-1}$, $k_{10}=0.2 \text{ h}^{-1}$, $k_a=10 \text{ h}^{-1}$, $V_1=4.5 \text{ L}$, and $\tau=12 \text{ hours}$.

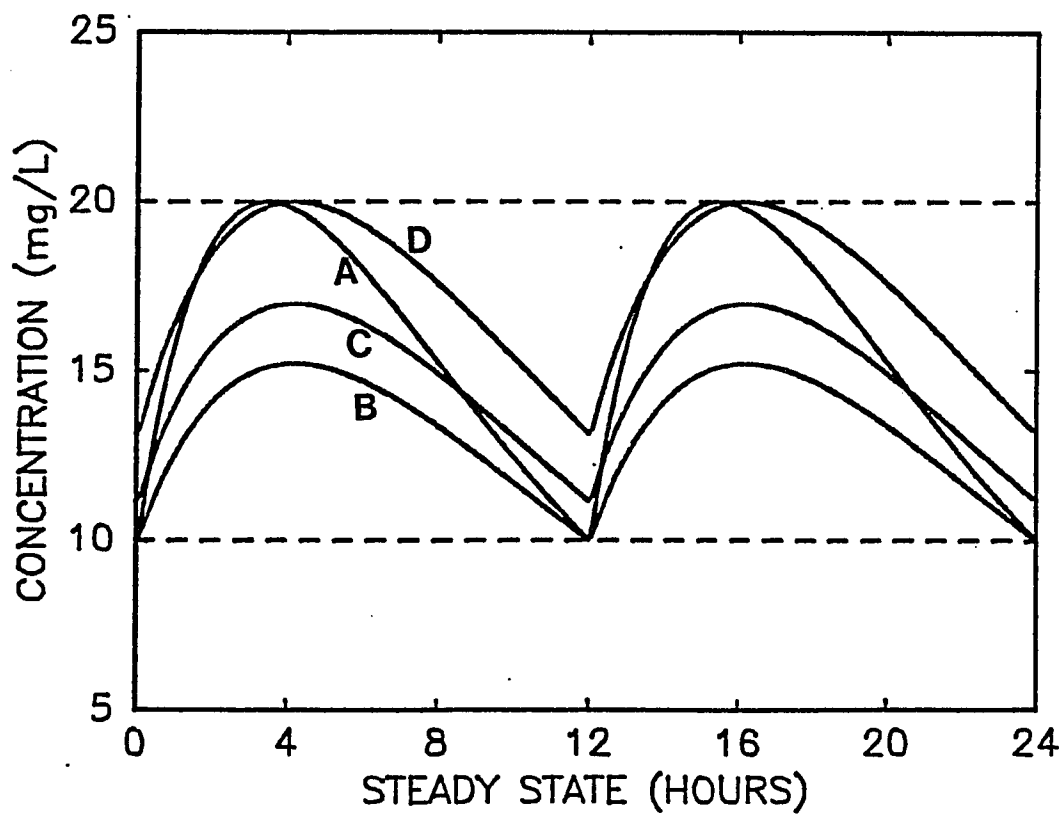


Figure 1.6: Steady state plasma concentration-time profiles for the corresponding DDS and doses indicated in Fig. 1.5

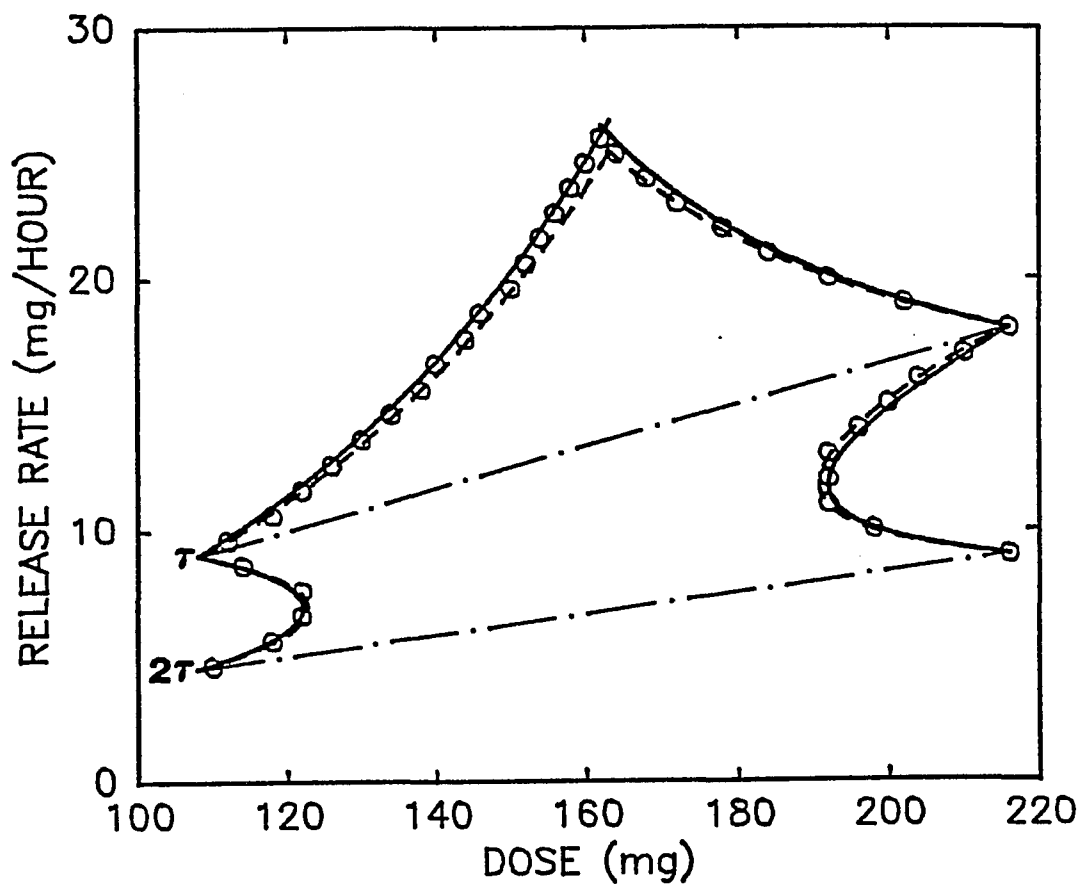


Figure 1.7: Release rate constant-dose profile for a zero-order DDS described by Scheme I. (o) represents profile predicted using reiterative simulation method. Solid curve (—) represents profile predicted using eqs. 1.16, 1.17, 1.20, and 1.21. Dashed curve (---) represents profile predicted using eqs. 1.18, 1.19, 1.22, and 1.23. Pharmacokinetic parameters used: $k_{12}=3.0 \text{ h}^{-1}$, $k_{21}=5.0 \text{ h}^{-1}$, $k_{10}=0.2 \text{ h}^{-1}$, $k_a=10 \text{ h}^{-1}$, $V_1=4.5 \text{ L}$, and $\tau=12 \text{ hours}$.

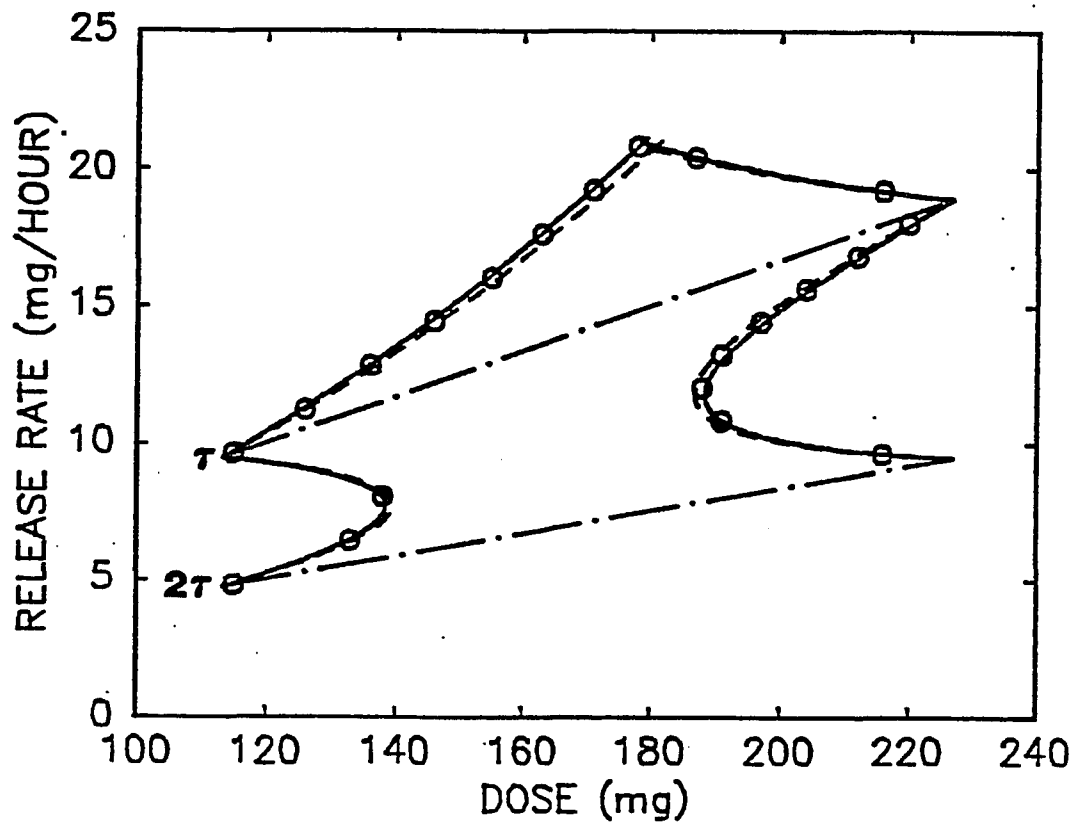


Figure 1.8: Release rate constant-dose profile for a zero-order DDS described by Scheme II. (o) represents profile predicted using reiterative simulation method. Solid curve (—) represents profile predicted using eqs. 1.26 - 1.29. Dashed curve (---) represents profile predicted using eqs. 1.30 - 1.33. Pharmacokinetic parameters used: $k=0.21 \text{ h}^{-1}$, $k_a=5.0 \text{ h}^{-1}$, $V=4.5 \text{ L}$, and $\tau=12 \text{ hours}$.

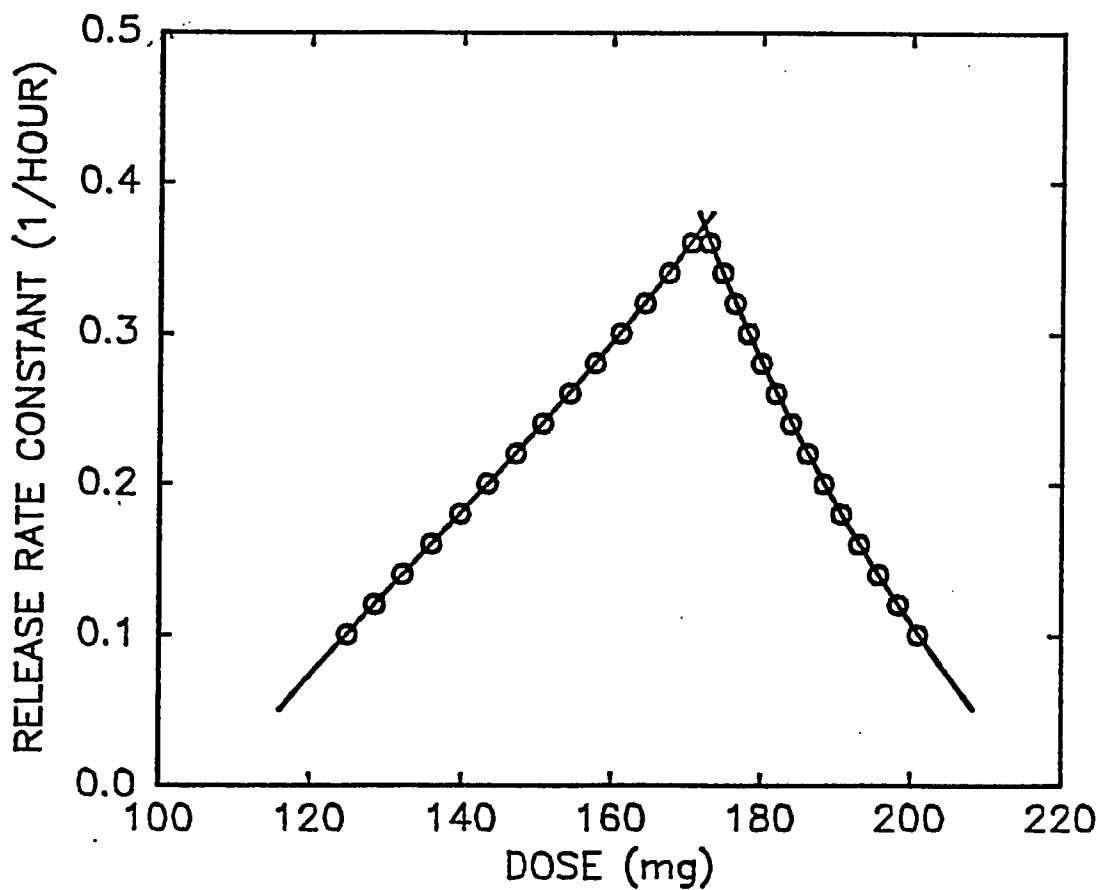


Figure 1.9: Release rate constant-dose profile for a first-order DDS described by Scheme I. (o) represents profile predicted using reiterative simulation method. Solid curve (—) represents profile predicted using eqs. 1.34 and 1.35. Pharmacokinetic parameters used: $k_{12}=3.0 \text{ h}^{-1}$, $k_{21}=5.0 \text{ h}^{-1}$, $k_{10}=0.2 \text{ h}^{-1}$, $k_a=10 \text{ h}^{-1}$, $V_1=4.5 \text{ L}$, and $\tau=12 \text{ hours}$.

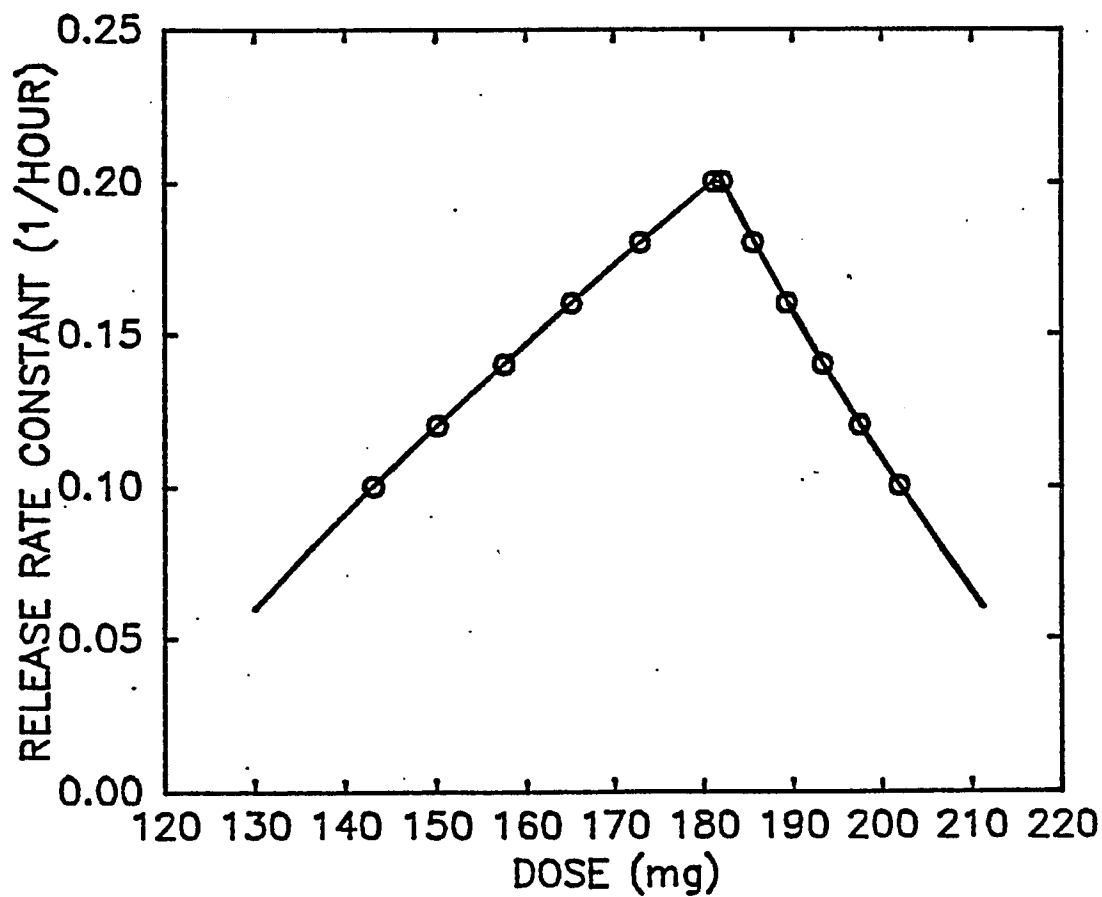


Figure 1.10:

Release rate constant-dose profile for a first-order DDS described by Scheme II. (o) represents profile predicted using reiterative simulation method. Solid curve (—) represents profile predicted using eqs. 1.36 and 1.37. Pharmacokinetic parameters used: $k=0.21 \text{ h}^{-1}$, $k_a=5.0 \text{ h}^{-1}$, $V=4.5 \text{ L}$, and $\tau=12$ hours.

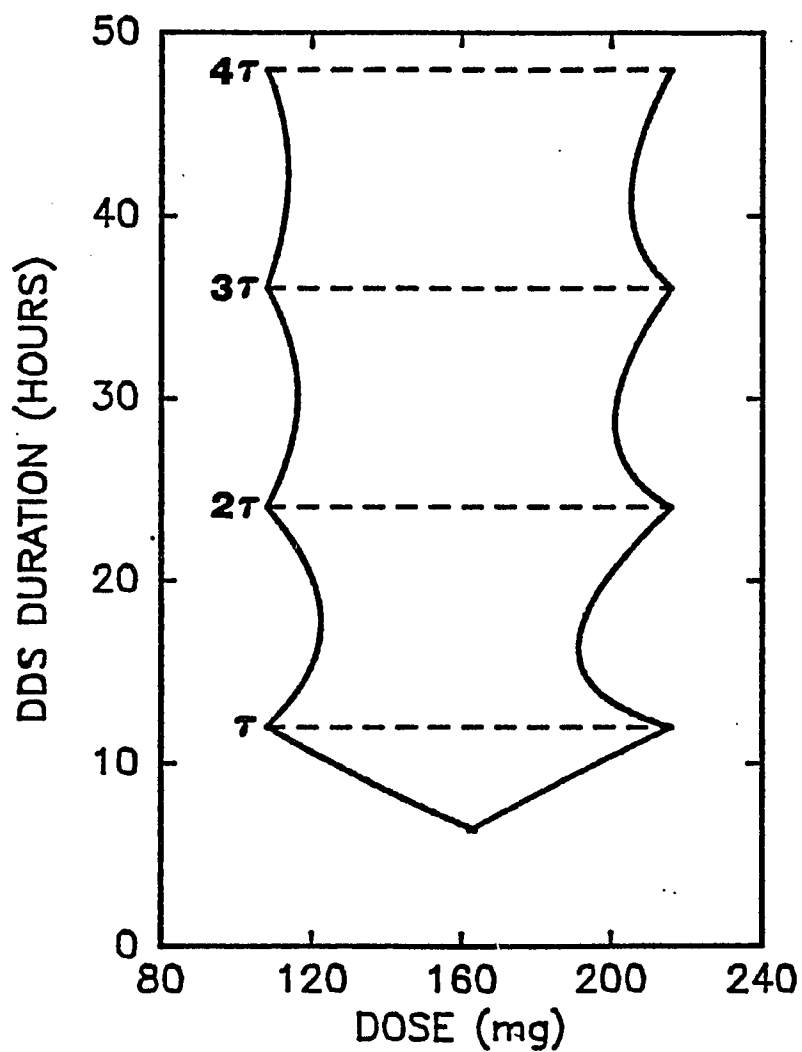


Figure 1.11: Release rate constant-dose profile for a zero-order DDS described by Scheme I with acceptable duration up to 4τ . Pharmacokinetic parameters used: $k_{12}=3.0 \text{ h}^{-1}$, $k_{21}=5.0 \text{ h}^{-1}$, $k_{10}=0.2 \text{ h}^{-1}$, $k_a=10 \text{ h}^{-1}$, $V_1=4.5 \text{ L}$, and $\tau=12 \text{ hours}$.

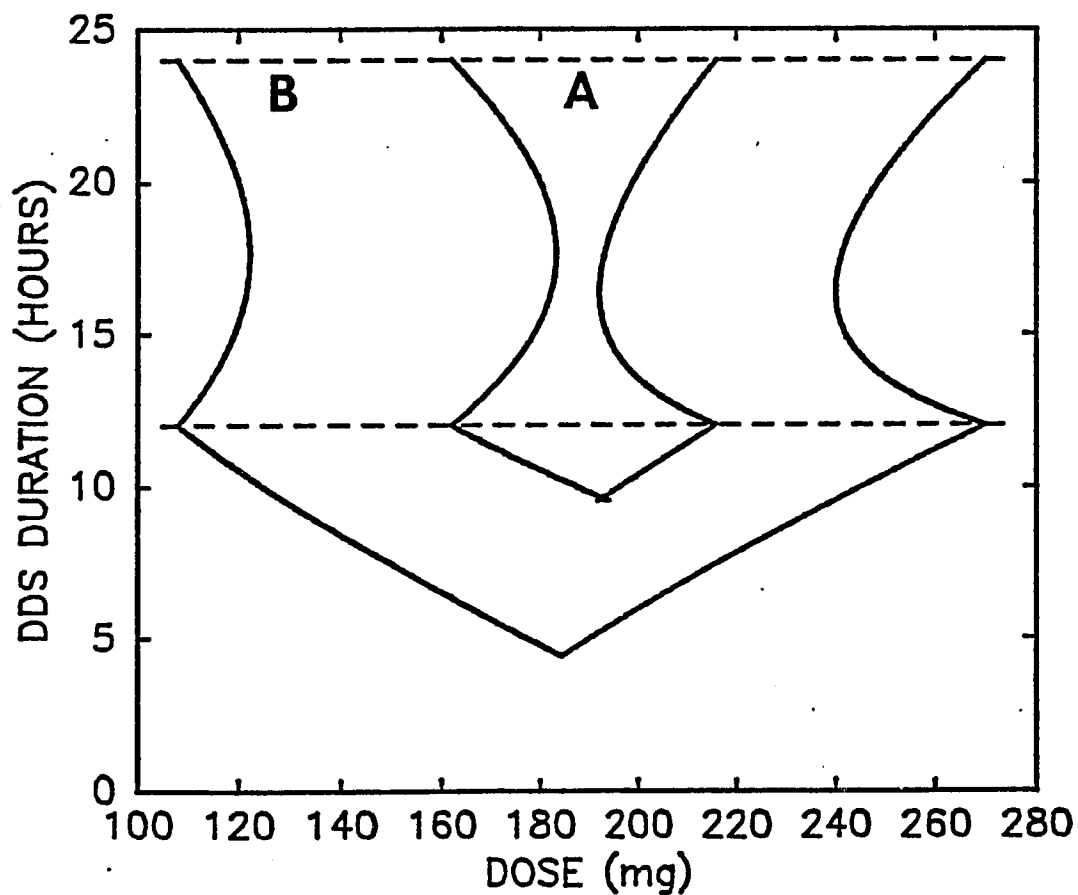


Figure 1.12: Influence of therapeutic window on the duration-dose profile for zero-order DDS. Therapeutic window: (A) 15 - 20 mg/L and (B) 10 - 25 mg/L. Pharmacokinetic parameters used: $k_{12}=3.0 \text{ h}^{-1}$, $k_{21}=5.0 \text{ h}^{-1}$, $k_{10}=0.2 \text{ h}^{-1}$, $k_a=10 \text{ h}^{-1}$, $V_1=4.5 \text{ L}$, and $\tau=12 \text{ hours}$.

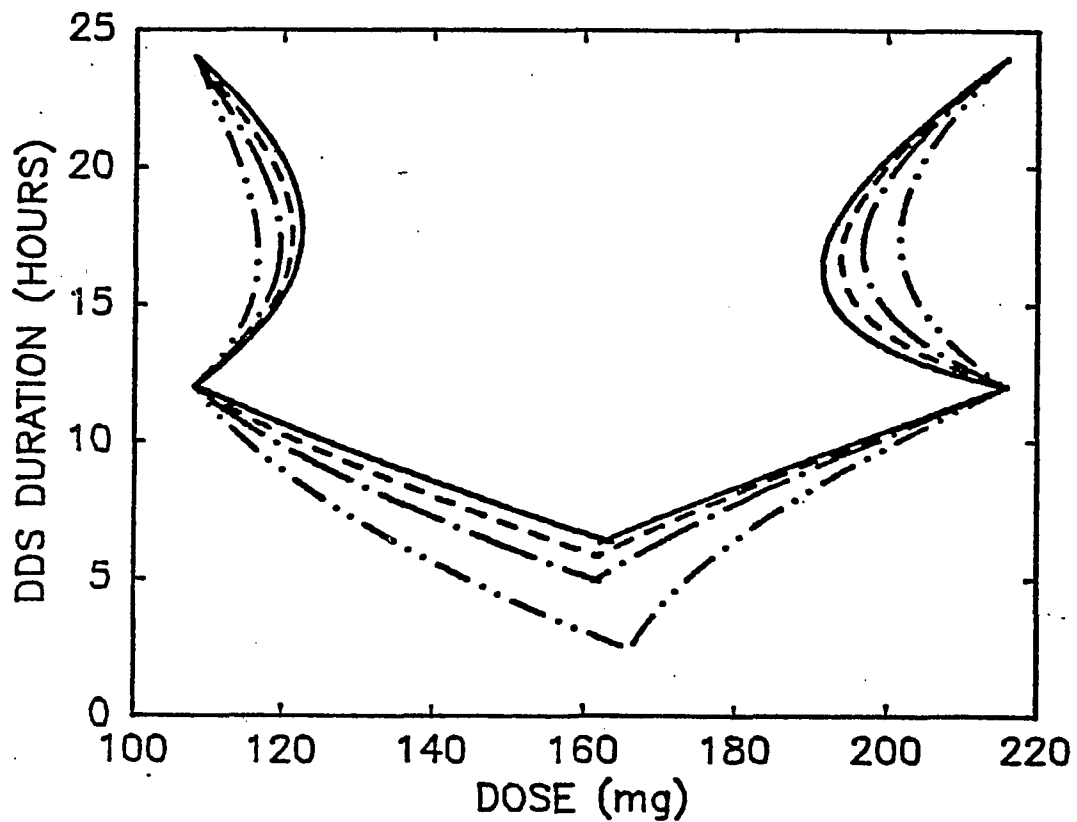


Figure 1.13: Influence of absorption on the duration-dose profile for zero-order DDS. k_a used: 0.5 h^{-1} (- • • -), 1.0 h^{-1} (- • -), 2.0 h^{-1} (----); and 10 h^{-1} (—). Pharmacokinetic parameters used: $k_{12}=3.0 \text{ h}^{-1}$, $k_{21}=5.0 \text{ h}^{-1}$, $k_{10}=0.2 \text{ h}^{-1}$, $V_1=4.5 \text{ L}$, and $\tau=12 \text{ hours}$.

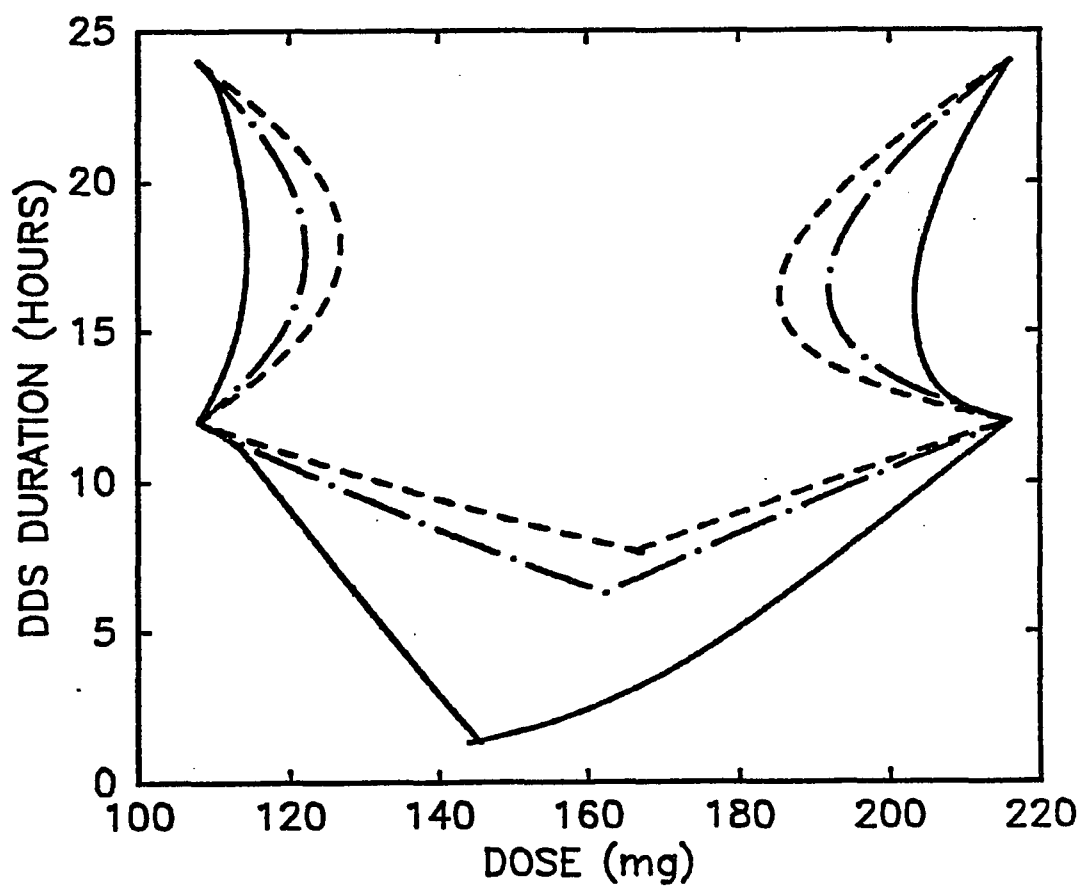


Figure 1.14: Influence of distribution on the duration-dose profile for zero-order DDS. k_{21}/k_{12} used: 5.0 (----); 1.67(- • -) and 0.5 (—). Pharmacokinetic parameters used: $k_{21} = 5.0 \text{ h}^{-1}$, $k_a = 10 \text{ h}^{-1}$, $k_{10} = 0.2 \text{ h}^{-1}$, $V_1 = 4.5 \text{ L}$, and $\tau = 12 \text{ hours}$.

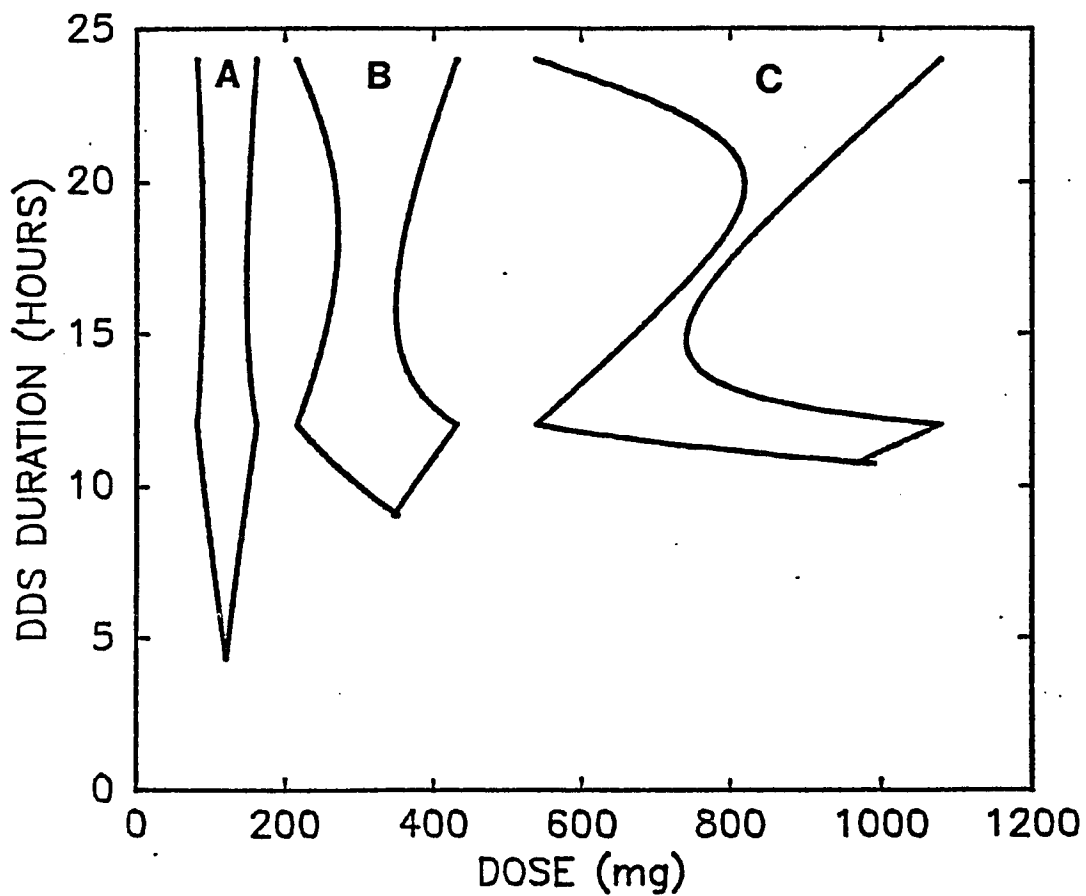


Figure 1.15: Influence of elimination on the duration-dose profile for zero-order DDS. k_{10} used: 0.2 (A); 0.4 (B); and 1.0 (C) h^{-1} . Pharmacokinetic parameters used: $k_{12}=3.0 \text{ h}^{-1}$, $k_{21}=5.0 \text{ h}^{-1}$, $k_a=10.0 \text{ h}^{-1}$, $V_1=4.5 \text{ L}$, and $\tau=12 \text{ hours}$.

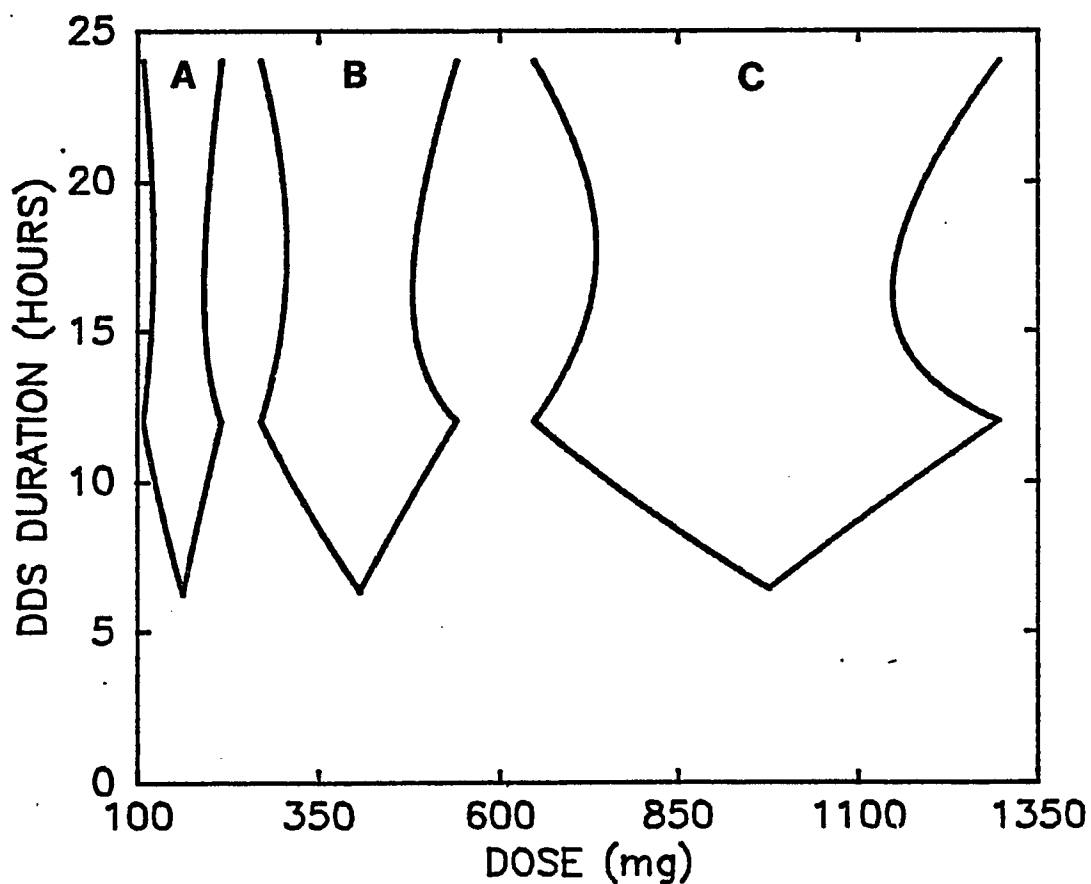


Figure 1.16: Influence of elimination on the duration-dose profile for zero-order DDS with constant β values. Pharmacokinetic parameters used: $k_a=10.0 \text{ h}^{-1}$, $V_1=4.5 \text{ L}$, and $\tau=12 \text{ hours}$. A: $k_{12}=3.0 \text{ h}^{-1}$, $k_{21}=5.0 \text{ h}^{-1}$, and $k_{10}=0.2 \text{ h}^{-1}$; B: $k_{12}=14.7 \text{ h}^{-1}$, $k_{21}=5.0 \text{ h}^{-1}$, and $k_{10}=0.5 \text{ h}^{-1}$; C: $k_{12}=42.2 \text{ h}^{-1}$, $k_{21}=5.0 \text{ h}^{-1}$, and $k_{10}=1.2 \text{ h}^{-1}$.

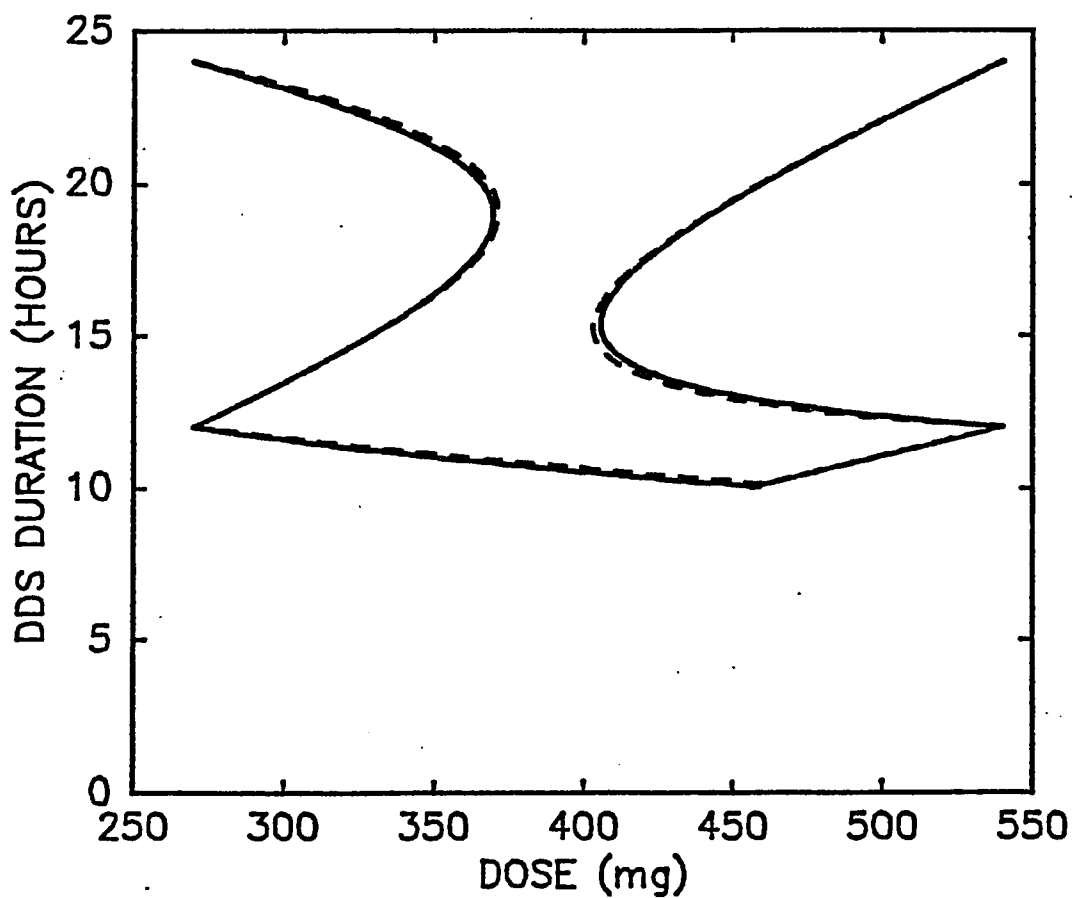


Figure 1.17:

Comparison of duration-dose profiles for a one and two compartment zero-order DDS. Pharmacokinetic parameters used: $k_a=10.0 \text{ h}^{-1}$ and $\tau=12$ hours. One compartment (—): $k=0.363 \text{ h}^{-1}$, and $V=6.206 \text{ L}$. Two compartment (----): $k_{12}=1.0 \text{ h}^{-1}$, $k_{21}=3.0 \text{ h}^{-1}$, $k_{10}=0.5 \text{ h}^{-1}$, and $V_1=4.5 \text{ L}$.

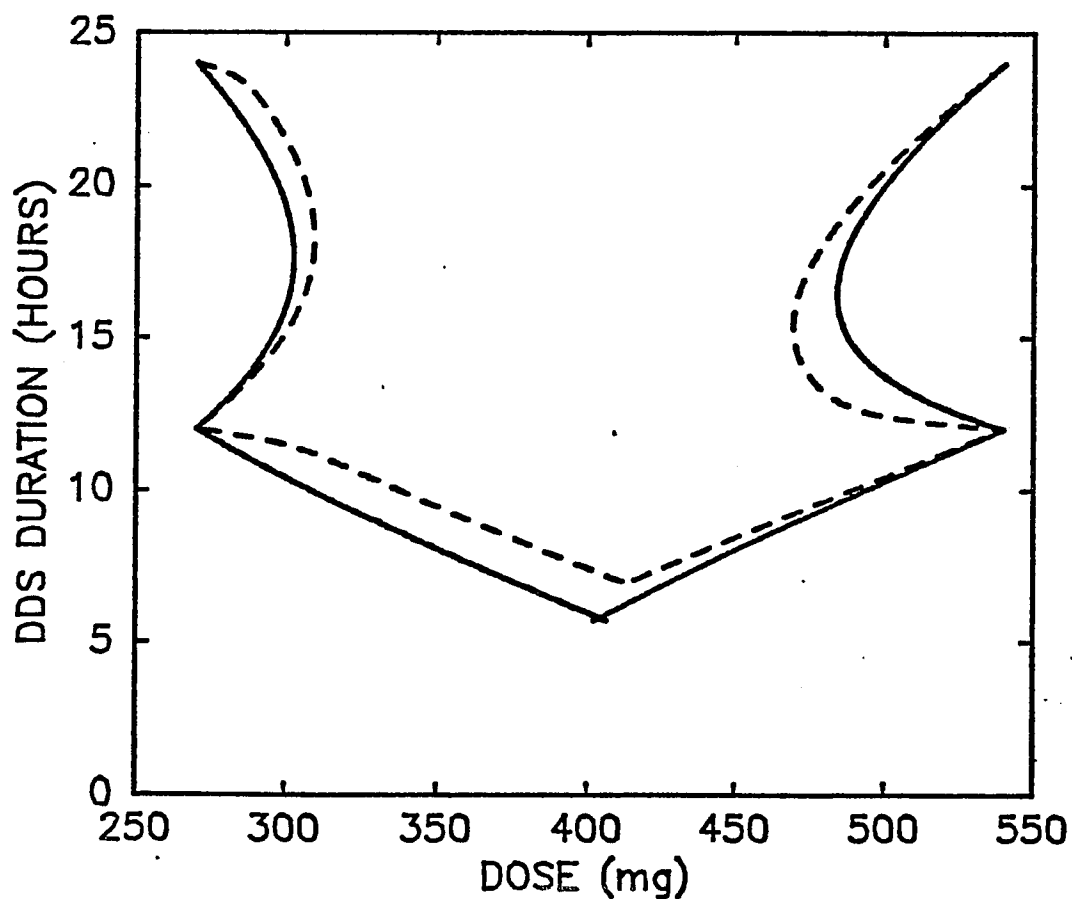


Figure 1.18:

Comparison of duration-dose profiles for a one and two compartment zero-order DDS. Pharmacokinetic parameters used: $k_a=10.0 \text{ h}^{-1}$ and $\tau=12$ hours. One compartment (—): $k=0.114 \text{ h}^{-1}$, and $V=19.74 \text{ L}$. Two compartment (----): $k_{12}=3.0 \text{ h}^{-1}$, $k_{21}=1.0 \text{ h}^{-1}$, $k_{10}=0.5 \text{ h}^{-1}$, and $V_1=4.5 \text{ L}$.

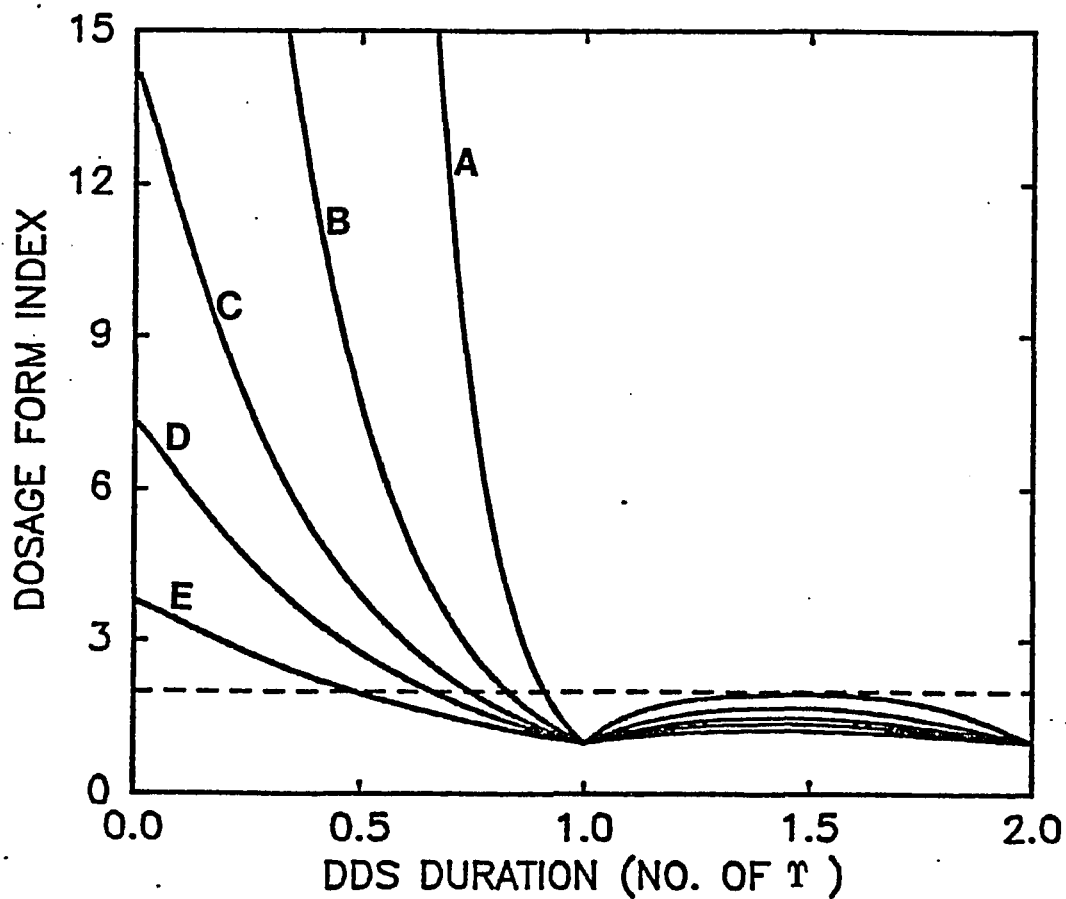


Figure 1.19: Dosage form index vs duration of DDS for one compartment zero-order DDS containing different half-lives drugs. Pharmacokinetic parameters used: $k_a=10.0 \text{ h}^{-1}$ $V=4.5 \text{ L}$, and $\tau=12 \text{ hours}$. Half-lives: 1(A), 2(B), 3(C), 4(D), and 6(E) hours. Dashed line (----) represents D.I. = 2.

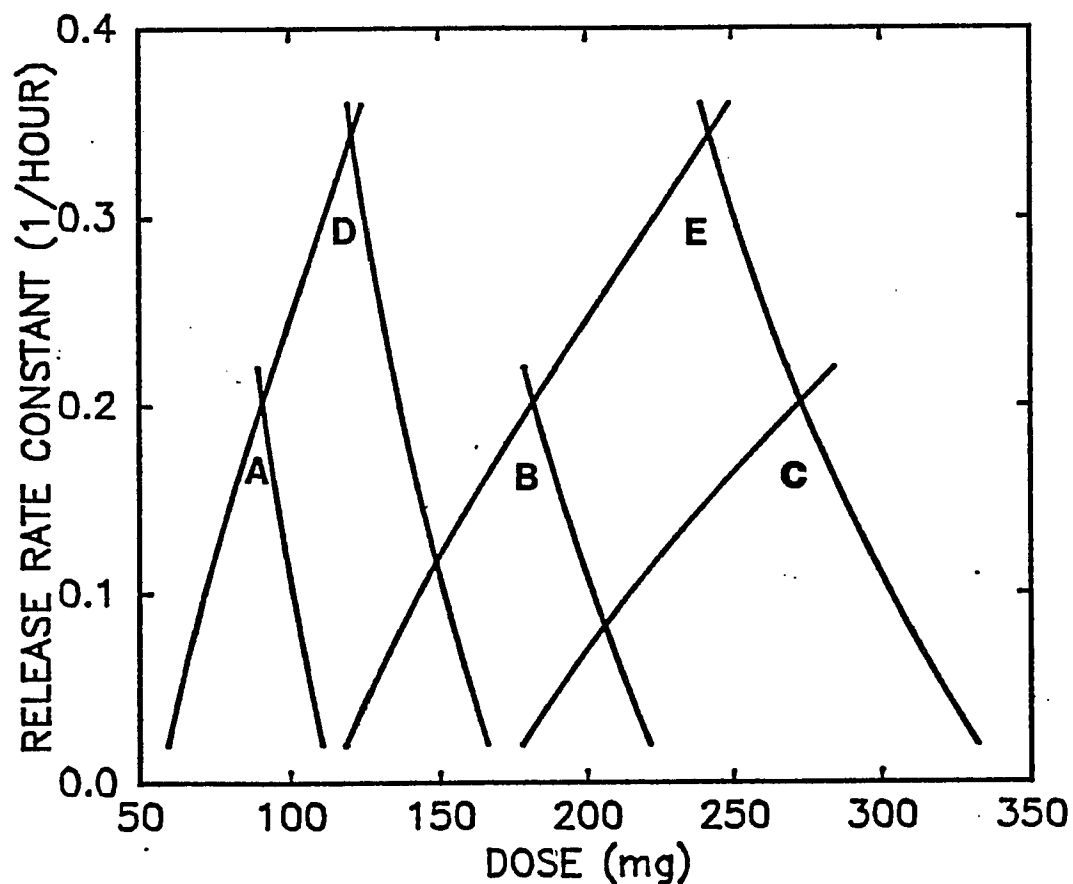


Figure 1.20:

Influence of therapeutic window on the release rate constant-dose profiles for a first-order DDS described by Scheme II. Therapeutic window: (A) 5-10 mg/L, (B) 10-20 mg/L, (C) 15-30 mg/L, (D) 5-15 mg/L, and (E) 10-30 mg/L. Pharmacokinetic parameters used: $k=0.21 \text{ h}^{-1}$, $k_a=5.0 \text{ h}^{-1}$, $V=4.5 \text{ L}$, and $\tau=12 \text{ hours}$.

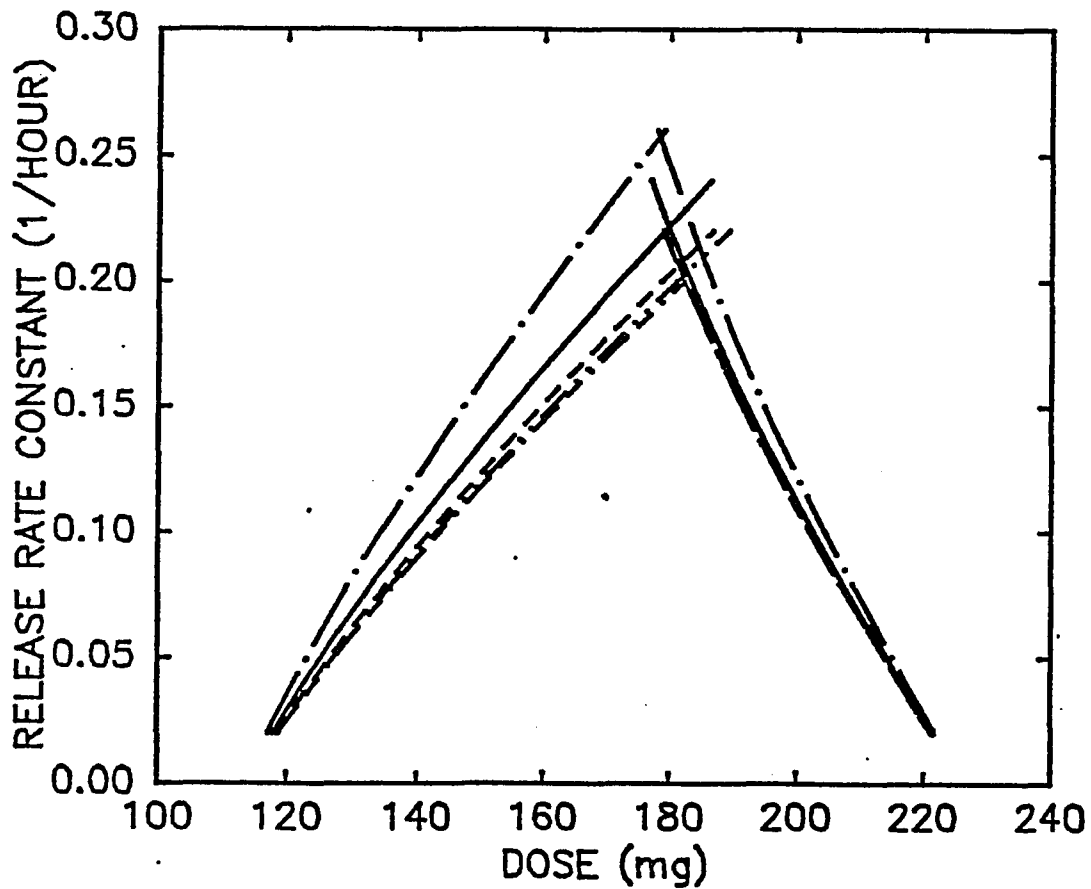


Figure 1.21: Influence of absorption on the release rate constant-dose profiles for a first-order DDS described by Scheme II. k_a used: 1.0 h^{-1} (— • —), 2.0 h^{-1} (—), 3.0 (----), 5.0 (— • • —), and 10 (- • -) h^{-1} Pharmacokinetic parameters used: $k=0.21 \text{ h}^{-1}$, $V=4.5 \text{ L}$, and $\tau=12$ hours.

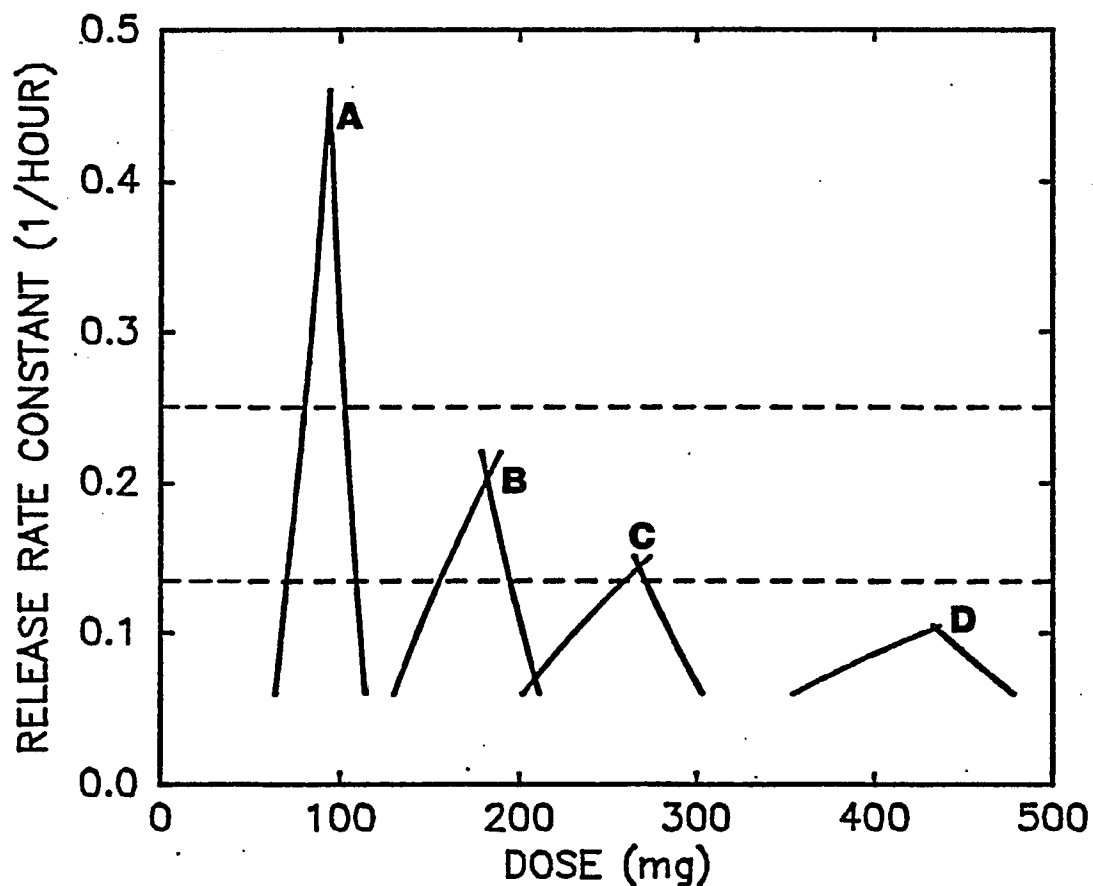


Figure 1.22:

Influence of elimination on the release rate constant-dose profiles for a first-order DDS described by Scheme II. k used: 0.11 (A), 0.21 (B), 0.31 (C), and 0.51 (D) h^{-1} . Pharmacokinetic parameters used: $k_a=10.0 \text{ h}^{-1}$, $V=4.5 \text{ L}$, and $\tau=12 \text{ hours}$. Dashed lines represent k required for a 95% ($k=0.250 \text{ h}^{-1}$) and 80% ($k=0.134 \text{ h}^{-1}$) payloads released during 12 hours interval.

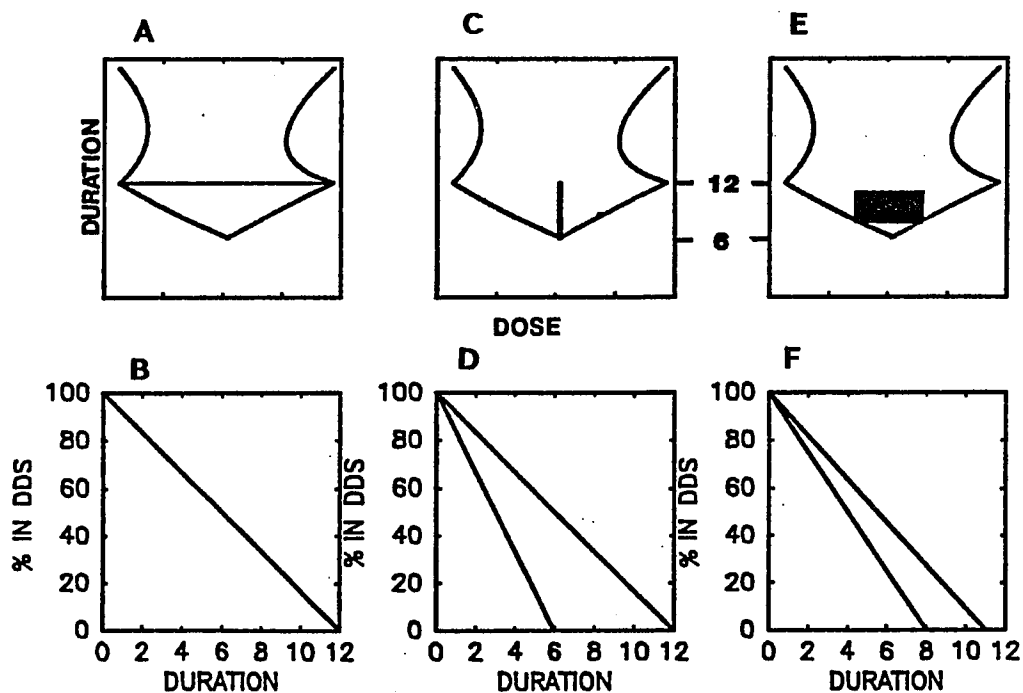


Figure 1.23: Possible specified targets for zero-order DDS design. A, C, and E are the duration-dose profile with different specified design target. B, D, and F are the corresponding release profiles for target A, C, and E, respectively. Explanations refer to the text.

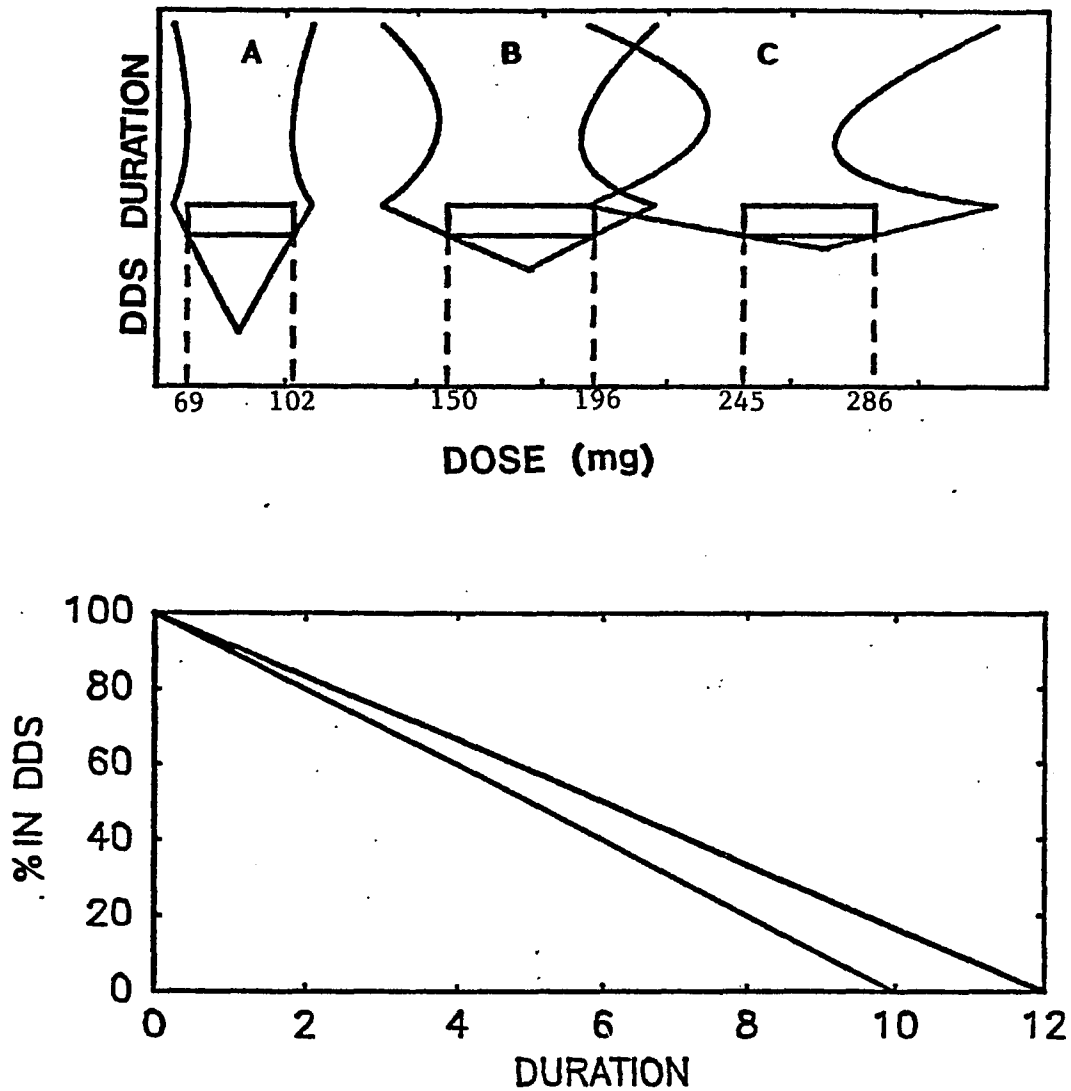


Figure 1.24: Determination of DDS specifications for a drug candidate with intersubject variation on the duration-dose profiles. A represents the duration-dose profiles for three patients. B represents the corresponding release profiles. Explanations refer to the text.

CHAPTER II
COMPUTER AIDED DOSAGE FORM DESIGN II:
CONTROLLED RELEASE THEOPHYLLINE DELIVERY
SYSTEMS

SUMMARY

The clinical pharmacokinetic properties of theophylline were used to define the required release rates and payloads for a controlled release drug delivery system (DDS). The selected goal was to describe oral delivery systems (zero-order and first-order) which would maintain steady state theophylline plasma concentrations between 10 and 20 mg/L when administered every 12 hours. Literature values for individual pharmacokinetic parameters for 10 children and 23 adults were employed. The individual required duration-dose profiles (zero-order DDS) and release rate constant-dose profiles (first-order DDS) were defined. In the case of zero-order systems, a minimum duration of 10 hours was required to accommodate all of the children and adults studied. However, the time required for first-order systems to release 90% of their payloads (T_{90}) was longer than 14 hours for adults and 18 hours for children in order to provide successful therapy for all of these patients. An apparent first-order controlled-release DDS having a release rate constant equal to 0.19 h^{-1} ($T_{90} = 12$ hours), while not ideal for every child, was also acceptable. Simulations using this DDS showed that the worst case did not differ significantly from the desired plasma concentrations. In addition, results show that different formulations are required for the pediatric and adult DDS. For the 10-hour duration zero-order system and the 12-hour T_{90} first-order system, a unit dose size of 120 mg is suggested for the pediatric DDS and 500 mg for the adult DDS. These represent the smallest theophylline payloads.

INTRODUCTION

The clinical pharmacokinetic properties of a candidate for a controlled release drug delivery system (DDS) can be employed to define, a priori, the release rates and payloads required to achieve the product goals.¹ The feasibility for success can be assessed by comparing these calculated specifications to what is possible using available technology. This approach provides a basis for establishing: (1) whether or not the drug is a good candidate for incorporation in the proposed drug delivery system; (2) the largest possible range of acceptable product specifications; (3) whether or not it is technically feasible to achieve specifications within this range, and (4) an ideal pattern to be used as a reference for the evaluation of product performance.

Theophylline was selected to illustrate the application of the previously developed theory to a specific drug.¹ Theophylline clinical pharmacokinetics and pharmacology in humans, together with the rationale for employing sustained release formulations, have been reviewed.^{2,3} In addition to the fact that extensive clinical pharmacokinetic data have been reported in humans, theophylline is also a drug with a well-documented, narrow, therapeutic window. This window, combined with high interpatient variability in clearance, necessitates carefully monitored administration with individualized dosage for safe and effective therapy.⁴ Theophylline therefore constitutes a challenging candidate for application of this theory since

the required pharmacokinetic data are known but the product specifications must take into account a narrow therapeutic window and a need for variable dosage requirements between patients.

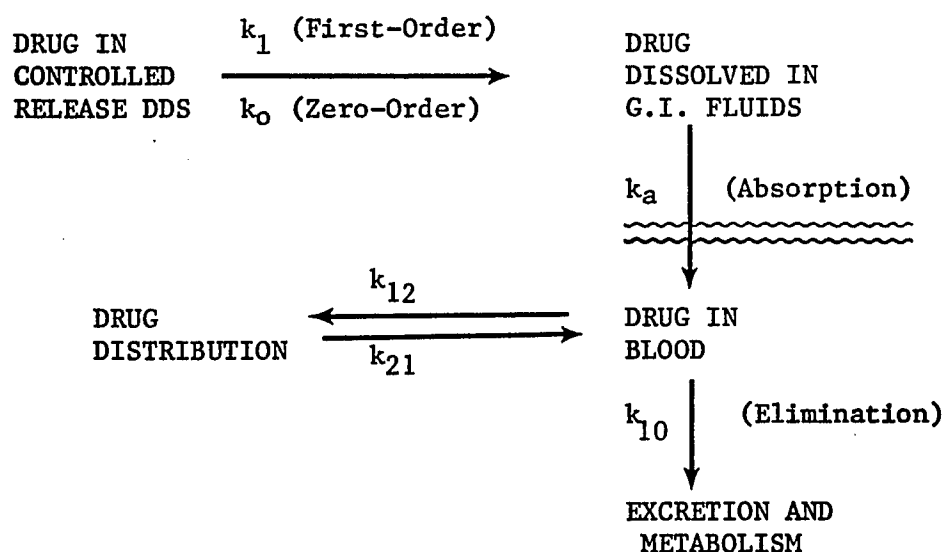
The selected goal for this computer-designed drug delivery system is to maintain steady-state plasma theophylline concentrations within the therapeutic window using a maintenance dosage interval of 12 hours. The specifications are based on two populations, adults and children, because of the well recognized higher clearance values in children relative to adults.⁴ Results will therefore be in the form of two different sets of product specifications.

THEORETICAL SECTION

The time course for the concentration (C) of theophylline in plasma following rapid intravenous administration has been described by:⁵⁻⁸

$$C = Ae^{-\alpha t} + Be^{-\beta t} \quad (2.1)$$

Therefore, Scheme I can be used to represent the oral administration of a drug delivery system (DDS) which releases theophylline with either a zero-order (k_0) or first-order (k_1) release rate constant.



Scheme I

The steady-state plasma concentration - time course equations for theophylline from a zero-order DDS are

$$\begin{aligned}
C^{SS} = \frac{1}{V_1} \left\{ \frac{(M+1)k_0k_a k_{21}}{k_a \alpha \beta} - \frac{k_0k_a(k_{21}-k_a)}{k_a(\alpha-k_a)(\beta-k_a)} \left(1 - \frac{(e^{k_a(\Delta t)}-1)e^{-k_a\tau}}{(1-e^{-k_a\tau})}\right) e^{-k_a t'} \right. \\
- \frac{k_0k_a(k_{21}-\alpha)}{\alpha(k_a-\alpha)(\beta-\alpha)} \left(1 - \frac{(e^{\alpha(\Delta t)}-1)e^{-\alpha\tau}}{(1-e^{-\alpha\tau})}\right) e^{-\alpha t'} - \frac{k_0k_a(k_{21}-\beta)}{\beta(k_a-\beta)(\alpha-\beta)} \left(1 - \frac{(e^{\beta(\Delta t)}-1)e^{-\beta\tau}}{(1-e^{-\beta\tau})}\right) e^{-\beta t'} \left. \right\} \quad (2.2)
\end{aligned}$$

where $0 \leq t' \leq \Delta t$ and

$$\begin{aligned}
C^{SS} = \frac{1}{V_1} \left\{ \frac{Mk_0k_a k_{21}}{k_a \alpha \beta} + \frac{k_0k_a(k_{21}-k_a)(e^{k_a(\Delta t)}-1)}{k_a(\alpha-k_a)(\beta-k_a)(1-e^{-k_a\tau})} e^{-k_a t'} + \right. \\
\left. \frac{k_0k_a(k_{21}-\alpha)(e^{\alpha(\Delta t)}-1)}{\alpha(k_a-\alpha)(\beta-\alpha)(1-e^{-\alpha\tau})} e^{-\alpha t'} + \frac{k_0k_a(k_{21}-\beta)(e^{\beta(\Delta t)}-1)}{\beta(k_a-\beta)(\alpha-\beta)(1-e^{-\beta\tau})} e^{-\beta t'} \right\} \quad (2.3)
\end{aligned}$$

where $\Delta t \leq t' \leq \tau$ and M and Δt are defined by

$$T = M(\tau) + \Delta t \quad (2.4)$$

The duration (T) of the DDS can be calculated from $T = D/k_0$ where D is the dose. Then M is the integer ratio between duration and the dosing interval (τ), $M = \text{INT}(T/\tau)$, and the remaining difference, Δt , has the limits $0 \leq \Delta t < \tau$.

In contrast, a single equation describes the steady-state concentration for a first-order release DDS.

$$C^{SS} = \frac{k_1 k_a D_0}{V_1} \left\{ \frac{(k_{21} - k_1)}{(k_a - k_1)(\alpha - k_1)(\beta - k_1)(1 - e^{-k_1 \tau})} e^{-k_1 t'} + \right. \\ \frac{(k_{21} - k_a)}{(k_1 - k_a)(\alpha - k_a)(\beta - k_a)(1 - e^{-k_a \tau})} e^{-k_a t'} + \\ \frac{(k_{21} - \alpha)}{(k_1 - \alpha)(k_a - \alpha)(\beta - \alpha)(1 - e^{-\alpha \tau})} e^{-\alpha t'} + \\ \left. \frac{(k_{21} - \beta)}{(k_1 - \beta)(k_a - \beta)(\alpha - \beta)(1 - e^{-\beta \tau})} e^{-\beta t'} \right\} \quad (2.5)$$

By using the reported pharmacokinetic parameters for theophylline⁵⁻⁷ in these steady-state equations, profiles representing the acceptable duration of the DDS versus the dose for a zero-order DDS and the release rate constant versus the dose for a first-order DDS can be established.¹

Duration-Dose Profiles for a Zero-Order Release Theophylline DDS --

The boundaries for the region of acceptable product specifications for successful zero-order release drug delivery systems can be determined by eqs. 2.6 and 2.7.

$$D_{\min} = \{C_{\min} V_1 (M\tau + \Delta t)\} \div \left\{ \frac{(M+1)}{k_{10}} - \frac{(k_{21} - \alpha)}{\alpha(\beta - \alpha)} \left[1 - \frac{(e^{\alpha(\Delta t)} - 1)e^{-\alpha \tau}}{(1 - e^{-\alpha \tau})} \right] e^{-\alpha t_{\min}} \right. \\ \left. - \frac{(k_{21} - \beta)}{\beta(\alpha - \beta)} \left[1 - \frac{(e^{\beta(\Delta t)} - 1)e^{-\beta \tau}}{(1 - e^{-\beta \tau})} \right] e^{-\beta t_{\min}} \right\} \quad (2.6)$$

$$D_{\max} = \{C_{\max}V_1(M\tau + \Delta t)\} \div \left\{ \frac{M}{k_{10}} + \frac{(k_{21} - \alpha)(e^{\alpha(\Delta t)} - 1)}{\alpha(\beta - \alpha)(1 - e^{-\alpha\tau})} e^{-\alpha t_{\max}} \right. \\ \left. + \frac{(k_{21} - \beta)(e^{\beta(\Delta t)} - 1)}{\beta(\alpha - \beta)(1 - e^{-\beta\tau})} e^{-\beta t_{\max}} \right\} \quad (2.7)$$

where t_{\min} and t_{\max} are the times of minimum and maximum steady-state plasma concentration during a single dosing interval respectively, where $0 \leq t \leq \tau$. The C_{\min} and C_{\max} values represent the plasma concentration range desired for the drug during therapy. These two equations can be further simplified to eqs. 2.8 and 2.9 with the approximations, $t_{\min} = 0$ and $t_{\max} = \Delta t$.¹

$$D_{\min} = \{C_{\min}V_1(M\tau + \Delta t)\} \div \left\{ \frac{(M+1)}{k_{10}} - \frac{(k_{21} - \alpha)}{\alpha(\beta - \alpha)} \left[1 - \frac{(e^{\alpha(\Delta t)} - 1)e^{-\alpha\tau}}{(1 - e^{-\alpha\tau})} \right] \right. \\ \left. - \frac{(k_{21} - \beta)}{\beta(\alpha - \beta)} \left[1 - \frac{(e^{\beta(\Delta t)} - 1)e^{-\beta\tau}}{(1 - e^{-\beta\tau})} \right] \right\} \quad (2.8)$$

$$D_{\max} = \{C_{\max}V_1(M\tau + \Delta t)\} \div \left\{ \frac{M}{k_{10}} + \frac{(k_{21} - \alpha)(1 - e^{-\alpha(\Delta t)})}{\alpha(\beta - \alpha)(1 - e^{-\alpha\tau})} \right. \\ \left. + \frac{(k_{21} - \beta)(1 - e^{-\beta(\Delta t)})}{\beta(\alpha - \beta)(1 - e^{-\beta\tau})} \right\} \quad (2.9)$$

Release Rate-Dose Profiles for a First-Order Release Theophylline DDS

-- As reported previously,¹ the product specification boundaries for successful first-order release theophylline delivery systems can be determined by eqs. 2.10 and 2.11.

$$D_{\min} = \left\{ \frac{C_{\min} V_1}{k_1 k_a} \right\} \div \left\{ \frac{(k_{21} - k_1)}{(k_a - k_1)(\alpha - k_1)(\beta - k_1)(1 - e^{-k_1 \tau})} e^{-k_1 t_{\min}} + \frac{(k_{21} - k_a)}{(k_1 - k_a)(\alpha - k_a)(\beta - k_a)(1 - e^{-k_a \tau})} e^{-k_a t_{\min}} + \frac{(k_{21} - \alpha)}{(k_1 - \alpha)(k_a - \alpha)(\beta - \alpha)(1 - e^{-\alpha \tau})} e^{-\alpha t_{\min}} + \frac{(k_{21} - \beta)}{(k_1 - \beta)(k_a - \beta)(\alpha - \beta)(1 - e^{-\beta \tau})} e^{-\beta t_{\min}} \right\} \quad (2.10)$$

$$D_{\max} = \left\{ \frac{C_{\max} V_1}{k_1 k_a} \right\} \div \left\{ \frac{(k_{21} - k_1)}{(k_a - k_1)(\alpha - k_1)(\beta - k_1)(1 - e^{-k_1 \tau})} e^{-k_1 t_{\max}} + \frac{(k_{21} - k_a)}{(k_1 - k_a)(\alpha - k_a)(\beta - k_a)(1 - e^{-k_a \tau})} e^{-k_a t_{\max}} + \frac{(k_{21} - \alpha)}{(k_1 - \alpha)(k_a - \alpha)(\beta - \alpha)(1 - e^{-\alpha \tau})} e^{-\alpha t_{\max}} + \frac{(k_{21} - \beta)}{(k_1 - \beta)(k_a - \beta)(\alpha - \beta)(1 - e^{-\beta \tau})} e^{-\beta t_{\max}} \right\} \quad (2.11)$$

Using the approximation $t_{\min} = 0$, eq. 2.10 can be further simplified to eq. 2.12. However, t_{\max} cannot be approximated and must be determined by computer reiterative techniques.⁹

$$\begin{aligned}
 D_{\min} = \left\{ \frac{C_{\min} V_1}{k_1 k_a} \right\} & \div \left\{ \frac{(k_{21} - k_1)}{(k_a - k_1)(\alpha - k_1)(\beta - k_1)(1 - e^{-k_1 \tau})} + \right. \\
 & \frac{(k_{21} - k_a)}{(k_1 - k_a)(\alpha - k_a)(\beta - k_a)(1 - e^{-k_a \tau})} + \\
 & \frac{(k_{21} - \alpha)}{(k_1 - \alpha)(k_a - \alpha)(\beta - \alpha)(1 - e^{-\alpha \tau})} + \\
 & \left. \frac{(k_{21} - \beta)}{(k_1 - \beta)(k_a - \beta)(\alpha - \beta)(1 - e^{-\beta \tau})} \right\} \quad (2.12)
 \end{aligned}$$

EXPERIMENTAL

Values for theophylline pharmacokinetic parameters (k_{12} , k_{21} , k_{10} and V_1) for each of ten children, ages 1 to 5 years old, reported by Loughnan *et al*⁶ and those for each of 7 adults determined by Kaumeier *et al*⁸ and 16 adults determined by Mitenko *et al*¹⁰ were used in the current study. However, due to the lack of reported body weight information in the Mitenko *et al*,¹⁰ study, those 16 patients were used only in the discussions of parameters that do not require the body weight. For parameters which require individual body weights, such as the individual required doses, data for the 7 adults and 10 children were used.

The oral absorption of theophylline in solution is known to be rapid and complete in children and adults.² Reported estimates for k_a (h^{-1}) in adults range from 2.9 to 8.9 h^{-1} .¹¹ An estimated mean k_a value of 2.6 h^{-1} following oral administration of an aqueous solution of choline theophylline in 6 children (0.6 to 4.5 years old) was reported by Bolme *et al*.¹⁰ The k_a values used in this study are 2.6 h^{-1} (children) and 2.9 h^{-1} (adults).

Calculations are based on oral administration of one controlled release theophylline delivery system to each of the ten children and twenty-three adults every 12 hours. The goal used was to maintain steady-state plasma theophylline concentrations (C^{SS}) within the therapeutic window of 10 to 20 mg/L.⁴ The acceptable duration-dose profiles (duration profiles) representing successful theophylline

zero-order systems were determined using eqs. 2.6 and 2.7 which calculate the minimum and maximum dose sizes for each specified duration. In the case of a first-order theophylline DDS, the release rate constant-dose profiles (delivery profiles) were defined by calculating the minimum and maximum required dose sizes for each individual release rate constant using eqs. 2.10 and 2.11. For the 16 adults studied by Mitenko et al,¹⁰ the absolute values for the volume of the central compartment (V_1 in L) cannot be determined since the body weights for these patients were not reported. Consequently, the dose sizes calculated for these patients using eqs. 2.6, 2.7, 2.10, and 2.11 provide dose per unit body weight (mg/kg) instead of total dose (mg). Therefore, only those seven adults reported by Kaumeier et al⁸ were used in the selection of dose size for the adult DDS.

RESULTS AND DISCUSSION

As previously demonstrated,¹ the product specifications for a successful zero-order or first-order release system can be defined using the observed clinical pharmacokinetic properties of the drug candidate. Therefore, each drug and dosage form presents a unique problem for the application of this approach. Theophylline was chosen to demonstrate how to apply this theory to the selection of performance characteristics for delivery systems employing a 12-hour dosing interval with a narrow therapeutic window and significant interpatient variability in clearance.

Zero-order Release -- The acceptable zero-order duration-dose profiles for two of the ten children (AP and GL) and that determined by the mean pharmacokinetic parameters for those ten children are shown in Fig. 2.1. In addition, the duration-dose profiles for each child are shown in Fig. 2.2. Figure 2.1 shows why profiles that are defined using mean values of pharmacokinetic parameters cannot be used to satisfy the individual patient's dosage requirements for theophylline. Figure 2.3 shows the acceptable duration-dose profiles for two of seven adults (1 and 7) and that determined by the mean values of the pharmacokinetic parameters for those seven adults. Figure 2.4 shows the profiles for all of those seven adults.

Each subject presents a unique profile and each profile has a different minimum required duration T_{\min} and effective dose range. The differences between these profiles are due mainly to intersubject

variability in clearance (CL).¹ Consequently, the selection of delivery system specifications must allow individualized theophylline dosing to provide successful therapy by considering each patient's requirements.

These duration-dose profiles are used to define both parameters of the DDS: ideal duration and dose size. Once these two parameters are selected, the release rate is determined since zero-order release rate is defined as dose/duration.

It is necessary to establish the T_{\min} value required for each subject in order to determine the ideal duration. These T_{\min} values can be observed in the duration-dose profiles constructed using eqs. 2.6 and 2.7 (Figs. 2.2 and 2.4) or from the duration-dose profiles determined using eqs. 2.8 and 2.9 when absorption is a sufficiently fast process. In addition, when absorption is fast and assuming that the steady state plasma concentration-time course during time period of $t' \geq \Delta t$ is approximately mono-exponential, the T_{\min} can be estimated using eq. 2.13,¹

$$T_{\min} = \tau - (\ln T.I. / \beta) \quad (2.13)$$

where the therapeutic index is defined as $T.I. = C_{\max}/C_{\min}$.¹³ Tables 2.1 and 2.2 summarize the T_{\min} values for children and adults.

The ideal delivery system duration should be equal to or longer than the minimum value observed for all of the patients. Figure 2.5 shows the relationship between the duration and the percentage of patients which would receive satisfactory therapy by combining this

duration with an appropriate dose size. As seen in this histogram, the minimum required duration to accommodate all of the patients is 9 hours for 7 adults or 10 hours for all 23 adults and 10 hours for children. The calculated duration for adults is in agreement with the reported duration of the zero-order release DDS, Theo-Dur, which was observed by Spangler et al. to be 9.2 hours.¹⁴

The required payload depends upon the duration of the DDS. When the duration is an exact integer multiple of τ , the dose size range can be determined by eqs. 2.14 and 2.15.

$$D_{\min}^{T=n\tau} = (C_{\min})(CL)(\tau) \quad (2.14)$$

$$D_{\max}^{T=n\tau} = (C_{\max})(CL)(\tau) \quad (2.15)$$

where CL is the total body clearance of the drug and $D_{\min}^{T=n\tau}$ and $D_{\max}^{T=n\tau}$ are the minimum and maximum dose sizes for a DDS with $T = n\tau$. Assuming all of the payload is absorbed, this is a reliable indication of the maximum dose range for a zero-order release DDS. This is a useful first step since it provides largest degree of dosage flexibility for each patient. However, it would be very restrictive to use this range for the design of a delivery system since it requires that the duration must be an integer multiple of τ .

Figure 2.6 is a histogram showing how the dosage ranges change as a function of product duration using two children as examples. Although the observed dosage ranges change markedly as the durations change, all of these ranges fall within the maximum range

calculated from eqs. 2.14 and 2.15. As illustrated by patient MG, the observed change in dose range is not significant in some patients. In contrast, this change can be too large to be ignored (patient JL). Whether this change in dose range as a function of duration is significant or not is dependent upon the drug clearance value in a particular patient. The larger the clearance, the more significant will be the change in dose range. Therefore, maximum flexibility for defining product specifications can only be realized by examining the duration-dose profiles for the entire group and not by the limited estimate at $T = n\tau$. This can be achieved as described below.

Theophylline pharmacokinetics show a high degree of intersubject variability. Each patient presents a unique dosing problem.⁴ As shown by the duration-dose profiles for these patients (Figs. 2.2 and 2.4), each subject has an individual required dose range. An ideal theophylline delivery system must allow clinical dosage adjustment to provide appropriate plasma levels for each patient. Tables 2.3 and 2.4 summarize the individual maintenance dose ranges for both children and adults using a 12 hour dosage interval. As seen in these tables, a 10 hour zero-order release DDS of 120 mg provides sufficient flexibility to dose all of the children in this study. A 500 mg 10-hour DDS would accommodate the 7 adults. The number of units to be given every 12 hours to each patient for acceptable individualization is also listed.

Even though the suggested maximum 12-hour maintenance dose for theophylline without serum monitoring is 300 mg for adults whose body weights range from 35 to 70 kg and 450 mg for those with body weights greater than 70 kg,¹⁵ some patients may require doses as high as 1600 mg.¹⁶ Using the steady state trough and peak levels observed during a multiple dose study with a commercially available zero-order theophylline sustained release product,¹⁴ 11 out of the 12 adults studied would require maintenance doses ranging from 280 to 1400 mg every 12 hours to provide a steady state plasma time course within the window of 10 to 20 mg/L assuming a body weight of 70 kg and linear kinetics to calculate the dose.

In addition, adults usually require a smaller dose than children when doses are normalized according to their total body weights.⁴ In this study, the normalized dose range for children is 6.8 to 39.3 mg/kg while that for adults is 4.4 to 24.9 mg/kg for 22 out of 23 subjects. However, it is necessary to design two different systems, specifically for adults and children, since the total dosage ranges for these two groups do not overlap (see selected DDS ranges).

First Order Release -- Although zero-order release is considered ideal, prolonged action can also be achieved through controlled exponential release (apparent first order).¹³ The release rate constant-dose profiles for first-order systems are shown in Figs. 2.7 (children) and 2.8 (adults). The mathematical solution for the duration required for 100% release from a first-order system is infinite time. It is therefore necessary to select a practical limit for the duration. If 12 hours is

selected as the time for 90% delivery, T_{90} , the release rate constant, k_1 , value is 0.192 h^{-1} . This value is indicated by the broken lines in Figs. 2.7 and 2.8. As seen in Fig. 2.7, only 5 of the 10 children would be maintained within the therapeutic window (10-20 mg/L) when properly dosed every 12 hours with this DDS. In contrast, all 7 adults in Fig. 2.8 would exhibit satisfactory concentrations taking the appropriate dose of a DDS with $k_1 = 0.192 \text{ h}^{-1}$ every 12 hours.

Figure 2.9 summarizes the relationship between the percentage of patients having acceptable steady-state theophylline concentrations and the T_{90} values for the delivery systems. As seen in this histogram, the minimum T_{90} value required to accommodate all 7 adults is only 8 hours ($k_1 = 0.288 \text{ h}^{-1}$) and 14 hours for all 23 adults ($k_1 = 0.164 \text{ h}^{-1}$) whereas that required for all 10 children is 18 hours ($k_1 = 0.128 \text{ h}^{-1}$). A DDS with a T_{90} value of 18 hours would deliver only 79% of the payload during a 12-hour period. This would predispose the product to bioavailability problems since gastrointestinal transit time may not be sufficiently long to allow adequate delivery. Although $T_{90} = 12$ hours accommodated only half the children (Fig. 2.9), simulations which combine this release rate constant with the dose corresponding to each peak k_1 value in Fig. 2.7, provided steady-state concentrations within or close to the therapeutic window in all cases. The greatest deviation was observed for patient GF (Fig. 2.7, No. 7) where the observed steady-state range was 8.2 to 22.9 mg/L. Of the two choices, $T_{90} = 12$ hours represents a more practical compromise than $T_{90} = 18$ hours since the observed deviation using the 12-hour

T90 is small. However, tailoring the dose size for at least half the subjects would become difficult due to the relatively narrow dose range (Table 2.3).

In addition to the selection of an adequate release rate constant, the unit dose size must also be determined. The approach used for zero-order systems can also be applied to first-order drug delivery. The dosage ranges associated with each release rate are listed for the individual subjects in Tables 2.3 and 2.4. Although the individual dosage ranges differ for the various release rates, a 120 mg unit size would accommodate all of the children (Table 2.3) and a 500 mg unit size all of the adults (Table 2.4) independent of the order. Individualization of regimens, which is required for theophylline, would be achieved by administering one to three units every 12 hours as shown in the tables. Theophylline serum concentrations would have to be used to individualize the regimen for each patient.

CONCLUSIONS

The clinical pharmacokinetic properties of a candidate for a controlled release drug delivery system (DDS) can be employed to define, a priori, the release rate constants and payloads required to achieve the product goal. The application of these methods to describe a theophylline DDS for children and adults has been used to illustrate the methodology. Although adults usually require less theophylline than children, when the doses are normalized according to total body weight,⁴ the results in this study show that adults require a larger DDS payload because they require a larger total dose of theophylline. This is primarily due to the differences in the total body weights. In addition, the product specifications for the adult system show a broader range of release patterns for both the zero-order and first-order systems. This is due to the fact that theophylline has a longer biological half-life and reduced clearance in adults relative to children.

Although both zero-order and first-order theophylline systems for children and adults were described in this report, the zero-order DDS represents a better choice for theophylline. The first-order theophylline DDS required at least 18 hours for 90% release in children and 14 hours in adults. Under these circumstances, bioavailability would become a primary limitation for the first-order systems. However, a zero-order DDS of 10 hour duration satisfied the requirements for both children and adults and this represents a more reasonable choice considering the gastrointestinal transit time.

The theories developed for defining the required product specifications of controlled release drug delivery systems using clinical pharmacokinetic approach not only provide the widest acceptable product specifications a priori, but also aid in choosing the release pattern goal for development of the DDS. Figure 2.10 shows the required release rate profiles for both zero-order and first-order theophylline DDS for children and adults. It indicates that zero-order technology is clearly more likely to succeed and easier to achieve. First-order systems for children require a release rate constant providing 90% release in 18 hours. While either zero- or first-order release may be acceptable for adults, zero-order still remains the better choice since it provides a range of acceptable release rates not observed for the first-order case.

REFERENCES

1. T.Y. Lee, Chapter I, this dissertation, p.1 (1986).
2. F.W.H.M. Merkus and L. Hendeles. Eds., Sustained Release Theophylline: A Biopharmaceutical Challenge to a Clinical Need, Excerpta Medica, Amsterdam, 1983.
3. J.H.G. Johnson, J.W. Jenne, and F.E.R. Simons, Eds., Sustained Release Theophylline in the Treatment of CRAO, Excerpta Medica, Amsterdam, 1984.
4. R.E. Notari, Biopharmaceutics and Clinical Pharmacokinetics an Introduction, 3rd. ed., Marcel Dekker, Inc., New York, N.Y., 1980.
5. G. Levy and R. Koysooko, Pharmacokinetic Analysis of the Effect of Theophylline on Pulmonary Function in Asthmatic Children, J. of Pediatrics, 86, 789 (1976).
6. E.F. Ellis, R. Koysooko, and G. Levy, Pharmacokinetics of Theophylline in Children with Asthma, Pediatrics, 58, 542 (1976).
7. P.M. Loughnan, D.S. Sitar, R.I. Ogilvie, A. Eisen, Z. Fox, and A.H. Neims, Pharmacokinetic Analysis of the Disposition of Intravenous Theophylline in Young Children, J. Pediatrics, 5, 874 (1976).
8. H.S. Kaumeier, O.H. Kehrhahn, G. Neugebauer, D. Schuppan, J.A. Schwarz, and A.H. Staib, A Cross-over Study of Oral and Intravenous Administration of Theophylline in Male Volunteers, Arzneim-Forsch, 34, 92 (1984).
9. M. Abramowitz and I.A. Stegun, Eds., Handbook of Mathematical Functions with Formulas, Graphs, and Mathematical Tables, National Bureau of Standards Applied Mathematics Series 55, U.S. Department of Commerce, U.S. Government Printing Office, Washington, D.C., 1972, p.18.
10. P.A. Mitenko and R.I. Ogilvie, Pharmacokinetics of Intravenous Theophylline, Clin. Pharmacol. Therap., 14, 509 (1973).
11. P.G. Welling, L.L. Lyons, W.A. Craig, and G.A. Trachta, Influence of Diet and Fluid on Bioavailability of Theophylline, Clinical Pharmacology and Therapeutics, 17, 475 (1975).

12. P. Bolme, M. Eriksson, G. Lonnerholm, and L. Paalzow, Pharmacokinetics and Dose Regimen of Theophylline in Children, *Acta Pharmacol. et. Toxicol.*, 51, 401 (1982).
13. P.R. Byron, R.E. Notari, and M-Y Huang, Pharmacokinetic Prediction of Optimum Drug Delivery Rates from Prodrugs Designed for Maximum Duration, *Intern. J. Pharm.*, 1, 219 (1978).
14. D.L.Spangler, D.D. Kalof, F.L. Bloom, and H.J. Wittig, Theophylline Bioavailability Following Oral Administration of Six Sustained-Release Preparations, *Annals of Allergy*, 40, 6 (1978).
15. E.R Barnhart (Publisher), *Physicians' Desk Reference*, 40th ed. Medical Economics Company Inc., Oradell, N.J., 1986, p. 972.
16. G.S. Avery, Ed., *Drug Treatment, Principles and Practice of Clinical Pharmacology and Therapeutics*, Publishing Sciences Group Inc., Acton, MA, 1976, p.571.

Table 2.1

The Minimum Required Duration (T_{\min}) of Theophylline
Zero-Order Release DDS for Children

Patient(No.) ^a	T_{\min} (Hours)		
	Predicted ^b	Observed ^c	Observed ^d
AP (1)	6.49	6.10	6.70
MG (2)	7.43	7.10	7.50
DN (3)	9.03	9.00	9.40
JM (4)	8.15	8.00	8.40
EC (5)	8.15	8.10	8.50
JC (6)	9.21	9.00	9.30
GF (7)	10.13	9.90	10.30
MA (8)	8.20	7.90	8.30
JL (9)	9.73	9.70	10.10
GL (10)	9.50	9.40	9.80

^aNumbers refer to Figure 2.1, initials refer to reference (7).

^bCalculated using $T_{\min} = \tau - \ln(T.I.)/\beta$.

^cObserved from duration-dose profiles determined using eqs. 2.5 and 2.6.

^dObserved from duration-dose profiles determined using eqs. 2.7 and 2.8.

Table 2.2

The Minimum Required Duration (T_{\min}) of Theophylline
Zero-Order Release DDS for Adults

Patient ^a	T_{\min} (Hours)		
	Predicted ^b	Observed ^c	Observed ^d
1	4.65	4.20	4.80
2	3.61	3.40	4.10
3	2.94	2.40	3.30
4	5.70	5.40	5.90
5	5.69	5.50	6.00
6	7.12	6.80	7.20
7	8.43	8.20	8.60

^aNumbers refer to reference (8).

^bCalculated using $T_{\min} = \tau - \ln(T.I.)/\beta$.

^cObserved from duration-dose profiles determined using eqs. 2.5 and 2.6.

^dObserved from duration-dose profiles determined using eqs. 2.7 and 2.8.

Table 2.3

Individual 12-Hour Maintenance Dose Range for Oral
Theophylline Delivery Systems in Children.

The Selected Drug Delivery System (DDS) Represents One Potential Unit Size.

Patient(No.) ^a	Dose Range (mg)			Selected DDS ^b	
	$k_o=D/10h$	T90=12h $k_1=0.190h^{-1}$	T90=18h $k_1=0.13h^{-1}$	(mg)	Units
AP (1)	88-140	99-135	92-140	120	1
MG (2)	105-161	120-153	110-160	120	1
DN (3)	150-190	(175) ^c	153-186	180	1.5
JM (4)	164-233	191-219	170-231	180	1.5
EC (5)	167-230	194-220	173-233	180	1.5
JC (6)	196-253	(233) ^c	204-247	240	2
GF (7)	235-244	(230) ^c	230	240	2
MA (8)	213-306	249-288	222-301	240	2
JL (9)	339-375	(350) ^c	335-359	360	3
GL (10)	363-432	(399) ^c	367-417	360	3

^aNumbers refer to Fig.2.1; Initials refer to reference (7).

^bUnit dose size = 120 mg/DDS.

^cTaken from the dose at peak k_1 value.

Table 2.4

**Individual 12-Hour Maintenance Dose Range for Oral
Theophylline Delivery Systems in Adults.**

The Selected Drug Delivery System (DDS) Represents One Potential DDS Unit Size.

Patient	Dose Range (mg)		Selected DDS ^a	
	$k_o = D/10h$	$T_{90}=12h$ $k_1=0.190h^{-1}$	(mg)	Units
1	364- 612	399- 598	500	1
2	371- 631	403- 620	500	1
3	500- 867	540- 852	750	1.5
4	499- 815	555- 791	750	1.5
5	575- 933	639- 906	750	1.5
6	629- 973	719- 932	750	1.5
7	1161-1630	1378-1525	1500	3

^aUnit dose size = 500 mg/DDS

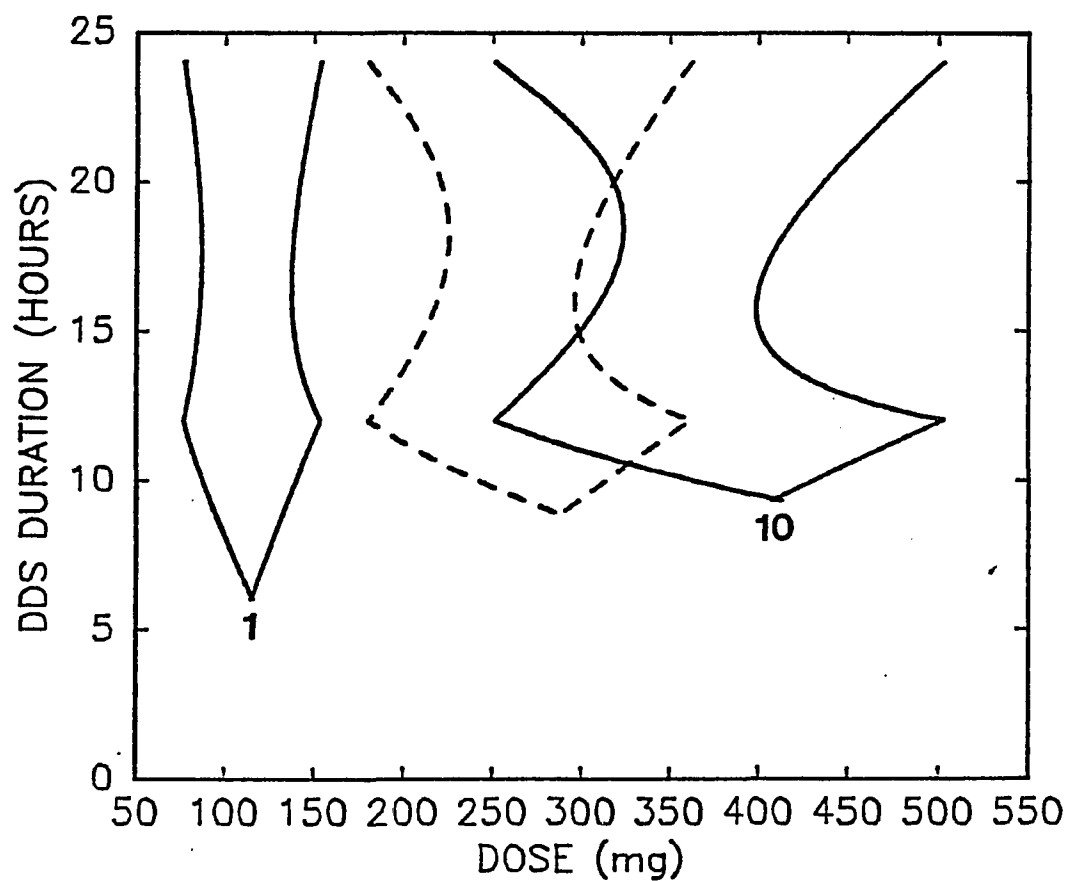


Figure 2.1: Duration versus dose profiles for zero-order delivery systems orally administered every 12 hours to children AP(1) and GL(10). The dashed curve profile is the profile defined by the mean values of pharmacokinetic parameters for the ten children in Table 2.1. The specifications within each profile provide steady state theophylline plasma concentrations within the range of 10 to 20 mg/L in the corresponding patient.

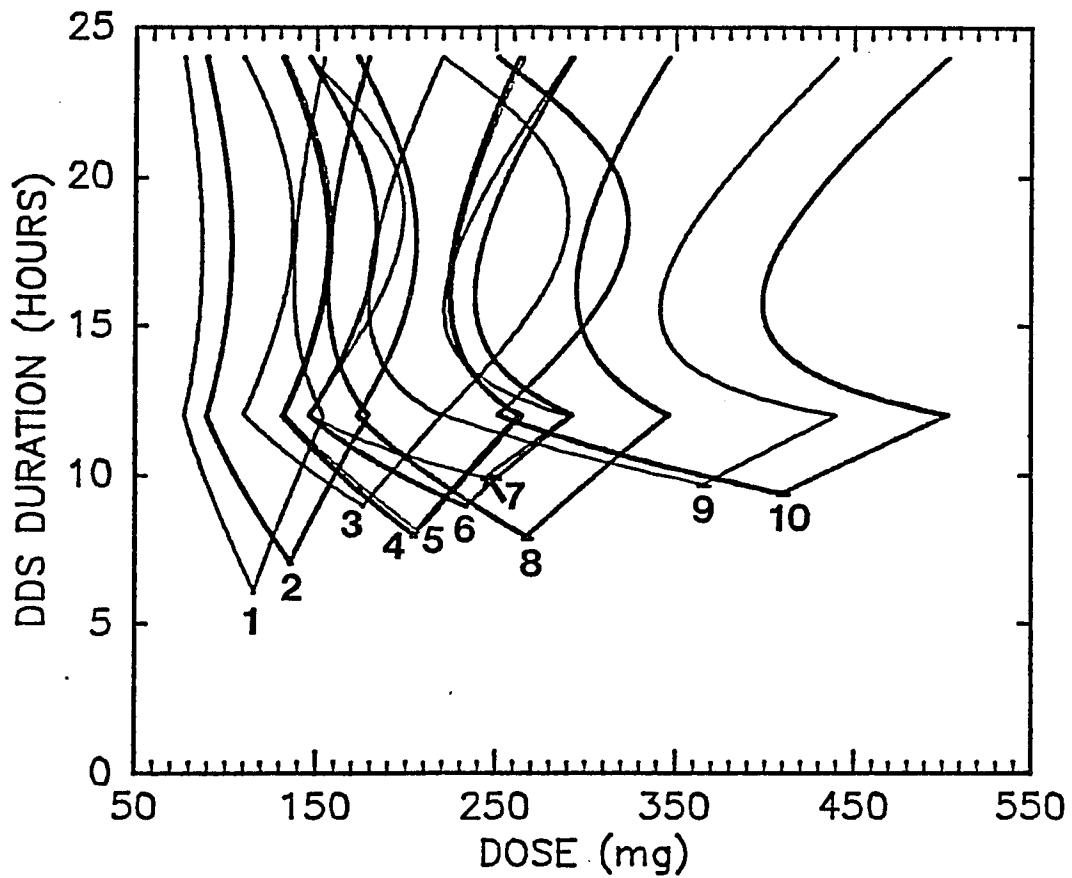


Figure 2.2: Duration versus dose profiles for zero-order delivery systems orally administered every 12 hours to the ten children in Table 2.1. The specifications within each profile provide steady state theophylline plasma concentrations within the range of 10 to 20 mg/L in the corresponding patient.

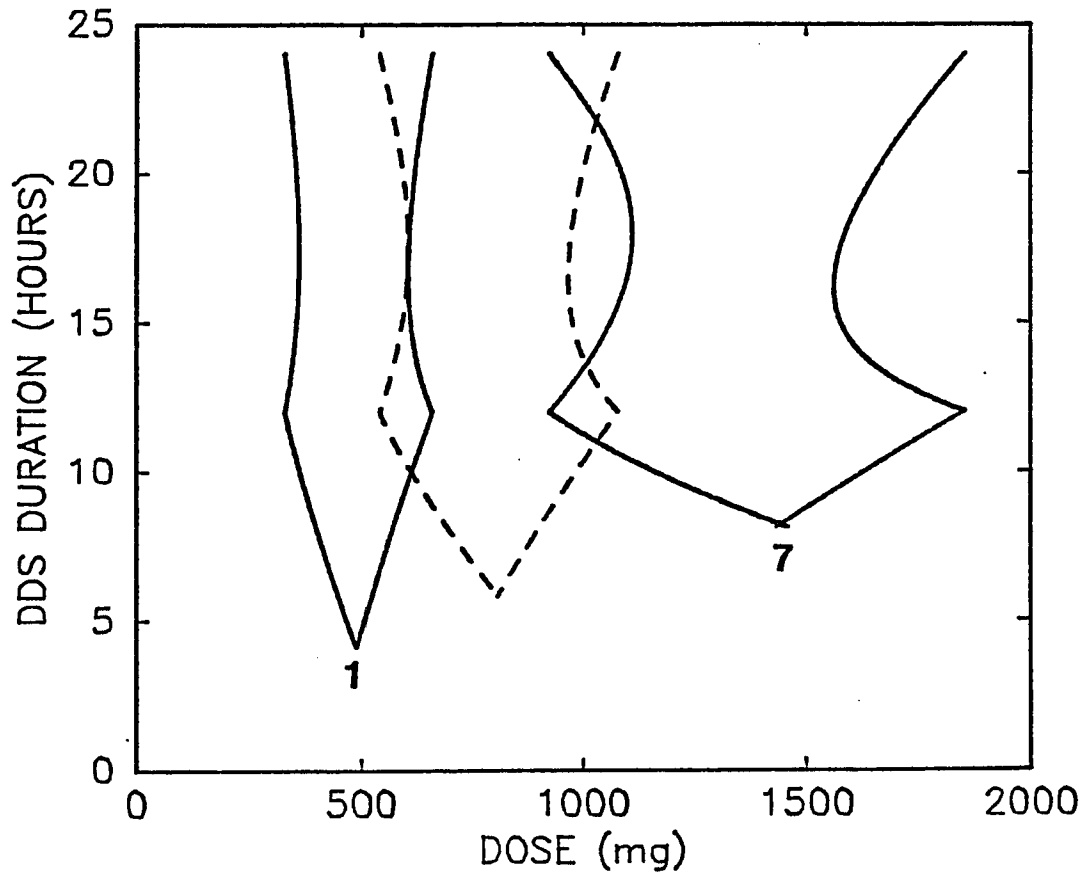


Figure 2.3: Duration versus dose profiles for zero-order delivery systems orally administered every 12 hours to adults (1 and 7). The dashed curve profile is the profile defined by the mean values of pharmacokinetic parameters for the seven adults in Table 2.2. The specifications within each profile provide steady state theophylline plasma concentrations within the range of 10 to 20 mg/L in the corresponding patient.

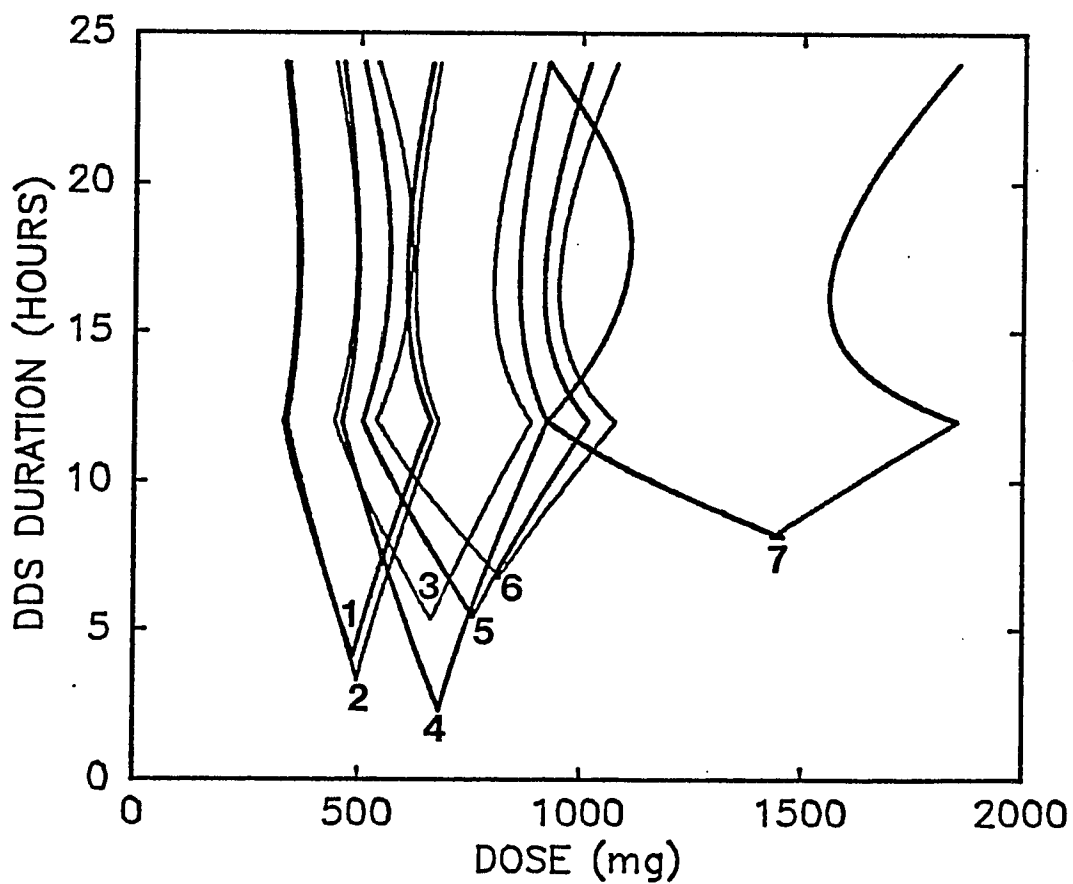


Figure 2.4: Zero-order dosage form duration versus dose profiles for the seven adults in Table 2.2 based on a 12-hour dosage interval which maintains steady-state theophylline plasma concentrations within the range of 10 to 20 mg/L.

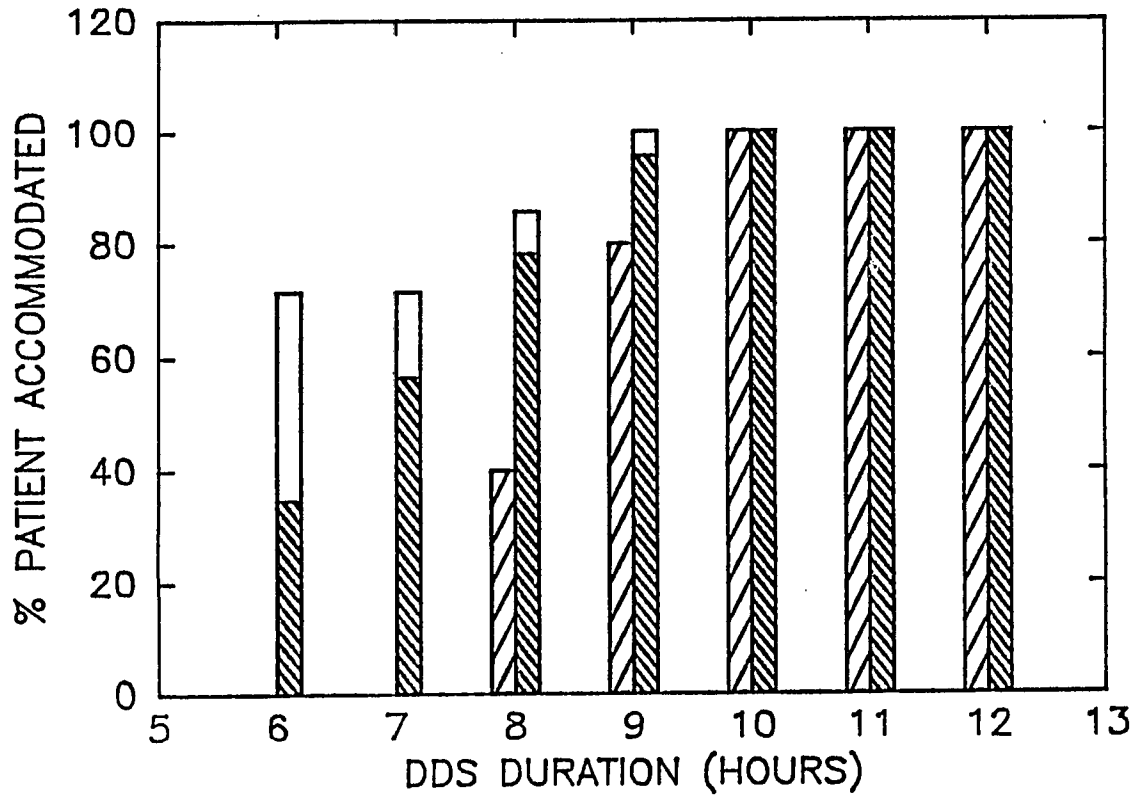


Figure 2.5: The percentage of patients having steady-state theophylline plasma concentrations between 10 and 20 mg/L as a function of the duration of the zero-order delivery systems given every 12 hours:
 ▨ children (n=10); ▩ adults (n=23),
 □ adults (n=7).

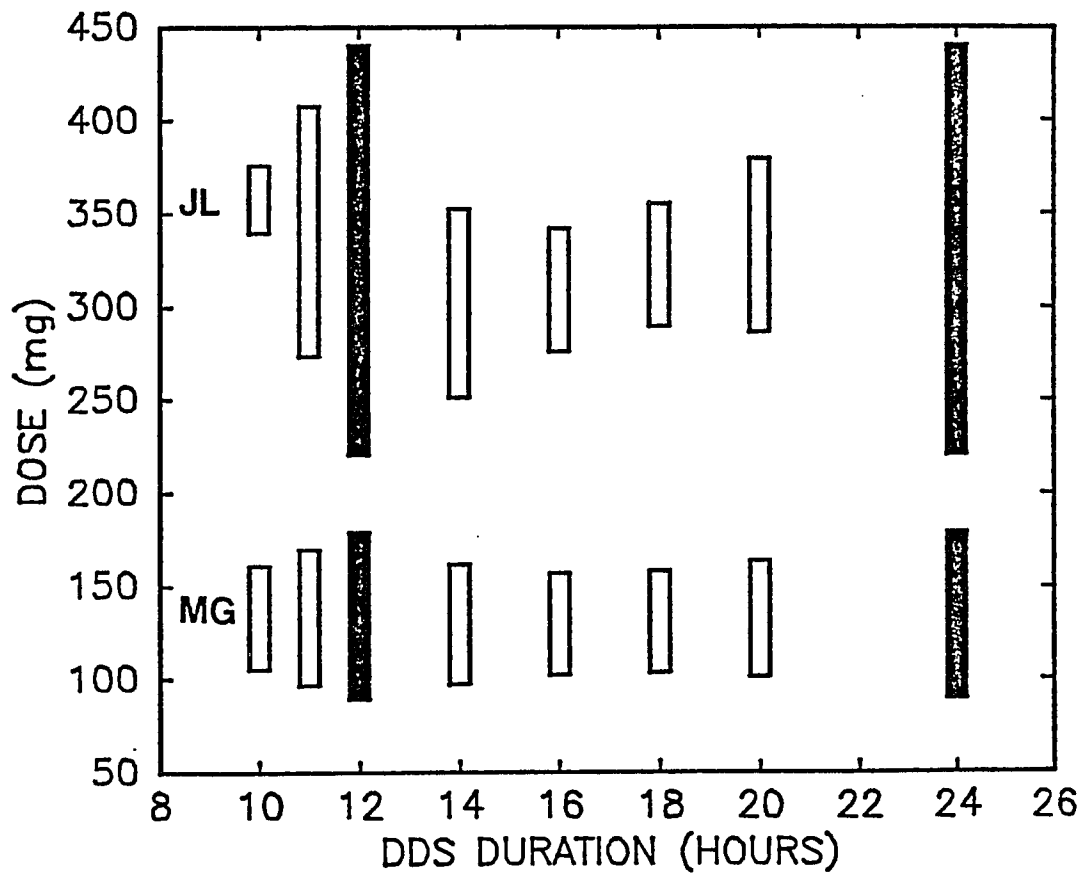


Figure 2.6: The range of the acceptable dose size as a function of the duration of the zero-order delivery system given every 12 hours as observed in Fig. 2.2 for patient JL (No. 9) and MG (No. 2). Maximum ranges are represented by the solid bars where $T = nt$ and $n=1,2$.

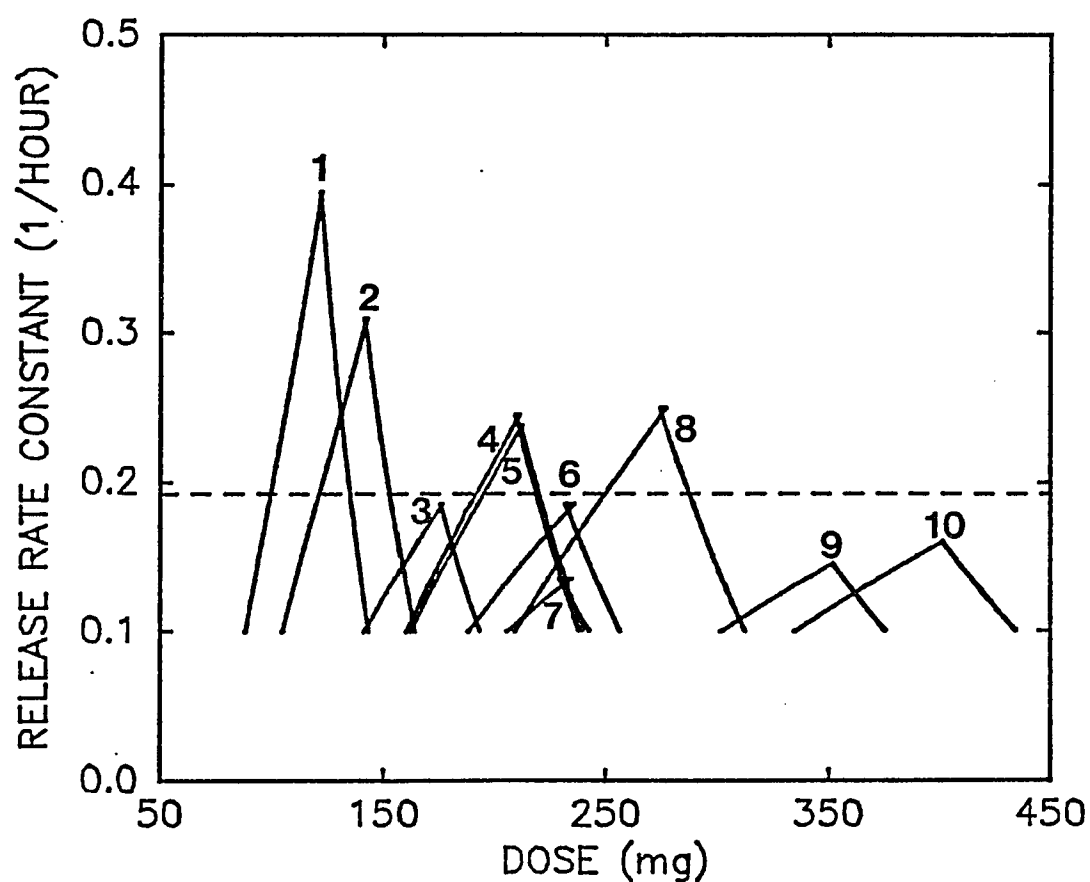


Figure 2.7: Release rate constant versus dose profiles for first-order systems administered orally every 12 hours to maintain 10 - 20 mg/L steady-state theophylline plasma concentrations in 10 children. Dashed line represents 90% release (T90) in 12 hours.

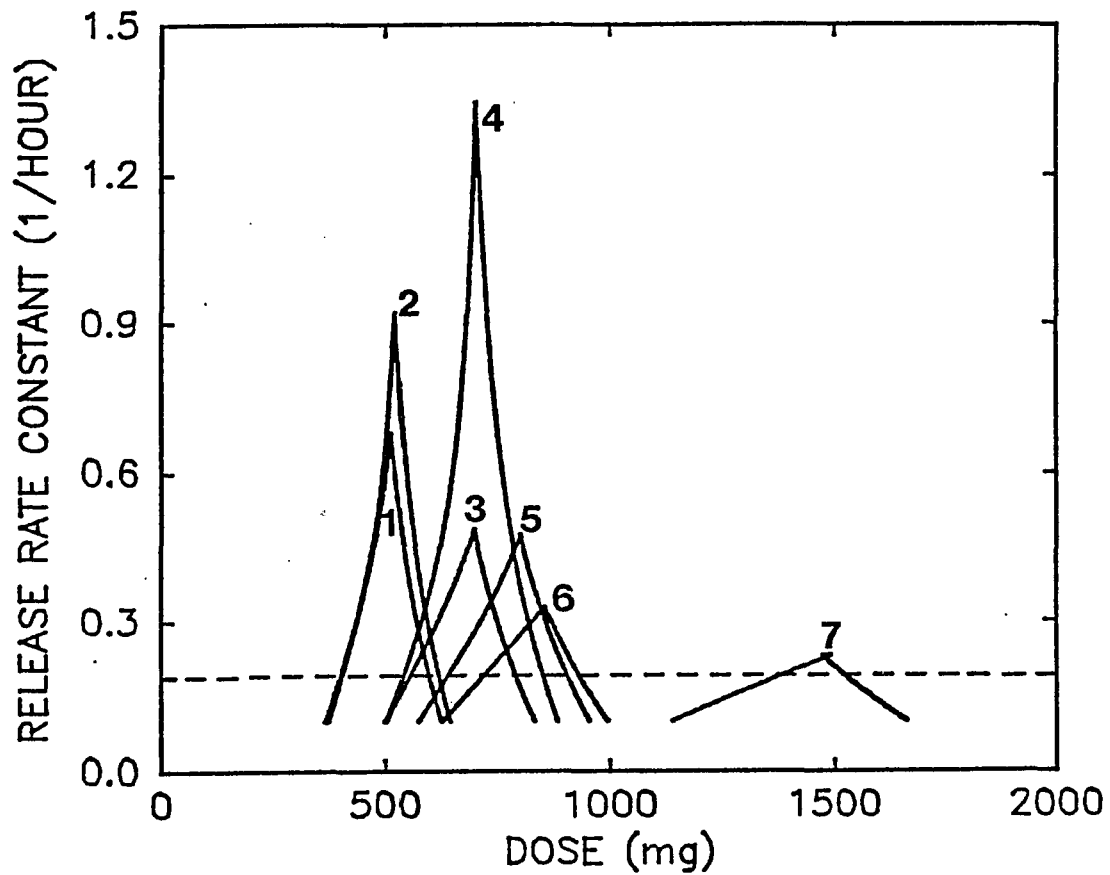


Figure 2.8: Release rate constant versus dose profiles for first-order systems administered orally every 12 hours to maintain 10 - 20 mg/L steady-state theophylline plasma concentrations in 7 adults. Dashed line represents 90% release (T90) in 12 hours.

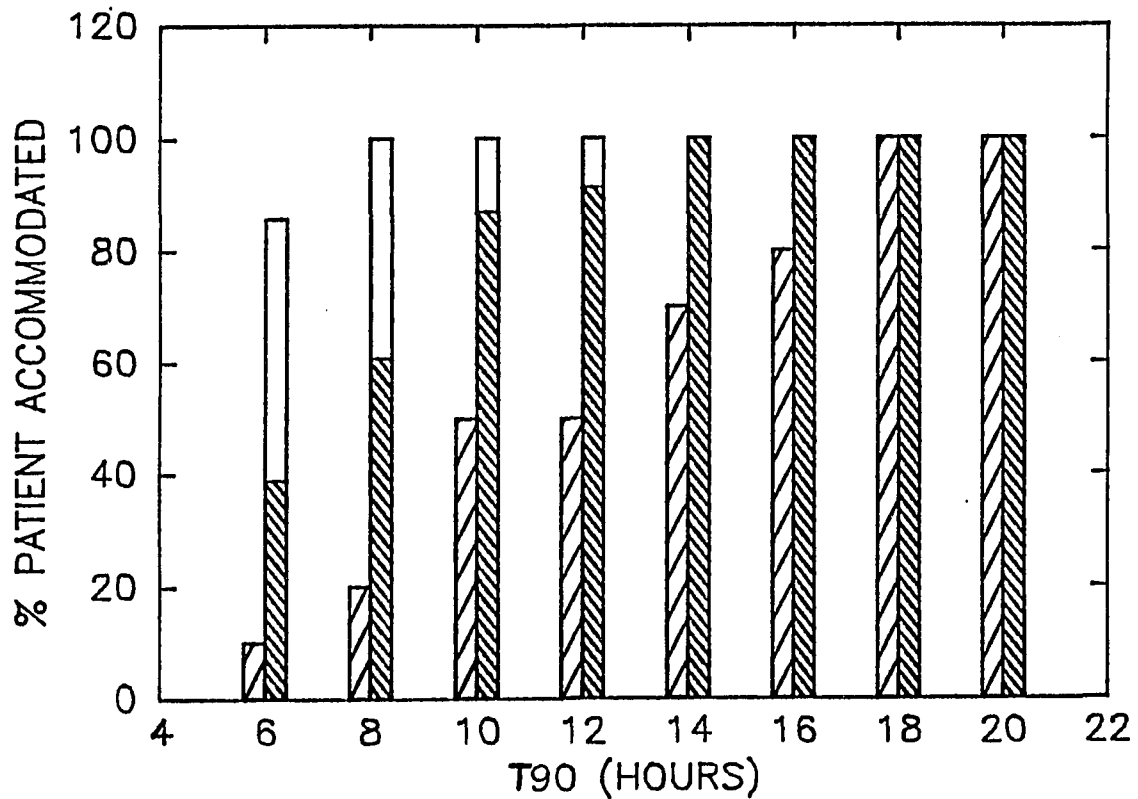


Figure 2.9: The percentage of patients having steady-state theophylline plasma concentrations between 10 and 20 mg/L as a function of the time required to deliver 90% of the payload (T_{90}) following oral administration of a first-order system every 12 hours:
 ▨ children (n=10); ▩ adults (n=23);
 □ adults (n=7).

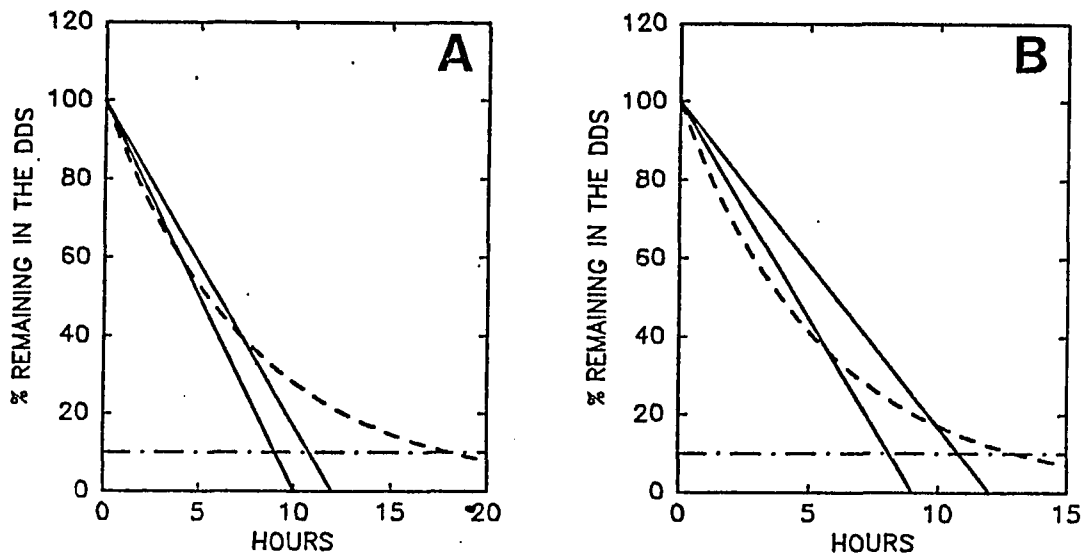


Figure 2.10:

Comparison of the calculated release rate profiles for zero-order and first-order theophylline delivery system for children (A) and adults (B): solid lines represent the ranges for zero-order systems where 12 hours is the selected maximum duration. Dashed curves represent the required release rate profiles for first-order systems. Systems are designed to maintain steady-state theophylline plasma concentrations between 10 to 20 mg/L when they are given orally every 12 hours. (-•-•-) represents 10% payloads remaining to be released from the system.

CHAPTER III
KINETICS AND MECHANISM OF CAPTOPRIL OXIDATION
IN AQUEOUS SOLUTIONS UNDER CONTROLLED OXYGEN
PARTIAL PRESSURE

SUMMARY

The stability of captopril in aqueous solutions was studied in the pH range 6.6 to 8.0 under controlled oxygen partial pressure (90 - 760 mmHg) with and without the addition of cupric ion at 32°C. The oxidative product, captopril disulfide, was found to be the sole degradation product under these conditions. A change in reaction rate from first order to zero order occurs as the captopril concentration decreases. The concentration at which the reaction order changes is a function of pH, oxygen partial pressure, and cupric ion concentration. The apparent first-order rate constants show a first-order dependency on both the oxygen partial pressure and cupric ion concentration. However, the apparent zero-order rate constants show a first-order dependency on oxygen partial pressure and a second-order dependency on cupric ion concentration. As the pH increases from 6.6 to 8.0, the first-order process becomes more predominant. A mechanism which consists of cupric ion and molecular oxygen catalyzed oxidation is proposed to explain those observations.

In order to characterize the progress of the oxidation and to elucidate the possible mechanism, studies which control the oxygen partial pressure are essential. The current studies investigate the oxidative mechanism of captopril in aqueous solutions under controlled oxygen partial pressure. In addition, it has been observed that cyclodextrins can form inclusion complexes with some compounds and stabilize them against oxidation by molecular oxygen.⁷⁻¹⁰ This study also examines the possible stabilization of captopril against oxidation by cyclodextrins.

EXPERIMENTAL

Apparatus -- The apparatus had to satisfy the following requirements: (1) to allow the selection of various oxygen partial pressures; (2) to maintain constant oxygen partial pressure throughout an experiment; (3) to permit rapid equilibrium between the oxygen gas phase and the reaction solution; (4) to provide convenient introduction of captopril stock solution and sampling. Therefore, the system had to be a closed system equipped with a gas source and sufficient stirring to provide efficient mixing between gas phase and reaction mixture. A modification of the apparatus used by Sokoloski and Higuchi¹¹ was employed.

The following experimental design (Fig. 3.1) was finalized using the studies described later in the "Selection of Experimental Methods". The 5 gallon jar, which serves as the oxygen source, was attached to the reaction vessel by pressure tubes. A three way valve connected the oxygen source to the reaction vessel and provided a convenient port to evaluate the head space of the reaction vessel by vacuum before introducing the oxygen into the reaction vessel. A mechanical stirring unit (ACE Glass Inc., Vineland, N.J.) was found to assure sufficient mixing between oxygen and the reaction mixture. The reaction vessel (a 50 mL three-neck flask) was immersed in an isothermal water bath (Haake, Model F, Berlin-Steglitz, West Germany) to maintain a constant temperature. Serum bottle stoppers were used to provide a closed system and to serve as a sampling port.

High Performance Liquid Chromatograph (HPLC) Analysis -- An HPLC method was developed for the assay of captopril (I) and its degradation product (II). The isocratic assay was carried out using a liquid chromatograph system (Model 332, Beckman Instruments, Inc., Irvine, CA) equipped with a variable wavelength ultraviolet detector (Model 1040A, Hewlett Packard, Inc., Waldbronn, West Germany), an integrator (Model 3090A, Hewlett Packard, Inc.), reversed-phase C-18 column (μ -Bondapak C18, Waters Associates), and injection loop size of 20 μ L.

Captopril and its disulfide were assayed in reaction mixtures by HPLC with UV detection at 210 nm due to the lack of significant absorbance at higher wavelengths (Table 3.1). The flow rate was 1 mL/min. using a mobile phase containing 25% acetonitrile (Omni Solv., EM Science, Gibbstown, N.J.) and 75% aqueous phosphoric acid (0.05%). The aqueous portion of the mobile phase was filtered and degassed before use. The resultant chromatographic characteristics for these compounds are summarized in Table 3.1. The ratio of the capacity factors yields an adequate resolution value of 2.68. The peak area versus concentration detection ranges are shown in Fig. 3.2. These calibration plots were prepared daily using fresh standard solutions.

Stability-Indicating Assay -- Figure 3.3 shows HPLC chromatograms for samples taken at various times during a reaction. These chromatograms clearly indicate the conversion of peak I to peak II.

Furthermore, the UV spectra taken at upslope, apex, and downslope for each peak (1040A detector, Hewlett Packard, Inc.) indicated that these two peak are consistent with the spectra for each of the two reference standards (Fig. 3.4).

In addition, mass balance during the reactions (Tables 3.2 - 3.4) indicates that captopril disulfide is the sole degradation product for the oxidation of captopril under these conditions. This mass balance also indicates that the assay is capable of following the progress of the reaction and quantitatively detecting all the components in the reaction.

Selection of Experimental Methods -- Two stirring methods (magnetic and mechanical) were evaluated for their ability to provide adequate mixing of oxygen with the reaction mixture. The oxidation of captopril as a function of time, at pH 6.62, 0.1 M phosphate buffer ($\mu = 0.18$) under 1 atm oxygen partial pressure, 32°C, was used to monitor the influence of these two stirring methods. The continuous diffusion oxygen bubbles through the reaction was used as a control. Initial slopes of semi-logrithmic plots show that mechanical stirring simulated the control condition but magnetic stirring did not (Table 3.5).

Methods for Captopril Oxidation Studies -- The 5 gallon jar was first filled with water (Fig. 3.1). The desired oxygen partial pressure was obtained by displacing known volumes of water with high purity of oxygen (U.S.P., Liquid Carbonic Co., Chicago, IL) and nitrogen

(AGA Gas, Inc., Cleveland, OH) through port H. The atmospheric pressure was determined by a barometer (Springfield Instrument Co., Hackensack, N.J.) at the time of preparing oxygen source. The oxygen partial pressure is calculated according to eq. 3.1.

$$pO_2 = P(V_O)/(V_N) - P_{HOH} \quad (3.1)$$

Where pO_2 , P , and P_{HOH} represent oxygen partial pressure, total pressure (barometer reading), and saturated water vapor pressure under the reaction condition; V_O and V_N represent the volumes of water displaced by oxygen and nitrogen, respectively.

Twenty-five milliliters buffer solutions using salts recrystallized from hot water to reduce trace metals (Table 3.6) were placed in the 50 mL three-neck round bottom flask. After evacuating the head space for 5 minutes at $32 \pm 0.2^\circ\text{C}$, the three way valve was turned to connect the reaction vessel to the oxygen source. The buffer solution was then equilibrated with oxygen with stirring for one hour. One milliliter of captopril aqueous stock solution (approximately 5.0×10^{-3} M) was introduced into the reaction mixture through the sampling port using a tuberculine syringe. The reaction mixture was protected from exposure to light by wrapping the entire water bath and reaction vessel with aluminum foil. The pH values of reaction mixtures before and after the reaction did not show significant changes. At predetermined time periods, approximately 0.8 mL samples of reaction mixture were taken using a tuberculine syringe. After cooling, 0.5 mL aliquots were quenched by dilution with equal volume of 1% or 2% phosphoric acid solution depended upon the pH of the reaction

mixture. The pH after this quench was approximately 2 to 3. For those studies with higher initial captopril concentrations, quenched samples were further diluted to the concentration range of the calibration curve using a mixture of equal volumes of reaction buffer and 1% or 2% phosphoric acid solution.

Influence of Cupric Ion (Cu^{++}) -- Various volumes (10 to 50 μL) of cupric acetate stock solution (7.04×10^{-3} M) were mixed with 25 mL of reaction buffer to provide Cu^{++} concentration ranging from 2.7×10^{-6} to 1.35×10^{-5} M. The reaction was studied using the procedure described previously.

Influence of Oxygen Partial Pressure -- Reactions were studied using various ratios of oxygen and nitrogen to provide an oxygen partial pressure ranging from 90 mmHg to ambient. The influence of oxygen partial pressure on the oxidation of captopril was examined at 32°C and pH 6.62 with a Cu^{++} concentration of 1.35×10^{-5} M.

Due to the decreased rate of oxidation of captopril under low oxygen partial pressure, initial rate studies were employed to characterize the reaction under these conditions. Three to four different initial concentrations of captopril (ranging from 1.0×10^{-4} to 5.0×10^{-4} M) were used in the studies. Loss of captopril and the formation of captopril disulfide were followed for the initial 10% of the reaction.

Influence of pH -- The effects of pH on the oxidation of captopril were examined from pH 6.6 to 8.0 at constant ionic strength ($\mu = 0.18$). The studies were performed under pure oxygen with Cu^{++} concentration of 1.35×10^{-5} M at 32°C .

Influence of Metal Chelating Agents -- Ethylenediaminetetraacetate (EDTA, G. Frederick Smith Chem. Co., Columbus, OH) and 8-hydroxyquinoline (Aldrich Chemical Co., Inc., Milwaukee, WI) at concentrations of 2.80×10^{-4} M were used to examine the influence of chelating agents on the oxidation of captopril at pH 6.62.

Influence of Cyclodextrins -- Three cyclodextrins (α -, β -, and γ -, P.L. Biochemicals Inc., Milwaukee, WI) were examined for their possible stabilization of captopril against oxidation by the formation of inclusion complexes. Three conditions were employed in this study:

- (1) A pH 6.62 buffer containing approximately 1.0×10^{-3} M cyclodextrin (α -, β -, or γ -) and 1.35×10^{-5} M Cu^{++} ion was prepared. Reactions were carried out by the addition of captopril in the usual manner.
- (2) Captopril (5.0×10^{-4} M) and cyclodextrin (2.5×10^{-3} M) were dissolved in 25 mL of 0.001 N hydrochloric acid solution and stirred under nitrogen at $59.0 \pm 0.1^\circ\text{C}$ overnight (approximately 18 hours). A 10 mL sample of this captopril-cyclodextrin mixture was mixed with 15 mL of pH 6.60 0.167 M phosphate buffer solution to make the final Cu^{++} concentration of 1.35×10^{-5} M.
- (3) The same experimental procedures described in (2) were

employed except that the reactions between captopril and the cyclodextrins were carried out at $32.0 \pm 0.1^\circ\text{C}$ instead of $59.0 \pm 0.1^\circ\text{C}$.

RESULTS

Identification of Degradation Products -- The conversion of peak I (captopril) to peak II was observed in a series of chromatograms during an experiment (Fig. 3.3). Peak II was identified as captopril disulfide by the comparison of its chromatographic behavior and its UV spectra at various positions on the HPLC peak to that of the reference standard. In addition, a mixture of a reference standard solution of known peak area of captopril disulfide shows only one peak at the retention time of peak II with the expected peak area when mixed with reaction mixture. The mass balance values (the concentration of captopril plus twice the concentration of captopril disulfide) are summarized in Table 3.2 to 3.4 and illustrated in Fig. 3.5. For all conditions in this study, the mass balance equals the initial captopril concentration throughout the entire period of reaction indicating that captopril disulfide is the only degradation product for captopril under these conditions.

Evaluation of Factors Influencing Concentration - Time Courses of

Captopril Oxidation -- The influence of oxygen partial pressure, cupric ion, and initial captopril concentration on the stability of captopril against oxidation were examined. Figure 3.6 shows the loss of captopril and the formation of captopril disulfide as a function of time at pH 6.62 under four different oxygen partial pressures. Figure 3.7 shows the loss of captopril and the formation of captopril disulfide as a function of time at pH 6.62, pure oxygen with four different concentrations of added cupric acetate.

The influence of initial concentration of captopril on the reaction was examined at pH 6.62 with pure oxygen in the presence of 1.35×10^{-5} M of Cu^{++} . The time courses for the loss of captopril and the formation of captopril disulfide are shown in Fig. 3.8. The profiles in Fig. 3.8A show that captopril loss is apparent zero order at low initial captopril concentrations and when the higher initial condition reactions fall below a certain level. In addition, the corresponding time courses for disulfide formation also appear zero order when the captopril concentrations are below a certain level (Fig. 3.8B).

However, the initial oxidation rate studies for the same range of captopril concentrations under low oxygen partial pressures (90 - 125 mmHg) suggest that this condition provides apparent first order loss. The relationship between initial rates and initial captopril concentrations is shown in Fig. 3.9.

These results indicated that oxidation of captopril cannot be described by a simple mechanism which applies to all conditions in this study. Both first-order and zero-order behavior are possible depending upon the experimental conditions.

Apparent Zero- and First-Order Rate Constants as a Function of Captopril Concentrations -- Figure 3.10 shows the first-order plots of captopril and captopril disulfide for the studies at pH 6.62 containing 1.35×10^{-5} M Cu^{++} with four different initial captopril concentrations under pure oxygen. The profiles indicate that oxidation of higher concentrations of captopril is initially first order. The zero-order

plots for these same data are shown in Fig. 3.8 which indicate that after the captopril concentration falls below 1.80×10^{-4} M, the reaction was apparent zero order. In addition, Fig. 3.10B indicates that the formation of captopril disulfide also follows an initial first-order process changing to zero-order when captopril concentrations are low. Therefore, first-order behavior is evident at high captopril concentrations while zero-order becomes predominant when captopril concentration falls below 1.8×10^{-4} M under these conditions. The resultant apparent first-order (k_1) and zero-order (k_0) rate constants are summarized in Table 3.7.

Apparent Zero- and First-Order Rate Constants as a Function of

Cupric Ion Concentrations -- The presence of Cu^{++} in the reaction mixture was also found to change the reaction rate from first-order to zero-order as shown in Fig. 3.11. The captopril concentration at which the reaction order changes from first to zero-order decrease as Cu^{++} concentration decreases. The resultant apparent first-order and zero-order rate constants for each Cu^{++} concentrations are summarized in Table 3.8.

Apparent Zero- and First-Order Rate Constants as a Function of

Oxygen Partial Pressure -- Figure 3.12 shows the zero-order and first-order plots for loss of captopril under four oxygen partial pressures. A change of order from first to zero-order during each of these reactions was also observed. However, the concentration of captopril at which the order changes from first to zero decreases as

the oxygen partial pressure decreases. At a lower oxygen partial pressure of 90 mmHg, only first-order behavior was studied since initial rate studies were used because of the slow rates. Table 3.9 summarizes the resultant apparent first-order and zero-order rate constants for these conditions.

Influence of pH and Buffer concentrations on the Oxidation of

Captopril -- The effect of pH on captopril oxidation was examined under pure oxygen in the presence of 1.35×10^{-5} M Cu^{++} at 32°C in the pH range 6.6 to 8.0. Figure 3.13 shows the zero-order and first-order plots for the loss of captopril under these conditions.

Both first-order and zero-order behavior was again observed.

Figure 3.14 shows the relationship between pH and the three pairs of apparent first-order and zero-order rate constants. In addition, the apparent influence of buffer species on the oxidation of captopril was insignificant (Fig. 3.14 insert).

Influence of Chelating Agents and Cyclodextrins on the Oxidation of

Captopril -- Figure 3.15 shows the loss of captopril as a function of time with and without the presence of chelating agents (EDTA and 8-hydroxyquinoline). The results indicated that the chelating agents have completely stabilized the captopril.

The effect of cyclodextrins (α -, β -, and γ -) were examined under conditions where the predominant reaction pathway is zero order. The results are summarized in Table 3.10. Since the resultant zero-order rate constants were similar to the control studies, either no

cyclodextrin-captopril inclusion complexes were formed or the inclusion process does not protect the thiol group against oxidation.

DISCUSSION

Reaction Order with respect to Captopril -- The oxidation of captopril in the presence and absence of added cupric ion was found to be a complex reaction. Results from the studies under pure oxygen and in the presence of 1.35×10^{-5} M Cu^{++} with various initial captopril concentrations show that the reaction is zero-order with respect to captopril when its concentration falls below a certain level (Fig. 3.8). In contrast, the results from the initial rate studies under low oxygen partial pressures suggest a first-order reaction with respect to captopril (Fig. 3.9). Therefore, both zero- and first-order reactions are possible depending upon the reaction conditions.

Examination of the data in Fig. 3.8 suggest that high captopril concentrations favor reactions which initially follow first-order kinetics but later change to zero-order when captopril concentrations decrease below a minimum level (Fig. 3.10). The results from studies on the influence of oxygen partial pressure, cupric ion concentration, and pH also suggest that a change in order occurs (Figs. 3.11 and 3.12). Based on these observations, the oxidation of captopril appears to follow a first-order process at the beginning of the reaction when captopril concentration is high and then change to zero order at lower concentrations. The concentration of captopril at which the reaction order changes depends upon the reaction conditions such as oxygen partial pressure, cupric ion concentration and pH.

Effects of Trace Metals on the Oxidation of Captopril -- The possible influence of trace metals in the reaction mixture was examined. The water used in preparing the buffer solutions and stock solutions of captopril was filtered (Milli-Q₂ System, Millipore Co., Bedford, MA) to minimize the possible contamination by trace metals. Successive recrystallization of buffer salts from hot water was used to remove the trace metals present in the commercially available buffer salts.¹² However, results indicated that either there is no significant amount of trace metals in the salts or the purification process did not remove the trace metals since no significant change in the oxidation rate was observed.

To further verify the catalysis by trace metals, two chelating agents were added to reaction mixtures. As shown in Fig. 3.15, no reaction was observed in the presence of either EDTA or 8-hydroxyquinoline. Since EDTA and 8-hydroxyquinoline represent two different chemical types of chelating agents, this retardation of the oxidation of captopril was believed to be due to the inactivation of trace metals in the reaction mixtures and not a direct participation by the agents themselves.

Cupric Ion Dependency of the Oxidation of Captopril -- The dependency of the apparent first-order and zero-order rate constants on the cupric ion concentration is shown in Fig. 3.16. The first-order rate constants show a linear relationship with the concentration of added cupric ion (Fig. 3.16A). The intercept in this

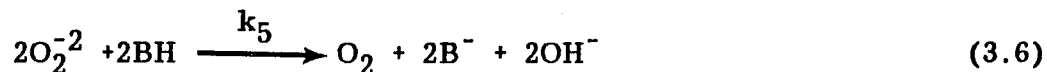
plot represents the first-order rate constant when there is no added Cu^{++} . This value is in agreement with the results determined for the captopril oxidation in the absence of additional Cu^{++} . In contrast, the zero-order rate constants represent a more complicated relationship to added Cu^{++} (Fig. 3.16B). This relationship can be described by a second-order dependency since k_0/Cu^{++} versus Cu^{++} is linear. In addition to the cupric ion dependency for both the apparent first- and zero-order rate constants, the concentration of captopril at which reaction changes from first- to zero-order decreases as the Cu^{++} concentration decreases.

Oxygen Dependency of the Oxidation of Captopril -- Figure 3.17

shows the dependency of apparent first- and zero-order rate constants on oxygen partial pressure. This indicates that oxygen molecules are involved in the rate limiting step for both cases in which the first-order and zero-order reaction is predominant. While the rate of loss of captopril may be either first-order or zero-order with respect to captopril, it is first order with respect to $[\text{O}_2]$

Mechanism -- The autooxidation of thiols by molecular oxygen has been previously studied and the following mechanism was proposed (Scheme I).¹³⁻¹⁵





Scheme I

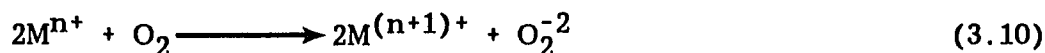
Using this scheme and applying steady state assumptions for $\text{RS}\cdot$ and O_2^{-2} , the reaction rate law can be described by eq. 3.7 which predicts a first-order dependency on thiol concentration after the initial lag time,

$$d[\text{RSH}]_{\text{T}}/dt = -2k_2\{K[\text{B}^-]/(K[\text{B}^-]+[\text{BH}])\}[\text{O}_2][\text{RSH}]_{\text{T}} \quad (3.7)$$

where $[\text{RSH}]_{\text{T}}$ represents total thiol concentration, K is the equilibrium constant for step 3.1, and $[\text{O}_2]$ is the dissolved oxygen concentration. However, results in this study show that first-order behavior was not followed under all conditions. In addition, this scheme cannot explain the rate change from first order to zero order. This phenomenon of order change has also been observed by Cullis *et al.*¹⁶ The existence of a zero-order process was reported by Rippie and Higuchi in the oxidation of 2,3-Dimercapto-1-propanol (BAL).^{17,18} Consequently, Scheme I cannot satisfy these observations.

A mechanism has previously been proposed for the case where heavy metal ions are present in the reaction mixture (Scheme II).¹⁹

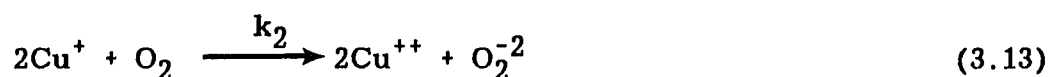
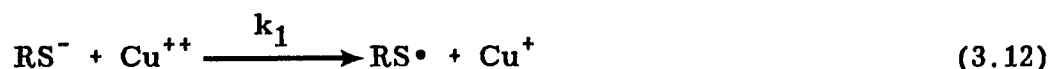




Scheme II

Cullis et al.²⁰ and Swan et al.²¹ observed that the reaction order with respect to thiol concentration is dependent upon the kind of heavy metal ions present. A zero-order reaction was observed when copper and cobalt were added while addition of nickel resulted in a first-order reaction. According to Scheme II, when step 3.10 becomes rate-limiting the reaction rate will become independent of thiol concentration and reaction order becomes zero with respect to thiol. On the other hand, when step 3.8 becomes rate-limiting, the reaction is first-order. In this study, reactions were first-order when the captopril concentration was high and zero-order when this concentration decreased. According to Scheme II, however, when the captopril concentration is high, step 3.10 should become rate-limiting and a zero-order reaction should result. This is contrary to the observed results.

Although the oxidation of thiol catalyzed by heavy metal ions is usually faster than that catalyzed by molecular oxygen, these two reactions co-exist when metal ions are present. The competition by these two pathways can explain the observations (Scheme III).





Scheme III

Employing the steady state assumptions for O_2^- , the rate of loss of captopril can be described by eq. 3.18.

$$d[\text{RS}^-]/dt = -k_1[\text{RS}^-][\text{Cu}^{++}] - 2k_3[\text{RS}^-][\text{O}_2] \quad (3.18)$$

Since the oxidation of cuprous (Cu^+) to cupric (Cu^{++}) ion is known to be the slow reaction when the pH of the reaction mixture is increased,²² reaction 3.13 can represent the rate-limiting step relative to reaction 3.12. Applying the steady state assumptions for Cu^{++} , eq. 3.18 can be rewritten as eq. 3.19.

$$d[\text{RS}^-]/dt = -2k_2[\text{Cu}^+]^2[\text{O}_2] - 2k_3[\text{RS}^-][\text{O}_2] \quad (3.19)$$

When the captopril concentration is small, the contribution of the second term in eq. 3.19 becomes insignificant and the reaction becomes zero-order with respect to captopril (eq. 3.20).

$$d[\text{RS}^-]/dt = -2k_2[\text{Cu}^+]^2[\text{O}_2] \quad (3.20)$$

However, when the captopril concentration is high, the direct oxidation of captopril by molecular oxygen becomes significant and the reaction becomes first-order with respect to captopril.

Both the observed first- and zero-order rate constants are dependent upon cupric ion concentrations. When the cupric ion concentration is low, the rate-limiting step for cupric-ion catalyzed

oxidation is reaction 3.12. Consequently, the reaction follows a first-order process with respect to captopril concentration (eq. 3.18). These first-order rate constants show a first-order dependency on cupric ion. In addition, as cupric ion concentration decreases, the change in the rate-limiting step from reaction 3.12 to 3.13 is observed at lower captopril concentrations. Consequently, the change in order was observed at lower captopril concentrations. When the cupric ion concentration was increased to a certain level, the importance of reaction 3.13 as rate-limiting step increases and the cupric ion catalyzed oxidation becomes zero-order. Therefore, the observed first-order rate constant becomes independent of cupric ion concentration. When the zero-order reaction was observed, the rate law indicates a second-order dependency on cupric ion concentration (eq. 3.20).

The saturated oxygen solubility can be described by Henry's law when oxygen pressure is under 1 atm,²³ $[O_2] = k[pO_2]$, where $[O_2]$ represents oxygen solubility and $[pO_2]$ represents the oxygen partial pressure above the solution. A first-order dependency on dissolved oxygen concentration for the rate of loss of captopril shown by eqs. 3.19 and 3.20 can be translated to first-order dependency on oxygen partial pressure. This is the type of behavior that was experimentally observed.

When the pH was increased from 6.62 to 7.94, the captopril concentration at which the reaction rate changes from first order to

zero order is decreased. As the pH increases, the concentration of thiol anion (RS^-) increases. Consequently, the direct oxidation of captopril by molecular oxygen becomes more significant and competes more favorably with cupric-ion catalyzed pathway. Therefore, the apparent first-order process becomes more dominant.

Based on the above discussions, Scheme III represents a mechanism which is consistent with the experimental observations.

CONCLUSION

The oxidation of captopril to its disulfide is the predominant degradation pathway in pH range of 6.6 to 8.0 with or without the presence of cupric ion. Depending upon the reaction conditions, the progress of the reaction follows first-order and zero-order kinetics with respect to captopril. Usually, a first-order reaction will change to zero order when captopril concentration decreases below minimum value. The concentration at which the order changes is a function of pH, cupric ion concentration, and oxygen partial pressure. The apparent first-order rate is first-order with respect to both the oxygen partial pressure and cupric ion concentration. However, the zero-order rate process shows a first-order dependency on the oxygen partial pressure and a second order dependency on cupric ion concentration.

It was found that previously proposed mechanisms for thiol oxidation in the presence and absence of heavy metal ions cannot adequately describe the observed results. A mechanism which involves both heavy metal ion catalyzed and direct molecular oxygen catalyzed oxidation is proposed. This proposed mechanism describes the experimental results including the observed change in rate-limiting step which occurs as a function of reaction conditions.

Although cyclodextrins have been reported to protect some compounds against oxidation, the rate of captopril oxidation was not reduced by α , β or γ cyclodextrin. This may be due either to

unsuccessful formation of inclusion complexes or the fact that inclusion complex formation does not protect captopril against oxidation.

REFERENCES

1. D.W. Cushman, H.S. Cheung, E.F. Sabo, and M.A. Ondetti, Design of Potent Competitive Inhibitors of Angiotensin-Converting Enzyme. Carboxyalkanoyl and Mercaptocalkanoyl Amino Acids, *Biochem.*, **16**, 5484 (1977).
2. R.K. Ferguson, H.R. Brunner, G.A. Turini, H. Gavras, and D.N. McKinstry, A Specific Orally Active Inhibitor of Angiotensin-Converting Enzyme in Man, *Lancet*, **1**, 775 (1977).
3. G. Capozzi and G. Modena, The Oxidation of Thiols, in "The Chemistry of Thiol Group", Vol. 2, S.Patai (Ed.), John Wiley, London, 1974, pp. 785-840.
4. P. Timmins, I.M. Jackson, and Y.J. Wang, Factors Affecting Captopril Stability in Aqueous Solutions, *INTERN. J. Pharm.*, **11**, 329 (1982).
5. Y. Kawahara, M. Hisaoka, Y. Yamazaki, A. Inage, and T. Morioka, Determination of Captopril in Blood and Urine by High-Performance Liquid Chromatography, *Chem. Pharm. Bull.*, **29**, 150 (1981).
6. H. Kadin, Captopril, in "Analytical Profiles of Drug Substances", Vol. 11, American Pharmaceutical Associations, Washington, D.C., 1982, pp. 79-137.
7. J. Szejtli, "Cyclodextrins and Their Inclusion Complexes", Akademiai Kiado, Budapest, 1982.
8. M.I. Bender and M. Komiyama, "Cyclodextrin Chemistry", Springer Verlag, Berlin, Heidelberg, New York, 1978.
9. J. Szejtli and E. Banky-Elod, Inclusion Complexes of Unsaturated Fatty Acids with Amylose and Cyclodextrin, *Die Starke*, **27**, 368 (1975).
10. H. Schlenk, D.M. Sand, and J.A. Tillotson, Stabilization of Autoxidizable Materials by Means of Inclusion, *J.A.C.S.*, **77**, 3587 (1955).
11. T.D. Sokoloski and T. Higuchi, Kinetics of Degradation in Solution of Epinephrine by Molecular Oxygen, *J. Pharm. Sci.*, **51**, 172 (1962).

12. D.D. Perrin and B. Dempsey, "Buffers for pH and Metal Ion Control", Chapman and Hall, New York, N.Y., 1974.
13. T.J. Wallace and A. Schriesheim, Solvent Effects in the Base-Catalyzed Oxidation of Mercaptans with Molecular Oxygen, *J. Org. Chem.* 27, 1514 (1962).
14. T.J. Wallace and A. Schriesheim, The Base-Catalyzed Oxidation of Aliphatic and Aromatic Thiols and Disulfides to Sulfonic Acids, *Tetrahedron*, 21, 2271 (1965).
15. T.J. Wallace, A. Schriesheim, and W. Bartok, The Base-Catalyzed Oxidation of Mercaptans. III. Role of the Solvent and Effect of Mercaptan Structure on the Rate Determining Step, *J. Org. Chem.* 28, 1311 (1963).
16. C.F. Cullis, J.D. Hopton, and D.L. Trimm, Oxidation of Thiols in Gas-Liquid Systems I. Reaction in the Absence of Added Metal Catalysts, *J. Appl. Chem.*, 18, 330 (1968).
17. E.G. Rippie and T. Higuchi, Kinetics of Copper Catalyzed Oxidation of 2,3-Dimercapto-1-propanol by Molecular Oxygen, *J. Pharm Sci.*, 51, 626 (1962).
18. E.G. Rippie and T. Higuchi, Kinetics of Reaction between Molecular Oxygen and 2,3-Dimercapto-1-propanol in Aqueous Solution, *J. Pharm Sci.*, 51, 776 (1962).
19. T.J. Wallace, A. Schriesheim, H. Hurwitz, and M.B. Glaser, *Ind. Engng. Chem., Process Des. Devel.*, 3, 237 (1964).
20. C.F. Cullis, J.D. Hopton, C.J. Swan, and D.L. Trimm, Oxidation of Thiols in Gas-Liquid Systems II. Reaction in the Presence of Added Metal Catalysts, *J. Appl. Chem.*, 18, 335 (1968).
21. C.J. Swan and D.J. Trimm, Oxidation of Thiols in Gas-Liquid Systems III. Oxidation of Ethanethiol in the Presence of Catalysts Containing Copper, Cobalt and Nickel, *J. Appl. Chem.*, 18, 340 (1968).
22. H. Nord, Kinetics of the Autoxidation of Cuprous Chloride in Hydrochloric Acid Solution, *Acta Chem. Scand.*, 9, 430 (1955).
23. M.L. Hitchman, "Measurement of Dissolved Oxygen", John Wiley & Sons, New York, N.Y., 1978.

Table 3.1

HPLC analyses and chromatographic characteristics for
captopril and captopril disulfide

Compound	$\lambda_{\text{max}}^{\text{a}}$ (nm)	Retention Time (mL)	Capacity Factor(k)	Detection Range(10^4M)	%CV ^b
Captopril	198	5.6	1.24	0.1-1.0	1.8
Captopril Disulfide	198	10.9	3.32	0.05-0.5	1.8

^aUV wavelength of maximum absorptivity in the mobile phase.

^bCoefficient of variation is based on the area under the peak from four replicate analyses of standard solutions containing 15.5 $\mu\text{g/mL}$ of captopril and 8.5 $\mu\text{g/mL}$ of captopril disulfide.

Table 3.2

Mass balance for captopril oxidation at pH 6.62, 0.1M phosphate buffer ($\mu=0.18$), $pO_2=732.9\text{mmHg}$, 32°C in absence of light

Time (min.)	Captopril (10^5 M)	Captopril Disulfide (10^5 M)	% Recovery ^a
3	18.32	0.21	98.8
10	18.09	0.25	98.0
20	17.51	0.49	97.4
30	16.41	0.74	94.3
45	16.22	1.10	97.1
61	15.02	1.55	95.5
90	13.41	2.29	94.9
120	12.04	2.92	94.3
180	9.57	4.05	93.2
240	7.19	5.29	93.7
300	3.66	6.97	92.7
360	0.95	8.39	93.4

$$\text{a}^{\circ} \% \text{ Recovery} = 100 \times (\text{Captopril} + 2 \times \text{Captopril Disulfide}) / \text{Cap}_0$$

Table 3.3

Mass balance for captopril oxidation at pH 6.62,
 $pO_2=729\text{mmHg}$, $Cu^{++}=1.35\times 10^{-5}\text{M}$, 32°C in absence of
light.

Time (min.)	Captopril (10^5 M)	Captopril Disulfide (10^5 M)	% Recovery ^a
2	31.52	1.17	98.9
15	30.20	1.93	99.5
30	27.42	2.97	97.5
50	24.29	4.63	98.0
70	21.28	6.08	97.7
90	18.31	7.62	98.1
120	14.34	9.35	96.6
150	11.37	11.49	100.4
180	7.64	12.98	98.2
210	5.13	15.25	104.5
270	--	17.03	99.5

$$^a\% \text{ Recovery} = 100 \times (\text{Captopril} + 2 \times \text{Captopril Disulfide}) / \text{Cap}_0$$

Table 3.4

Mass balance for captopril oxidation at pH 6.62,
 $pO_2=322\text{mmHg}$, $Cu^{++}=1.35 \times 10^{-5}\text{M}$, 32°C in absence of
light.

Time (min.)	Captopril (10^5 M)	Captopril Disulfide (10^5 M)	% Recovery ^a
2	16.93	0.78	99.4
15	15.94	1.07	97.2
30	15.60	1.38	98.7
45	14.52	1.91	98.6
60	13.28	2.15	94.6
80	13.00	2.79	99.9
150	9.85	4.50	101.3
180	8.16	5.09	98.6
210	7.23	5.82	101.4
240	5.34	6.18	95.1
270	3.99	7.19	98.8
300	2.66	7.82	98.4
360	0.53	8.55	94.8
600	--	8.56	92.0

$$^a\% \text{ Recovery} = 100 \times (\text{Captopril} + 2 \times \text{Captopril Disulfide}) / \text{Cap}_0$$

Table 3.5

Selection of experimental conditions which simulate the continuous flow of oxygen bubbles through the reaction mixture.^a

Method	Slope ^b	% Residual ^c
Magnetic Stirring	3.16 ₋ 0.11	50%
Mechanical Stirring	4.04 ₋ 0.08	40%
Control ^d	3.99 ₋ 0.14	35%

^aExperimental condition: pH 6.62, 0.1M phosphate buffer ($\mu=0.18$), 1 atm O₂ at 32°C.

^bAverage(+S.D.) slope of semi-logarithmic plots for 3 reactions.

^cFinal value as % initial captopril concentration on log-linear plot.

Table 3.6

Summary of reaction conditions at 32°C

pH	Buffer (M)		
	NaH ₂ PO ₄	Na ₂ HPO ₄	NaCl ^a
6.62	0.063	0.038	----
	0.030	0.020	0.09
7.44	0.015	0.055	----
7.94	0.005	0.055	0.01

^aIonic strength was adjusted to 0.18 by sodium chloride.

Table 3.7

Effect of captopril initial concentration on observed rates.^a

Captopril Concentration (10^4 M)	k_0 (10^6 M/min)	k_1 (min. ⁻¹)
5.26 \pm 0.01	1.14 \pm 0.02	6.01
3.55 \pm 0.13	1.05 \pm 0.01	6.35 \pm 0.02
1.93 \pm 0.02	1.02 \pm 0.01	--
1.31	0.936	--

^a0.1M phosphate buffer, pH 6.62, $\mu=0.18$, $[Cu^{++}]=1.35 \times 10^{-5}M$,
pure O_2 at 32°C.

Table 3.8

Effect of added cupric ion on observed rates.^a

Cu^{++} (10^6M)	k_0 (10^7 M/min)	k_1 (10^3 min.^{-1})
13.50	10.20 \pm 0.12	6.24 \pm 0.20
10.79	7.37 \pm 0.13	6.95 \pm 0.30
6.74	5.19 \pm 0.13	5.91 \pm 0.34
2.70	3.27 \pm 0.12	4.52 \pm 0.06
0	2.83 \pm 0.04	3.41 \pm 0.17

^a0.1M phosphate buffer, pH 6.62, $\mu=0.18$, pure O_2 at 32°C .

Table 3.9

Effect of oxygen partial pressure on observed rates.^a

pO_2 (mmHg)	k_0 (10^7 M/min)	k_1 (10^3min.^{-1})
724.0 \pm 2.5	10.20 \pm 0.12	6.24 \pm 0.20
525.7 \pm 17.3	7.59 \pm 0.17	3.96 \pm 0.13
315.6 \pm 7.1	4.83 \pm 0.04	2.49 \pm 0.10
189.5 \pm 4.6	3.82 \pm 0.04	--
123.5 \pm 5.2 ^b	--	0.95
92.0 \pm 2.6 ^b	--	1.01

^a0.1M phosphate buffer, pH 6.62, $\mu=0.18$, $[Cu^{++}]=1.35 \times 10^{-5}M$ at 32°C.

^bFrom initial rate studies.

Table 3.10

Effect of cyclodextrins on observed rates of captopril oxidation.^a

Process ^b	A	$k_0(10^7\text{M}/\text{min.})$ B	C
Cyclodextrin			
α	10.17±0.27	10.70±0.29	10.42
β	10.46±0.24	10.46	9.04±0.34 ^c
γ	--	9.90	10.23
Control ^d	10.30±0.68		

^a0.1M phosphate buffer, pH 6.62, $\mu=0.18$, $[\text{Cu}^{++}]=1.35 \times 10^{-5}\text{M}$ at 32°C.

^bSee experimental section for description of processes A, B, and C.

^cTerminal slopes from linear plots.

^dNo cyclodextrins were added.

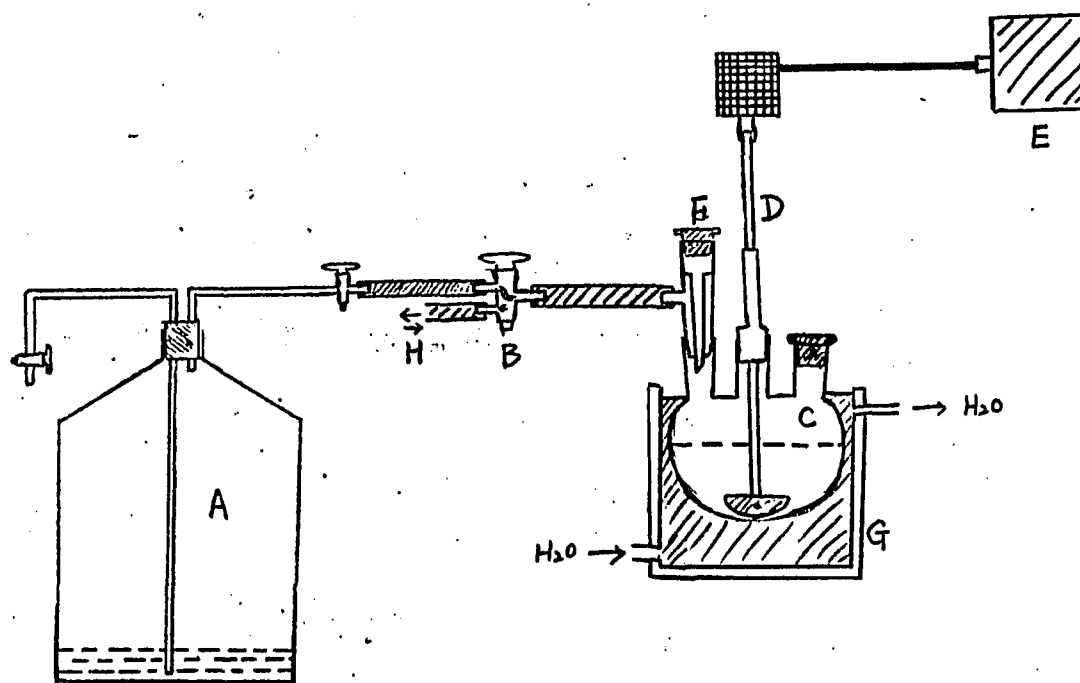


Figure 3.1: Schematic representation of the reaction vessel used in the study of captopril oxidation under various oxygen pressures. A. 5 gallon jar serves as oxygen atmosphere; B. Three way valve; C. 50 mL three-neck round bottom flask; D. Mechanical stirrer unit; E. Transformer; F. Serum bottle stopper (sampling port); G. Isothermal water bath flow cell unit; H. Gas inlet and vacuum port.

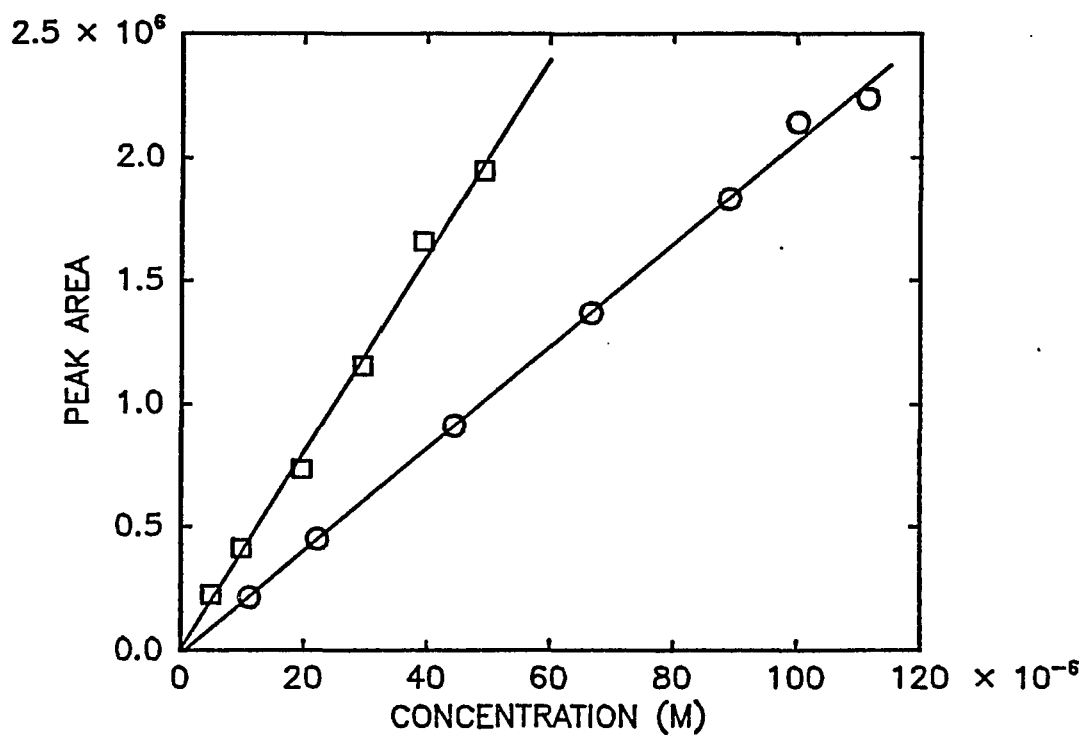


Figure 3.2: Standard curves for captopril and captopril disulfide. (o): captopril, (□): captopril disulfide.

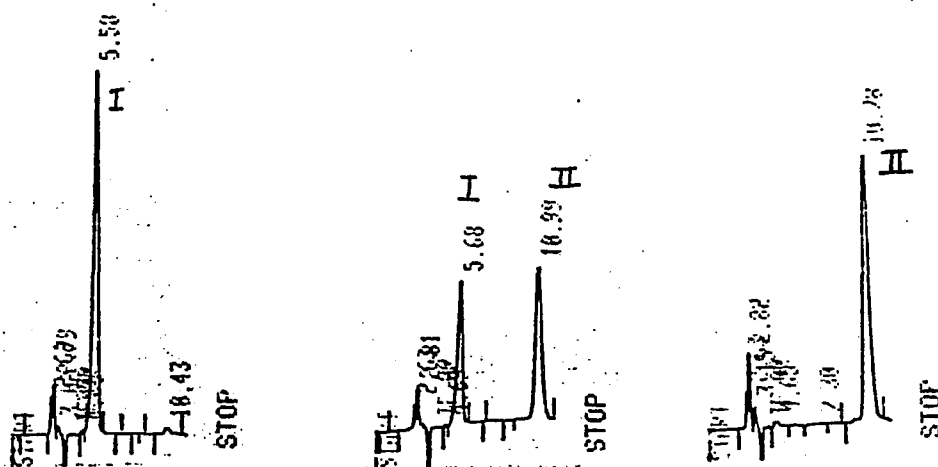


Figure 3.3: HPLC Chromatograms of reaction mixture samples taken at different time points during the reaction. I: captopril, II: captopril disulfide.

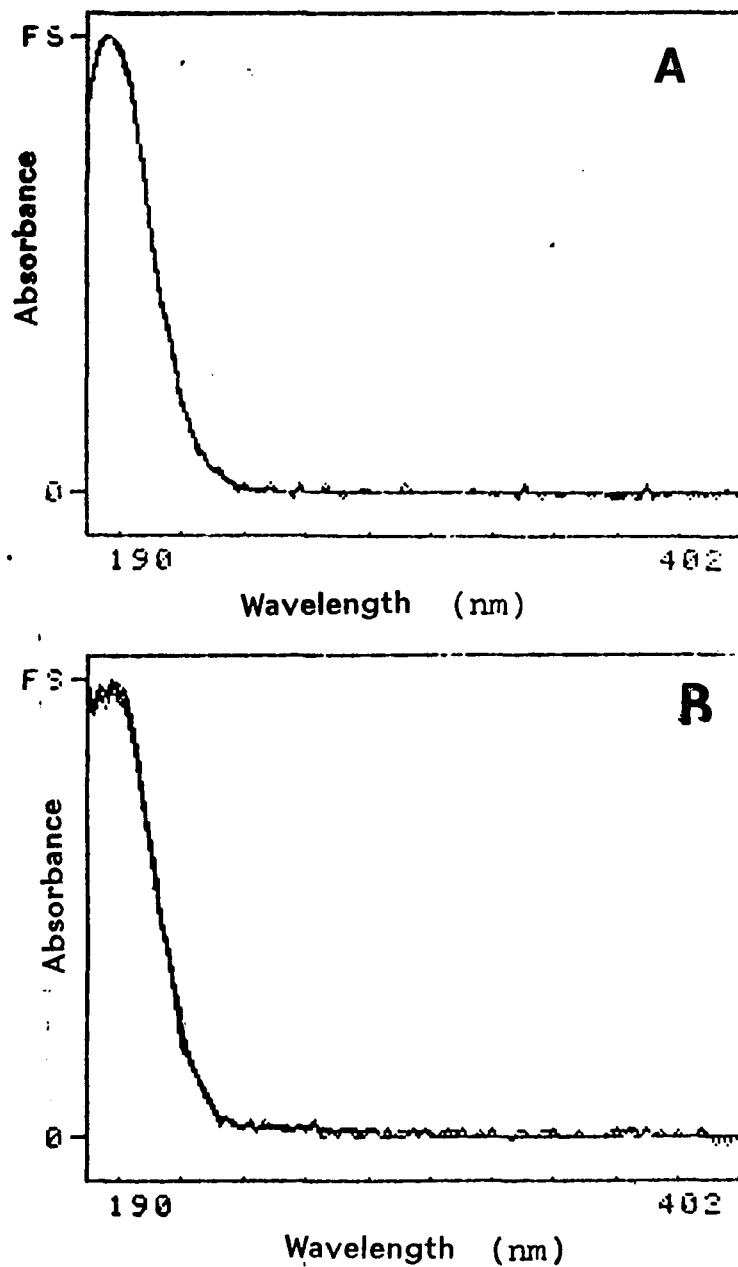


Figure 3.4: UV spectra taken at various points of the peak and that of reference standards for captopril (A) and captopril disulfide (B)

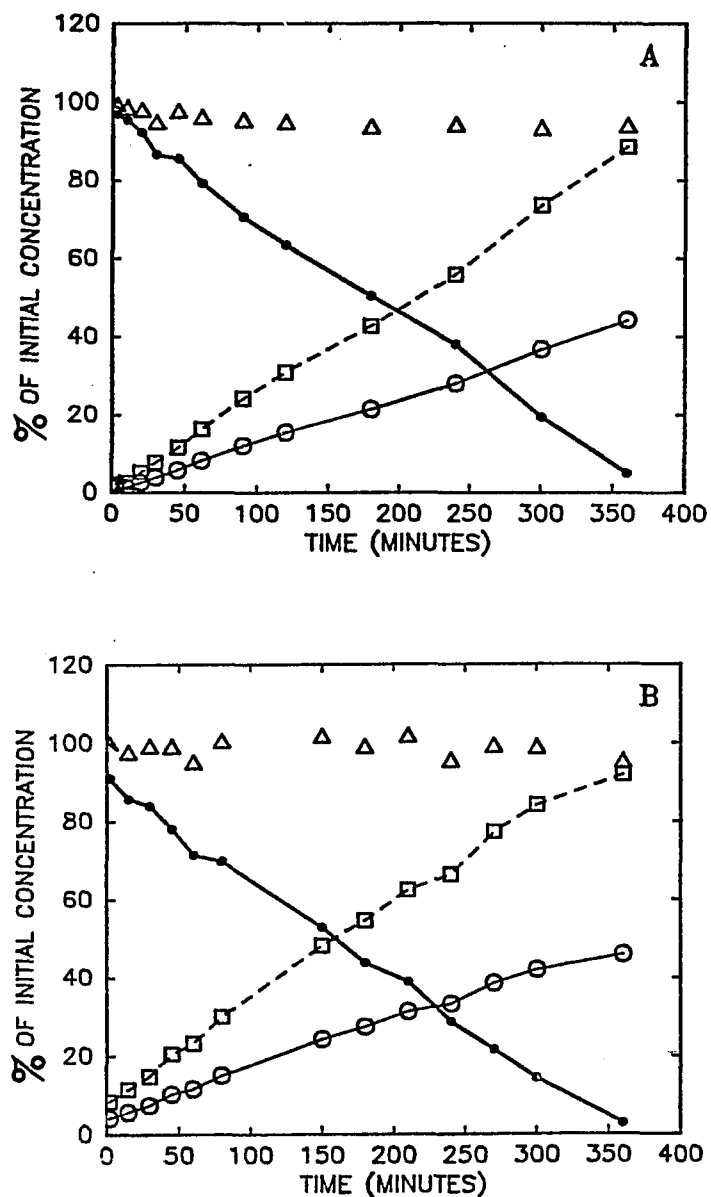


Figure 3.5: Examples of mass balance for captopril oxidation. (A) pH 6.62, 0.1 M phosphate buffer ($\mu=0.18$), $[\text{Cu}^{++}] = 1.35 \times 10^{-5} \text{ M}$, $p\text{O}_2 = 322 \text{ mmHg}$ at 32°C . (B) pH 6.62, 0.1 M phosphate buffer ($\mu=0.18$), $[\text{Cu}^{++}] = 0$, $p\text{O}_2 = 733 \text{ mmHg}$ at 32°C . (●): captopril (○): captopril disulfide, (□): two times captopril disulfide (Δ): total recovery.

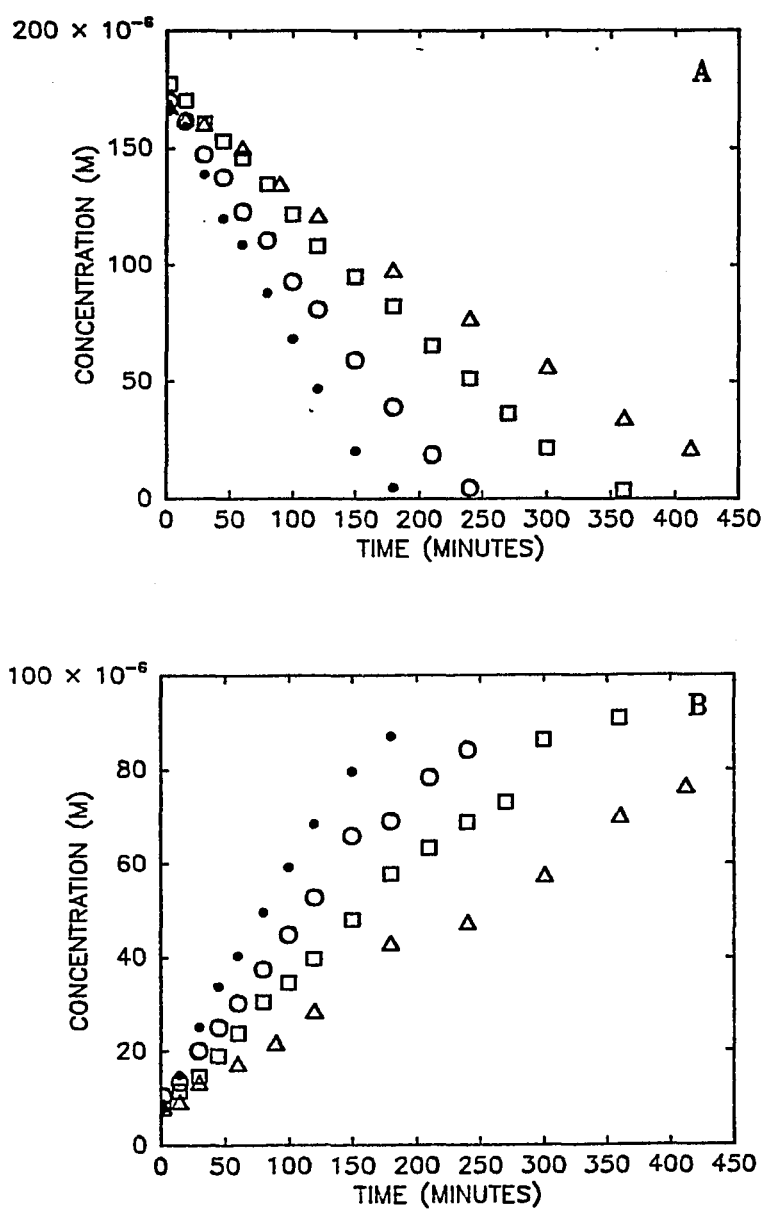


Figure 3.6: Captopril (A) and captopril disulfide (B) concentrations as a function of time under various oxygen partial pressures. pH 6.62, 0.1 M phosphate buffer ($\mu=0.18$), $[\text{Cu}^{++}]=1.35 \times 10^{-5} \text{ M}$ at 32°C . $p\text{O}_2 = 721(\bullet)$, $526(\circ)$, $338(\square)$, and $185 \text{ mmHg}(\Delta)$.

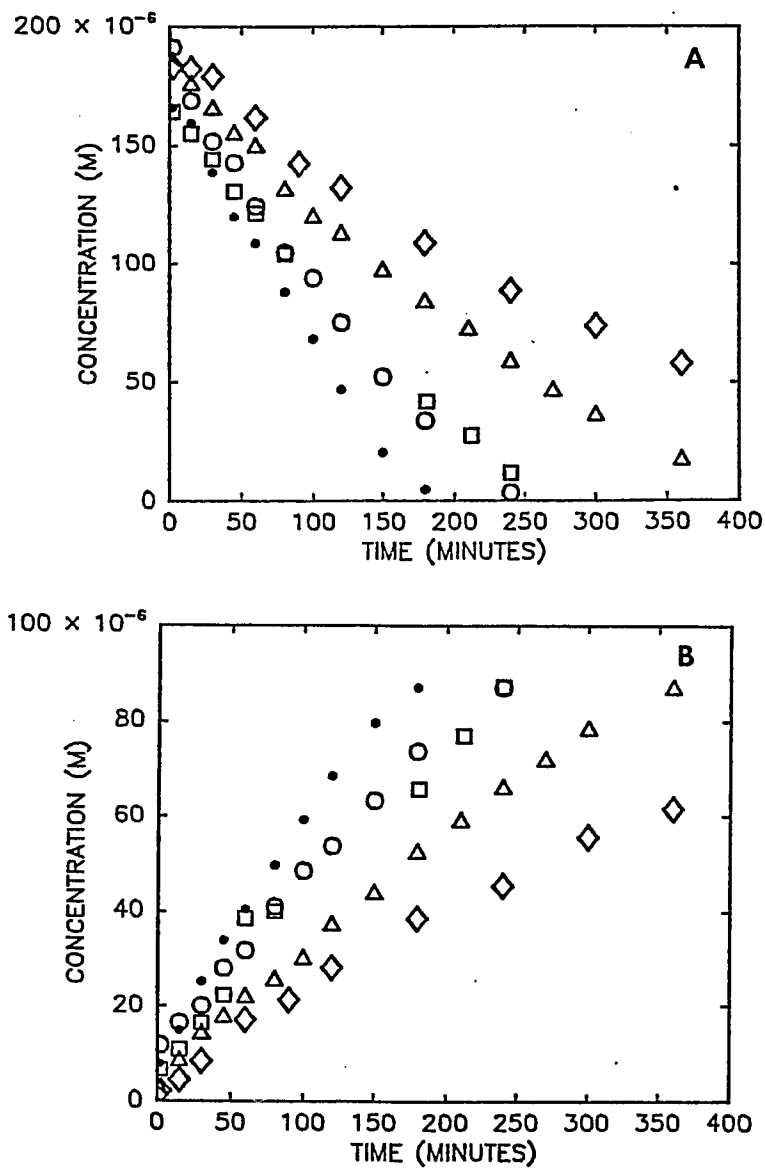


Figure 3.7: Captopril (A) and captopril disulfide (B) concentrations as a function of time under various Cupric ion concentrations. pH 6.62, 0.1 M phosphate buffer ($\mu=0.18$), pure O_2 , at $32^\circ C$. $[Cu^{++}] = 1.35 \times 10^{-5}$ (\bullet), 1.08×10^{-5} (\circ), 6.74×10^{-6} (\square), 2.70×10^{-6} (Δ), and 0 M (\diamond).

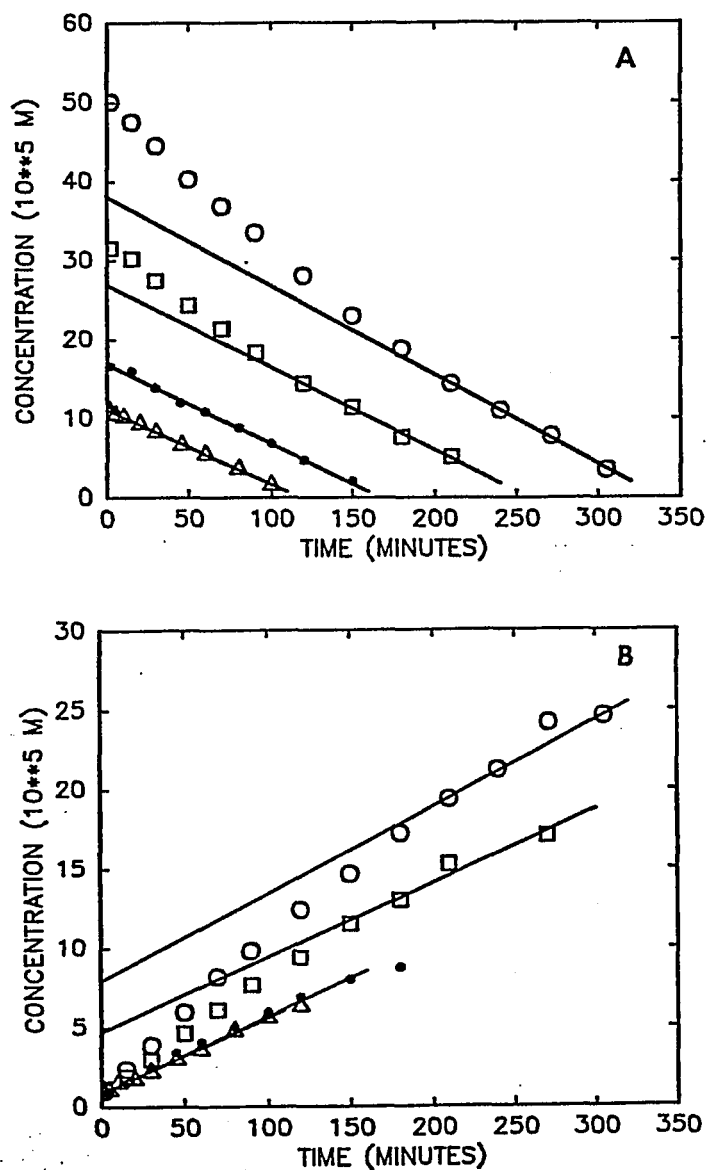


Figure 3.8: Captopril (A) and captopril disulfide (B) concentrations as a function of time with various initial captopril concentrations. pH 6.62, 0.1 M phosphate buffer ($\mu=0.18$), pure O_2 , $[Cu^{++}]=1.35 \times 10^{-5} M$ at $32^\circ C$. Initial captopril concentrations: 5.244×10^{-4} (o), 3.421×10^{-4} (\square), 1.945×10^{-6} (\bullet), and 1.315×10^{-6} (Δ).

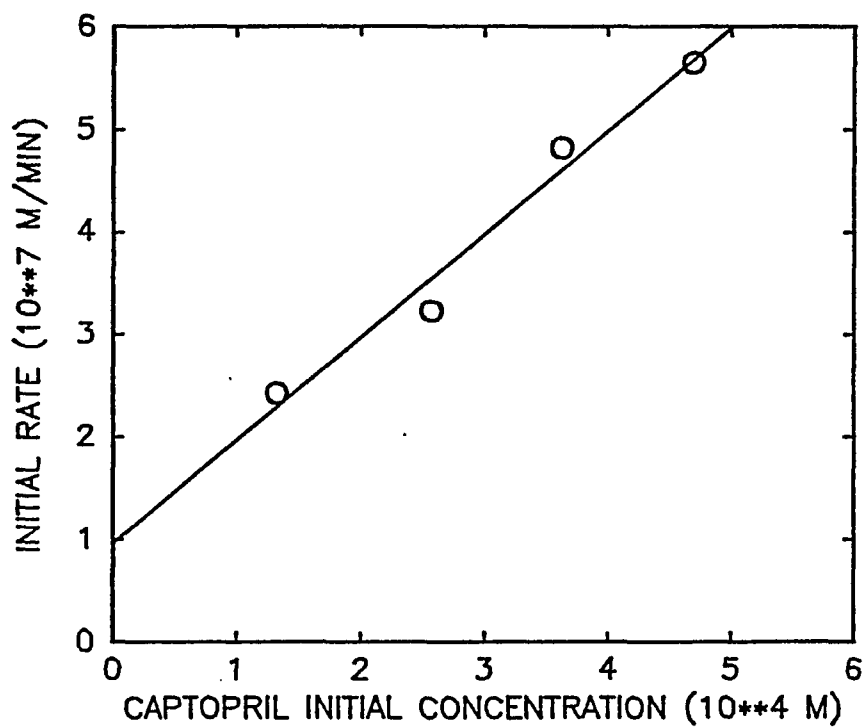


Figure 3.9: Initial rates as a function of initial captopril concentrations. pH 6.62, 0.1 M phosphate buffer ($\mu=0.18$), $pO_2=92\text{mmHg}$, $[Cu^{++}]=1.35 \times 10^{-5}\text{M}$ at 32°C .

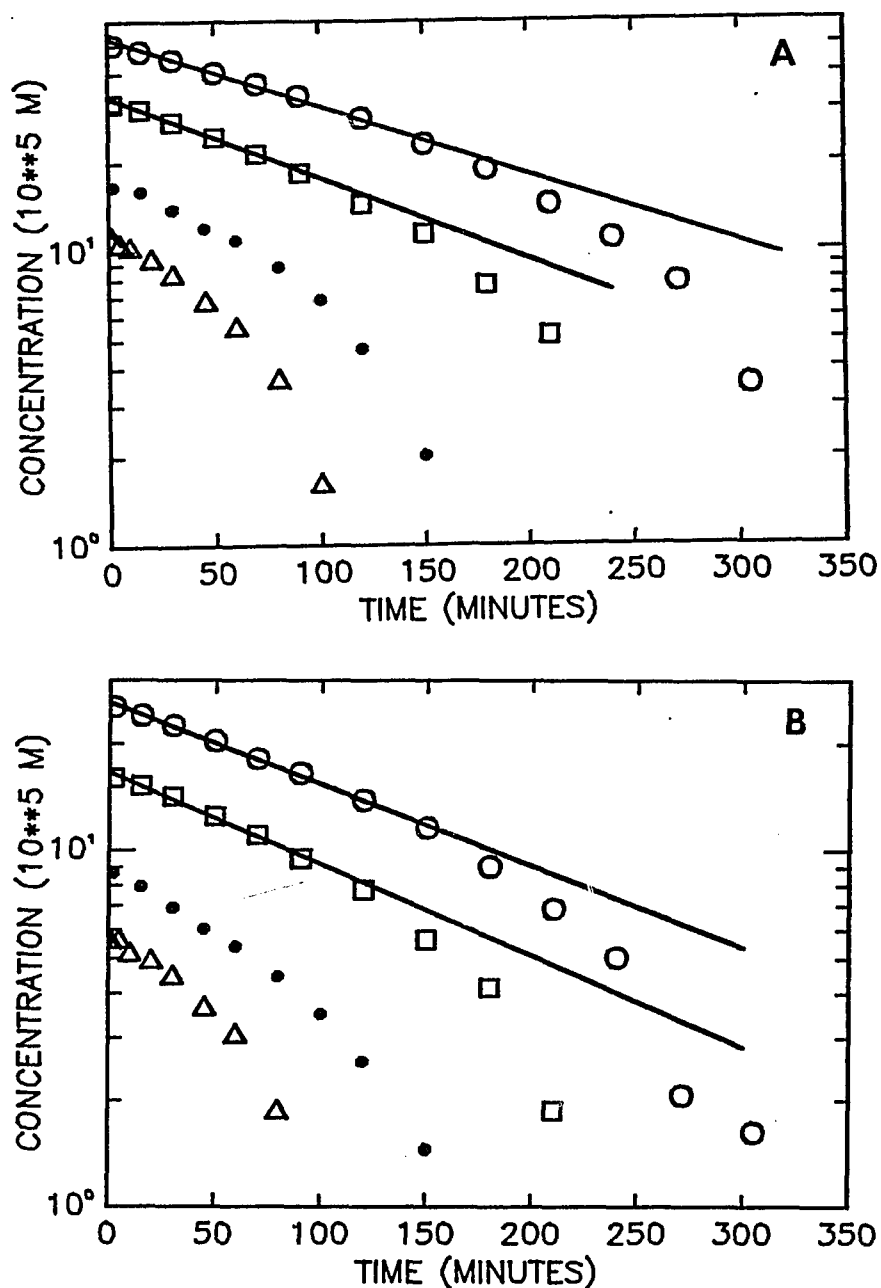


Figure 3.10:

Semi-logarithmic plots of captopril (A) and captopril disulfide (B) vs time with various initial captopril concentrations. pH 6.62, 0.1 M phosphate buffer ($\mu=0.18$), pure O_2 , $[Cu^{++}]=1.35 \times 10^{-5} M$ at $32^\circ C$. Initial captopril concentrations: 5.244×10^{-4} (o), 3.421×10^{-4} (□), 1.945×10^{-6} (•), and 1.315×10^{-6} (Δ).

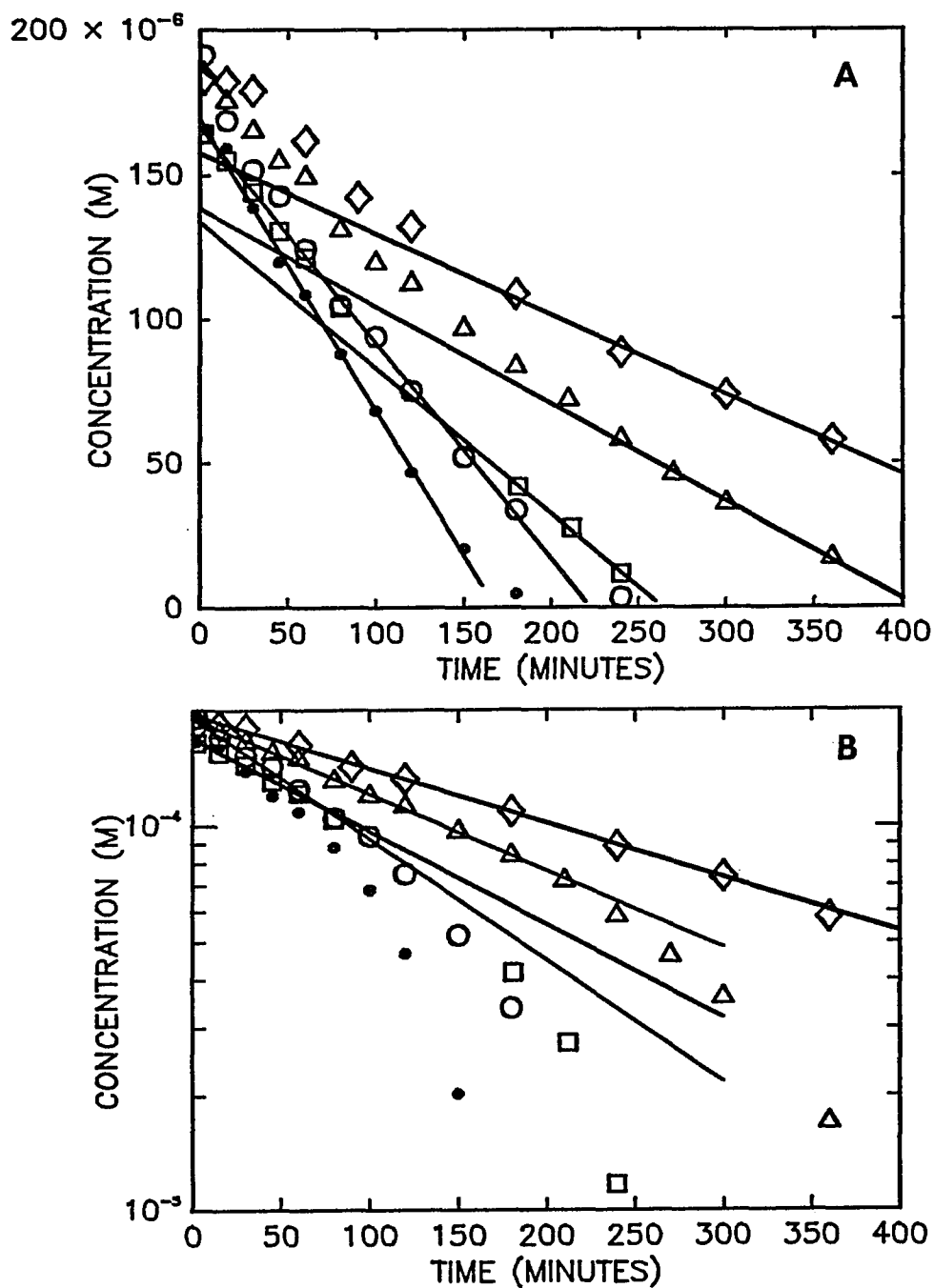


Figure 3.11: Zero-order(A) and first-order(B) plots of captopril as a function of time under various Cupric ion concentrations. pH 6.62, 0.1 M phosphate buffer ($\mu=0.18$), pure O_2 , at $32^\circ C$. $[Cu^{++}] = 1.35 \times 10^{-5}$ (\bullet), 1.08×10^{-5} (\circ), 6.74×10^{-6} (\square), 2.70×10^{-6} (Δ), and 0 M (\diamond).

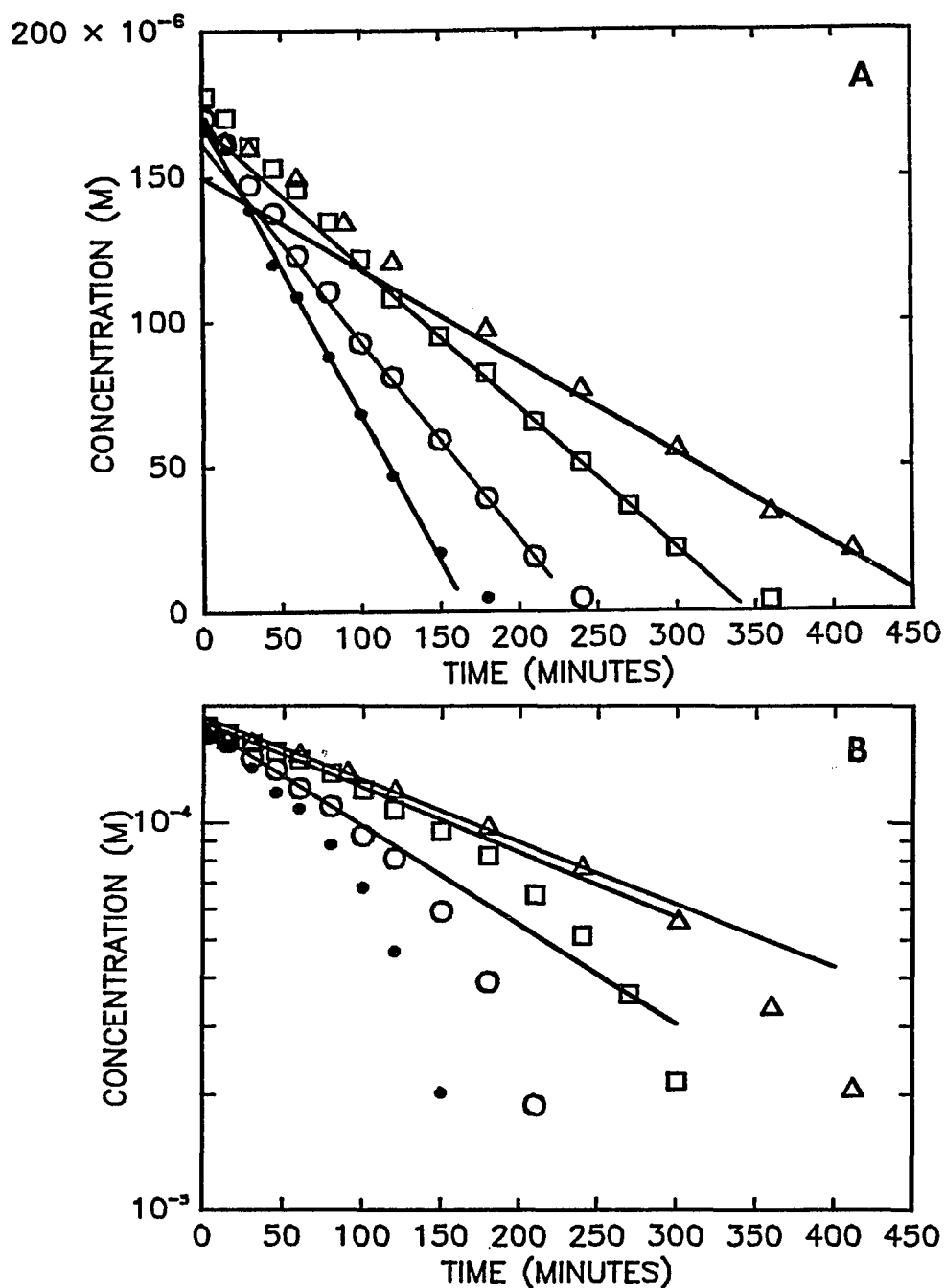


Figure 3.12: Zero-order(A) and first-order(B) plots of captopril as a function of time under various oxygen partial pressures. pH 6.62, 0.1 M phosphate buffer ($\mu=0.18$), $[\text{Cu}^{++}]=1.35 \times 10^{-5} \text{M}$ at 32°C . $p\text{O}_2 = 721(\bullet)$, 526(\circ), 338(\square), and 185 mmHg(Δ).

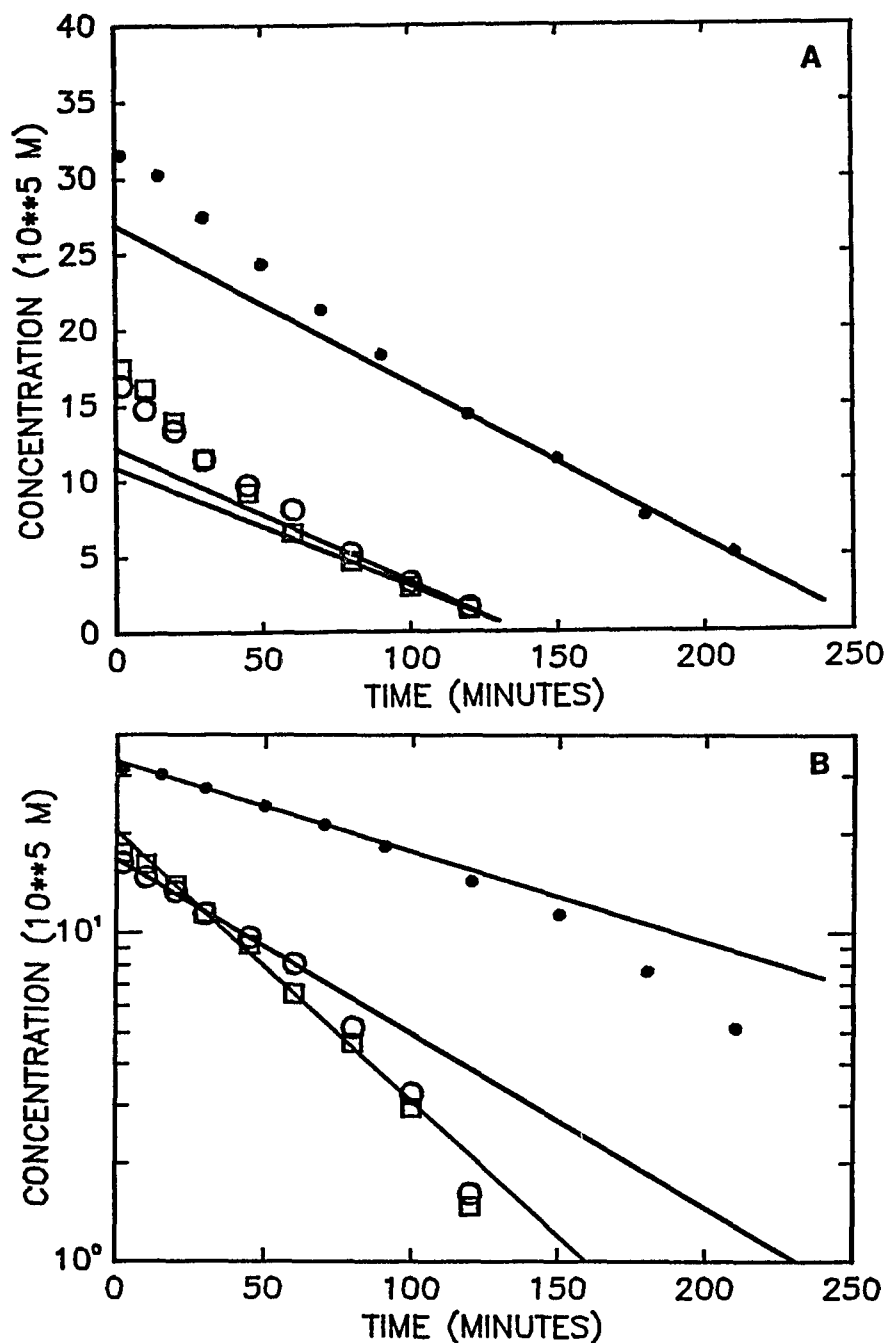


Figure 3.13: Zero-order(A) and first-order(B) plots of captopril as a function of time at various pH. $[\text{Cu}^{++}] = 1.35 \times 10^{-5}$ M at 32°C , with pure oxygen. pH: 6.62(\bullet), 7.44(\circ), and 7.94(\square).

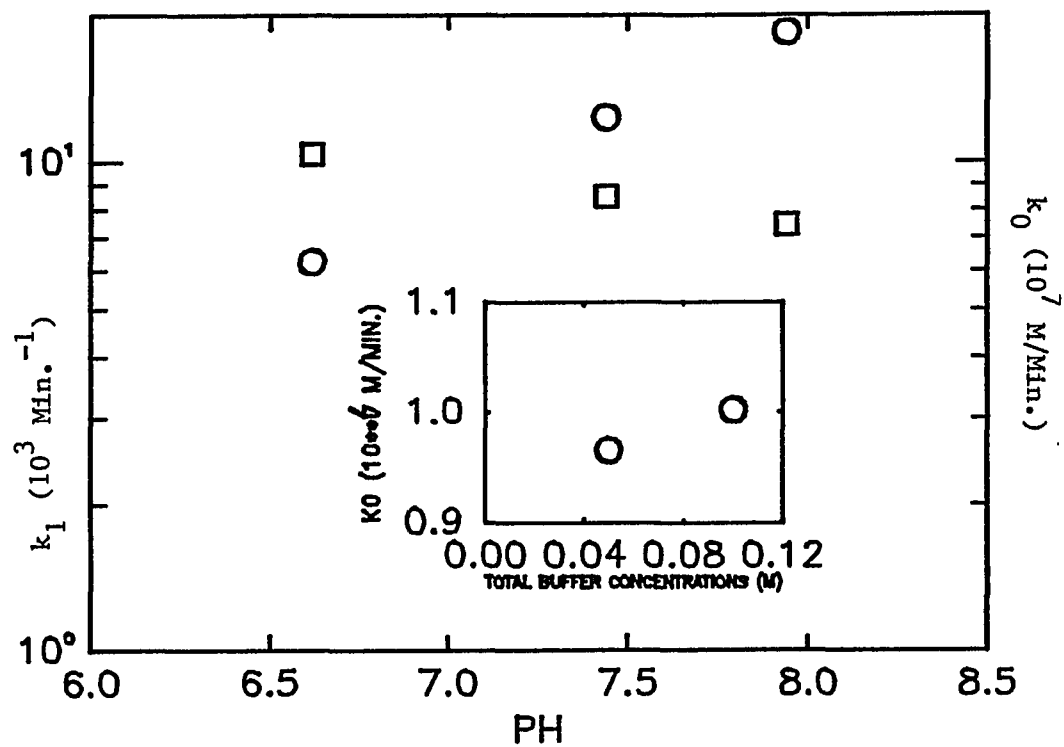


Figure 3.14: Paired apparent zero- (\square) and first-order (\circ) rate constants as a function of pH. $[\text{Cu}^{++}] = 1.35 \times 10^{-5} \text{ M}$ at 32°C . with pure oxygen. Insert is the comparison of apparent rate constants under different buffer concentrations.

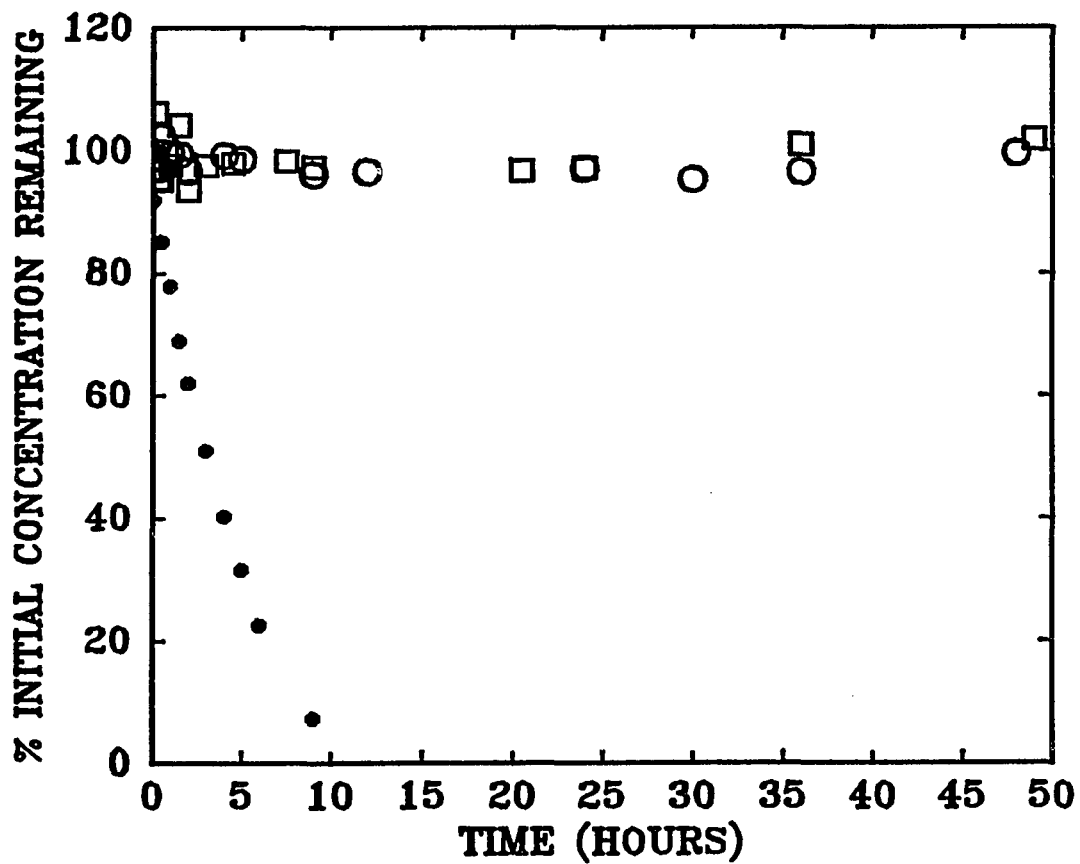


Figure 3.15: Comparison of captopril concentration as a function of time with the presence of chelating agents. (○): EDTA (□): 8-hydroxyquinoline and (●): no chelating agent added. pH 6.62, 0.1 M phosphate buffer ($\mu=0.18$), $[\text{Cu}^{++}]=0$, pure O_2 at 32°C .

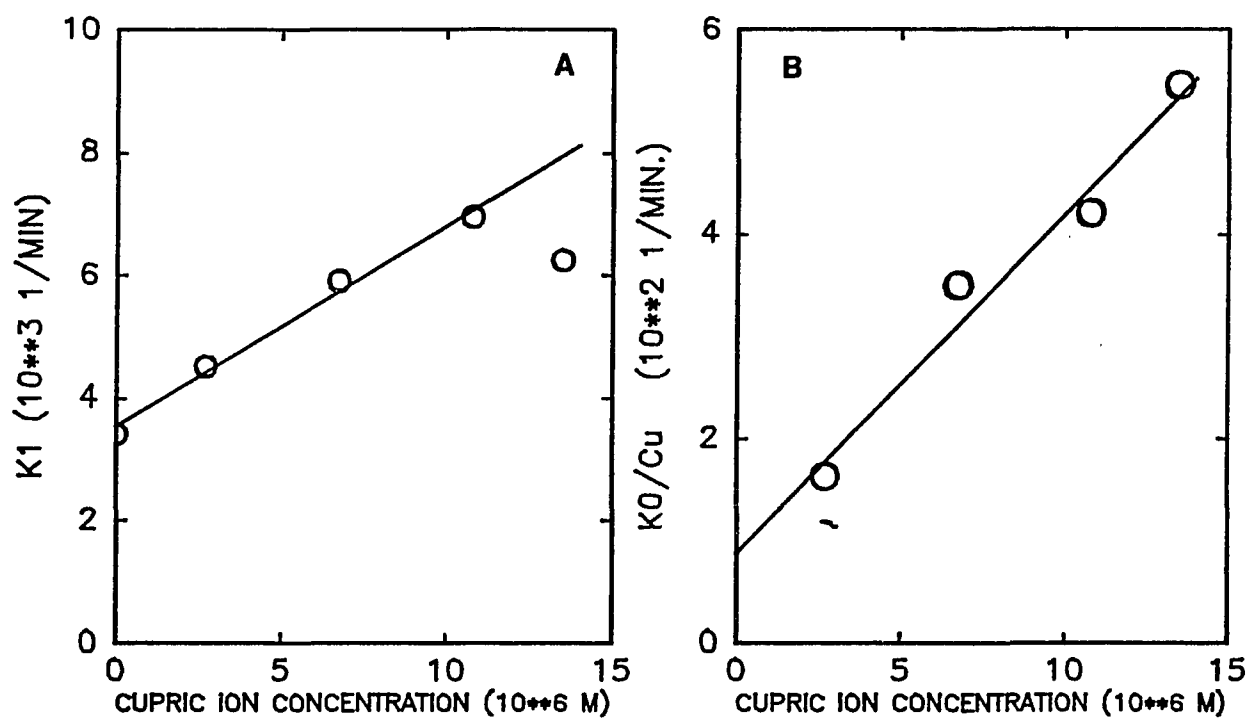


Figure 3.16:

Apparent first-order(A) and zero-order(B) rate constants as a function of cupric ion concentration. pH 6.62, 0.1 M phosphate buffer ($\mu=0.18$), pure O_2 at 32°C .

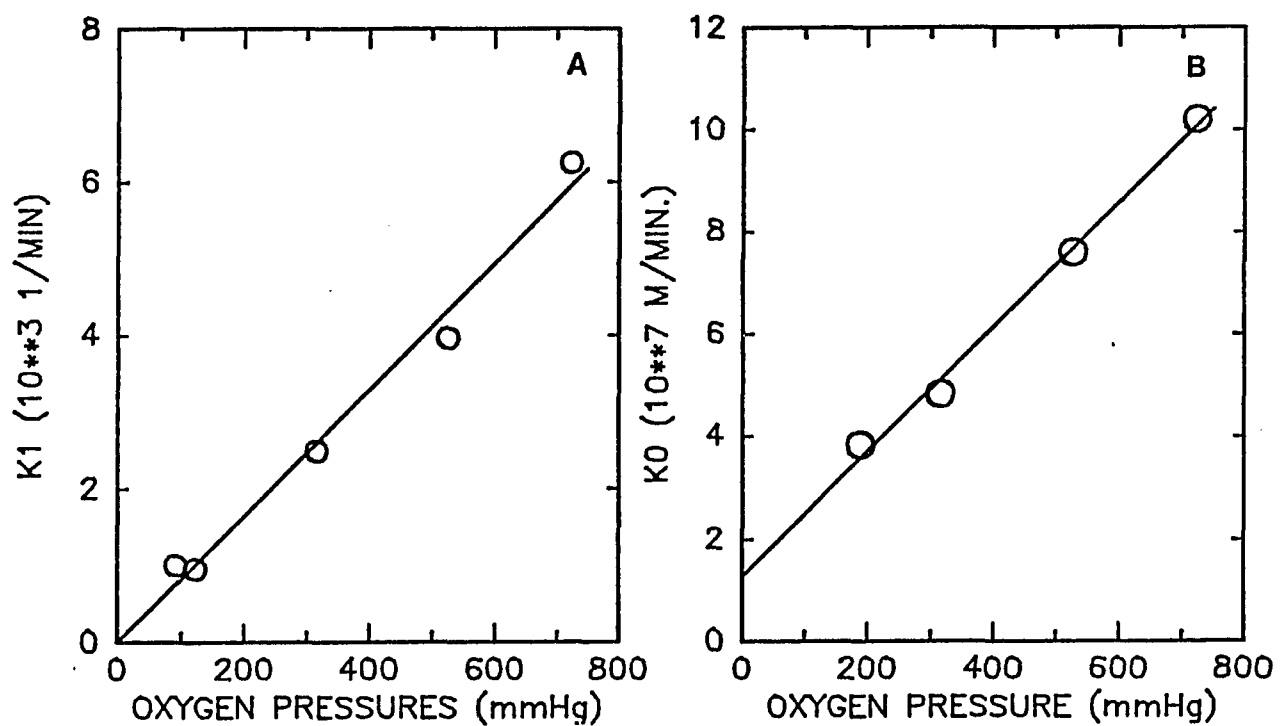


Figure 3.17:

Apparent first-order(A) and zero-order(B) rate constants as a function of oxygen partial pressure. pH 6.62, 0.1 M phosphate buffer ($\mu=0.18$), $[\text{Cu}^{++}]=1.35 \times 10^{-5} \text{M}$ at 32°C .